CALCIUM/CALMODULIN DEPENDENT PROTEIN KINASE II SIGNALING AND IGFR SIGNALING ARE COUNTER-BALANCED TO REGULATE PROTEIN DEGRADATION IN *C. ELEGANS* MUSCLE

by

Caitlin Feather

B.S., Edinboro University of Pennsylvania, 2006

Submitted to the Graduate Faculty of the

Kenneth P. Dietrich School of Arts and Sciences in partial fulfillment

of the requirements for the degree of

Doctor of Philosophy

University of Pittsburgh

2013

UNIVERSITY OF PITTSBURGH

DEITRICH SCHOOL OF ARTS AND SCIENCES

This dissertation was presented

by

Caitlin Feather

It was defended on

09-10-13

and approved by

Paula Grabowski, Professor, Department of Biological Sciences

Beth Stronach, Associate Professor, Microbiology and Molecular Genetics

Kirill Kiselyov, Associate Professor, Department of Biological Sciences

Gary Silverman, Chief, UPMC, Newborn Medicine Program, Department of Cell Biology

Lewis Jacobson, Professor, Department of Biological Sciences

CALCIUM-CALMODULIN ACTIVATED KINASE II SIGNALING AND IGFR SIGNALING ARE COUNTER-BALANCED TO REGULATE PROTEIN DEGRADATION IN *C. ELEGANS* MUSCLE

Caitlin Feather, PhD

University of Pittsburgh, 2013

The signal transduction network controlling protein degradation in the striated body-wall muscle of *C. elegans* has been shown to be composed of stimulatory signaling from the FGF receptor and inhibitory signaling from the IGF receptor engaged in cross talk at the level of the Raf-MEK-MAPK cascade. Calcium/calmodulin-dependent protein kinase II (CaMKII) is an additional, pro-degradation input into the network at the level of Raf. Splice forms of CaMKII may play a role in effective CaMKII signaling. The IGFR/FGFR/CaMKII network regulates protein degradation via autophagy. Degradation caused by increase of the pro-degradation signal from CaMKII can be suppressed by increase of opposing IGFR signaling, and degradation caused by decrease in the IGFR signal can be suppressed by decreased CaMKII signaling. This implies that regulation of protein degradation is based on integration of multiple signals by Raf and not on absolute amounts of individual signals.

TABLE OF CONTENTS

LIST OF TABLES

LIST OF FIGURES

LIST OF ABBREVIATIONS AND GENES

PREFACE

At the outset, I want to thank all the people who have made this work possible. It is as much a product of the people who have helped and guided me as it is my own. Some of the people I wish to thank are listed below, but many go unnamed. Thank you all.

To Karen Curto (KAC) and Evan O'Brian (ESO), who have worked with me on different aspects of this project, I am grateful for insight, as well as experimental contributions.

To Karen Curto and Valerie Oke, I am grateful for teaching and career advice and support.

To Swarna Mohan, I am thankful for reminding me of every important deadline.

To Paula Grabowski, Kirill Kiselyov, Beth Stronach, and Gary Silverman, I am thankful for serving on my committee. Your guidance had been much appreciated.

To Lew Jacobson (LAJ) for being my advocate and advisor. I will be forever grateful to you for taking me on as a mentee and doing the work of training me to be a scientist.

To my families, both the family that raised me and my husband's family, I am thankful for many, many things. Growing up, you encouraged curiosity and determination; these qualities have seen me through my education. In the nearer term, you have fed me wholesome food, provided countless hours of childcare so I could prepare this document, and given me unwavering emotional support. Michal, my husband, has kept my boat afloat, and, with our daughter, Gabriela, has made life fun.

1.0 INTRODUCTION

Muscle is a tissue of interest for many groups of people, including athletes, astronauts, the injured, and the elderly, just to name a few. Athletes seek to maximize muscle performance and avoid injury, while astronauts, the injured, and the elderly seek to avoid or reverse loss of muscle mass. While these groups may have an increased awareness of the importance of muscle, all people require muscle for movement (skeletal muscle), breathing (smooth muscle), and beating of the heart (cardiac muscle). Although dysfunction of muscle, particularly skeletal muscle, caused by aging or medical problems is not always a direct cause of death, function of muscle contributes to quality of life. As we come to focus more on "health span", we are likely to also focus more on our muscle and its role in our lives [7].

Skeletal muscle is the type of muscle we use for locomotion, and perhaps less obviously, as a metabolic reserve of protein. When one compares the muscle of, for example, a young athlete and an elderly person, one notices differences in both strength and mass. While the structural differences between the muscles in these individuals are well-catalogued [8-13], the molecular biology and biochemistry of each state are more complicated. This study attempts to broaden our understanding of how muscle responds to the signaling environment to determine the appropriate extent of protein catabolism. We do this using *C. elegans* body-wall muscle as a model, since it is related to human skeletal muscle and *C. elegans* offers many benefits as a model system. Perhaps the most important advantage is that by using *C. elegans* we can look at muscle *in situ*, an

important benefit when one considers the various paracrine and endocrine signals a tissue is exposed to in a whole, living animal. Using this system, I will show calcium/calmodulin-dependent protein kinase (CaMKII) promotes degradation through interaction with other known signaling pathways and that these pathways regulate protein degradation via autophagy. I will start to define the rules by which signaling through these multiple pathways is integrated and offer some data on the role that a specific isoform of CaMKII may be playing in promoting CaMKII activation and degradation.

In the following introduction to this work, I will first discuss the different types of muscle, focusing on skeletal muscle and its contractile and metabolic roles. I will then describe the effects of skeletal muscle hypotrophy and the degradative mechanisms by which it occurs. Having described relevant muscle types and processes in vertebrates, I will describe the parallel structures and processes in *C. elegans*, as well as the signaling pathways regulating muscle protein degradation that we have thus far identified using this system. Lastly, I will turn to calcium signaling and the role it is known to play in muscle protein homeostasis, preparing the reader for my studies of CaMKII, a protein most succinctly described as a calcium sensor, and its role in muscle protein degradation.

1.1 ROLE OF MUSCLE IN HEALTHY ANIMALS

1.1.1 Types of muscle

In vertebrates, there are three different types of muscle: smooth, cardiac, and skeletal. Smooth muscle is non-striated, while cardiac and skeletal muscle are striated [14].

Developmentally, skeletal muscle originates from somites, which are segments of the paraxial mesoderm that lie in pairs along the neural tube. Each somite differentiates to produce dermomyotome, which goes on to produce muscle precursors that migrate to the limbs and body wall and become the muscles of the back [15]. Cardiac muscle is derived from two populations of cells in the anterolateral plate mesoderm called the right and left heart fields. The two fields merge anteriorly and then form a tubular heart, which is specified along its anteroposterior axis to form what will become the compartments of the mature heart. The tube undergoes looping and acquires contractile activity [16]. Smooth muscle cells have diverse origins, both from the ectoderm and mesoderm. Some smooth muscle cells arise from the cardiac neural crest, while others arise from the local mesenchyme [17].

All three types of muscle express some of the same muscle-specific genes from embryogenesis, while they also each express genes unique to their particular muscle type. This allows all three tissues to be defined as "muscle", but gives them unique contractile, metabolic, and electrophysiological properties [15, 18]. These muscle-specific genes that are differentially expressed in the various muscle types are regulated by the binding of transcription factors. With each gene able to bind multiple transcription factors, it is the combination of factors bound to regulatory regions of the gene that confers level of expression [15]. The combinations of genes that are expressed then define a muscle type and gives rise to its particular muscle structure and function.

As stated above, smooth muscle is a non-striated form of muscle. Layers of smooth muscle are contained in the walls of various organs and blood vessels. Their contraction serves to move the luminal contents of the organ or vessel in which they reside [19]. Although they are not striated, contraction still occurs through interaction of myosin with actin stimulated by a change

in electrical potential of the cell membrane. Upon stimulation, calcium is released from the internal sarcoplasmic reticulum (SR) stores and enters from the extracellular space. Calcium then binds to calmodulin, which binds myosin light chain kinase (MLCK). Binding of calcium/calmodulin to MLCK results in removal of the autoinhibitory domain from the active site and activation of the kinase [20]. MLCK then goes on to phosphorylate myosin light chain, promoting myosin's ATPase activity and causing cross-bridge cycling and contraction. Relaxation is promoted by decreased activity of MLCK and increased activity of myosin light chain phosphatase. Interestingly, activity of autophosphorylated CaMKII (see section 1.4.3) promotes relaxation of smooth muscle by phosphorylating MLCK on a site that prevents binding of calcium/calmodulin [21].

Cardiac muscle is a type of striated muscle more closely related to skeletal muscle. In the heart, myocytes are arranged in muscle fibers, which are organized to form the myocardium and the ventricles of the heart [22]. Electrical stimulation of the myocytes causes them to contract and increase the pressure inside the ventricle to the point where the valve opens. When the valve opens, the tissue is deformed and blood is ejected [22]. There are two different types of myocytes, work cells and pacemaker cells. Work cells have a more stable resting potential, while pacemaker cells have unstable resting potentials and spontaneously depolarize to generate the auto-rhythmicity of the heart [23]. Influx of calcium into the myocyte from the extracellular space stimulates further release of calcium from the SR. Unlike smooth muscle, cardiac muscle contains troponin, which is associated with the actin filament and prevents interaction of myosin with actin. Binding of calcium to troponin causes a conformational shift that permits the interaction of actin and myosin. The activity of myosin in cardiac muscle does not require MLCK, but its activity can be modulated by it. Additionally, MLCK in cardiac muscle has roles in maintaining sarcomere

structure [24]. In cardiomyocytes, activated CaMKII is linked to heart failures and arrhythmias through phosphorylation of diverse downstream substrates [25].

Skeletal muscle is multinucleate and striated. Bundles of multinucleate fibers are bound to form the whole muscle, which is sheathed in connective tissue continuous with the tendons at the end of the muscles [2]. Contraction of skeletal muscle allows for movement. In skeletal muscle, depolarization activates a calcium channel in the plasma membrane (the L-type channel) that physically interacts with the calcium channel in the SR (the ryanodine receptor, RyR). This activation results in a small influx of calcium and activation of the opposing channel on the SR, which releases a large amount of calcium into the muscle cytoplasm. Excitation-contraction coupling is similar to that in cardiac muscle and MLCK plays a negligible role [24]. The structural features of skeletal muscle will be further discussed in the following section.

1.1.2 Structure of skeletal muscle

Developmentally, skeletal muscle arises from structures of the paraxial mesoderm, called somites. Dorsally, each somite contains dermomyotome, which differentiates to produce dermatome and myotome [26]. The dorso-medial dermatome and myotome produces the back muscles, while the ventro-lateral dermatome produces the trunk and limb muscles [27]. These populations give rise to the direct precursors of muscle cells, myoblasts. Myoblasts are mononucleate cells that are defined by their expression of myogenic regulatory factors [27]. Myoblasts fuse and migrate to their future location, where they attach to the appropriate tendon [28].

The same embryonic myogenic precursor cells that give rise to muscle also give rise to satellite cells [26], which are non-differentiated, muscle-precursor cells that are external to, but associated with muscle fibers [2]. Upon stimulation, satellite cells differentiate into myoblasts that are capable of differentiating into adult muscle fibers [5]. These cells are essential for muscle growth, repair, and adaptation [2].

The basic structural unit of a skeletal muscle is a muscle fiber (Figure 1). A muscle fiber is a multinucleated cell containing many parallel myofibrils, the contractile apparatus of the muscle cell. Each muscle fiber is innervated by a single branch of a motor neuron [5] and is surrounded by connective tissues called endomysium [2] One muscle fiber combined with other muscle fibers and innervated by the same neuron compose a motor unit. In contrast to smooth muscle and cardiac muscle, skeletal muscle activation is voluntary, with a motor unit being the smallest group of muscle fibers that can be voluntarily activated, as all fibers in a motor unit will contract simultaneously as they are depolarized by a nerve impulse. Motor units range in size from several dozen to thousands of fibers [5]. Muscle fibers are bundled in fasciculi, which are surrounded by perimysium [2]. Fibers in different motor units can be in the same fasciculus, and vice versa, although all fibers in the same motor unit are of the same type, as will be discussed below. Fasciculi are bundled to form the complete muscle, which is sheathed in epimysium [2]. (Figure 1)

The basic contractile unit of a muscle fiber is the sarcomere, with an array of parallel, longitudinally repeating sarcomeres forming a myofibril [2]. As muscle develops post-natally and through adulthood, muscle fiber increases in length by adding sarcomeres longitudinally [29]. A sarcomere is composed of overlapping thin (actin) and thick (myosin) filaments that slide across each other during muscle contraction [5]. Thin filaments are composed of actin, tropomyosin, and

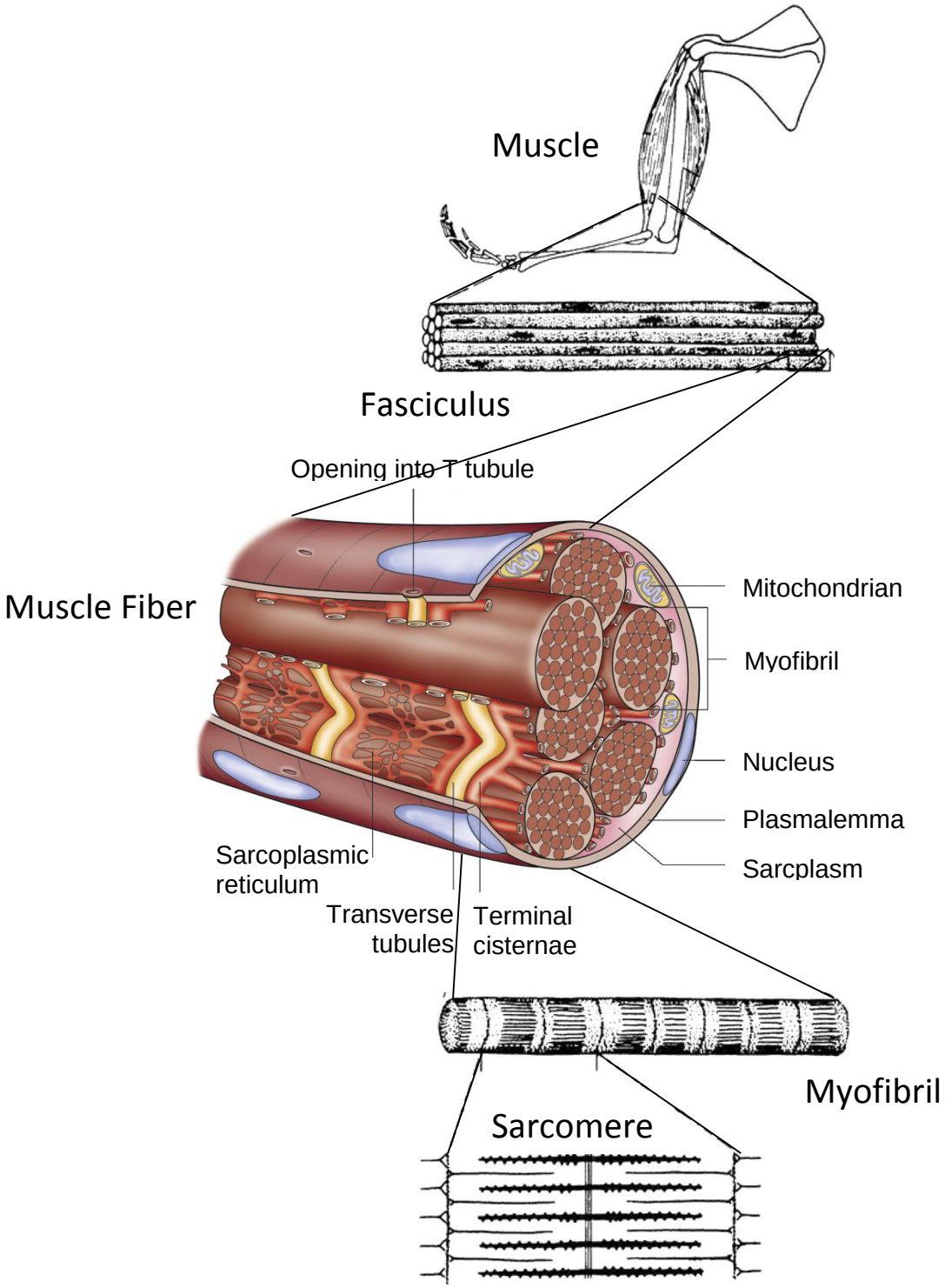

Figure 1

Structure of a mammalian muscle. Longitudinally repeating sarcomeres are arranged in parallel to form a myofibril. Several myofibrils are bundled to form a muscle fiber. Bundled muscle fibers form a fasiculus. Many fasciculi form the complete muscle. Adapted from Exeter, 2010 [2] and Brooks, 2003 [5]

troponin. Two chains of actin and a chain of tropomyosin are twisted together in a helix. Troponin is a globular protein consisting of three subunits and is bound to tropomyosin [2]. Thick filaments are composed of myosin heavy chain (MHC) proteins arranged in bundles of two, with each bundle having a rod-like portion and two globular heads [2]. At the neck of the head, myosin light chain is associated. It is the head of the MHC that binds actin and ATP [2].

Contraction of the muscle cell depends on calcium binding to troponin, leading to an alteration in the conformation of the thin filament such that the myosin head can bind it. Calcium enters the sarcoplasm of the muscle cell from both the external environment and the internal stores of the SR. The SR is closely associated with the myofibrils, such that the calcium that is released from the SR upon stimulation of the muscle cell will be at its site of action. To avoid the classic surface/volume ratio problem in communicating a nerve impulse to all the myofibrils in a muscle fiber, the plasma membrane has a system of deep invaginations that form tubules. These are called transverse (T) tubules. Each T tubule is abutted on either side by dilations of the sarcoplasmic reticulum, in an arrangement called a triad [2]. The role of these structures in contraction will be discussed in the following section, as will the implications of modulation of these structures on muscle strength.

1.1.3 Muscle as a means for doing mechanical work

In order to contract, the muscle must be stimulated by a nerve impulse. A nerve impulse results in release of acetylcholine (ACh) into the neuromuscular junction (NMJ). Binding of acetylcholine to ligand-gated sodium channels (acetylcholine receptor, AChR) results in flux of sodium into the muscle cell, leading to depolarization of the muscle membrane [2]. This

depolarization enters the T-tubule and causes a change of conformation of the dihydropyridine receptor (DHPR), an L-type calcium channel. Some calcium can enter the cell through the DHPR, but this is not required for muscle contraction [30]. Instead, physical interactions between the DHPR and the RyR during depolarization stimulate release of SR stores of calcium through the RyR into the muscle cytoplasm [30].

In order for contraction to occur, the globular head of MHC must ratchet along the actin filament in a series of events known as cross-bridge cycling, with a "cross-bridge" being the interaction between the myosin head and actin, and "cycling" referring to the fact that contraction occurs by a cycle of binding and release of the actin filament by myosin. Upon stimulation of the muscle cell, the calcium released from the sarcoplasmic reticulum binds troponin. This initiates a conformation shift in the actin filament, exposing the myosin binding sites. Myosin-bound to ATP is then able to bind actin, marking the start of the cross-bridge cycle. Next, myosin hydrolyzes the ATP, releasing ADP and inorganic phosphate and causing distortion of the myosin head, to pull on the actin filament. Rebinding of ATP to myosin causes release of the actin filament and return of the myosin head to its original conformation. Repetition of this cycle causes the actin and myosin filaments to slide along each other and the sarcomere to shorten. [31]

When stimulation of the muscle cell ceases, calcium is returned to the SR via the Sarco/Endoplasmic Reticulum ATPase pump (SERCA). SERCA pumps two calcium ions into the SR for every mole of ATP converted to ADP, P_i, and heat, creating a 10,000-fold concentration gradient [32]. Return of calcium to the SR results in loss of cross-bridging.

It is the rate of the cross-bridge cycle that determines the velocity with which a muscle fiber can shorten. The rate of cycling is determined by the ATPase activity of the MHC [5], of which there are many isoforms, each with characteristic ATPase activity. The types of MHC

expressed in a muscle will determine the shortening velocity of that muscle. The power of a contraction [33] is equal to force times velocity, with force being determined by the cross-sectional area of the fiber, or the number of myofibrils in parallel [29]. The various MHC isoforms do not have different abilities to generate force, so variations in power output by muscle expressing different MHC isoforms is based on differences in shortening velocity [5]. It is muscle power that is needed for athletic movements. During growth and adaptation, the isoforms of MHC expressed in a muscle changes [29].

Another important component of muscle performance is resistance to fatigue. This depends on continuation of the cross-bridge cycle. ATP is required for the cross-bridge cycle to turn, therefore it is the availability of ATP that determines fatigue resistance. ATP is generated by oxidative metabolism, requiring mitochondria. To increase fatigue resistance, muscle increases the number of mitochondria. However, due to space considerations, an increase in mitochondria reduces the packing density of the myofibrils, which reduces the amount of force that can be generated. Therefore, there is trade-off between power and endurance. Based on the demands placed on a motor unit, its component fibers will be fast-twitch and favor the fast type of MHC with fewer mitochondria, or slow-twitch and favor the slow type of MHC with more mitochondria. It is not entirely understood how these changes in gene expression occur. [29]

Another way a muscle can increase power output is by adding sarcomeres longitudinally to the muscle fiber in order to produce sarcomeres of optimum length for power output [29]. Stretching and stimulation induces lengthening of the muscle fiber and is associated with increased protein synthesis [29]. This change is thought to require not so much a change in what genes are expressed by the muscle, but by the amount of translation of expressed genes [29].

With age, muscle mass and maximal power output decrease (sarcopenia). This is largely due to loss of muscle fibers, with fast fibers more prone to loss than slow fibers [34]. This loss is caused by denervation of the fast muscle fibers, which may or may not be re-innervated by sprouts from the nerves that innervate slow muscle fibers. Those that are not re-innervated are lost [34]. Aging muscle is also less able to generate force per muscle fiber cross-sectional area than younger muscle. This deficit is thought to be the result of accumulation of insufficiently repaired contraction-induced damage [5], the repair of which is thought to be the primary mechanism by which muscle adaptation occurs [2].

1.1.4 Muscle in metabolism

Muscle is classically regarded as a tissue whose primary role is to produce movement. While its role in locomotion is important, it has an equally important metabolic role. In this metabolic role, it serves both as the body's "furnace" through thermogenesis [35] and as the body's primary location of stored protein [36]. All heat production in muscle is ultimately tied to hydrolysis of ATP [32]. Hydrolysis of ATP during muscle contraction produces heat, but skeletal muscle is likely also responsible for a significant amount of resting, basal heat production [32]. This heat may be produced by maintenance of muscle tone [32], as a byproduct of absorption and storage of nutrients [37], or, majorly, by calcium ion recycling [32]. It is thought [32] that the steep calcium gradient between the SR and the cytoplasm causes leakage of calcium from the RyR. This "leaked" calcium is pumped back into the SR by SERCA, generating heat through hydrolysis of ATP [32]. Production of heat is balanced by heat dissipation, resulting in maintenance of basal body temperature, 37C for humans [38]. Mutation of proteins involved in calcium recycling (often

the RyR) can cause malignant hyperthermia with use of anesthetics [32]. Anesthetics cause increased calcium leakage through mutant RyR, leading to an increase in intracellular calcium. This increased intracellular calcium causes a decrease in cytoplasmic ATP and an increase in glycolysis, generating heat [32]. Excess calcium is taken up by the mitochondria, increasing oxidative metabolism and heat production [32]. Untreated, malignant hyperthermia results in death.

Muscle's role as a protein-storage organ in likewise important. Muscle contains half of all protein in a healthy human and acts as a protein reservoir [36]. This protein reservoir is maintained so that in times of need, such as starvation or disease, it can be readily tapped as a source of amino acids for energy metabolism or biosynthesis by organs which require a steady source of amino acids [39]. During fasting, muscle releases amino acids into the circulation, as well as gluconeogenic precursors. The amino acids are used by other tissues for essential protein synthesis [40], while the gluconeogenic precursors are used by the liver for production of the glucose needed to keep the body alive and feed the brain [41]. In fasting and non-fasting states, muscle also provides the amino acids required for neurotransmitter synthesis and acid/base balance [29].

During catabolic conditions, such as cancer, diabetes, burn injury, or sepsis, the muscle releases amino acids that are used not only as described above, but also for wound healing and the synthesis of antibodies and acute-phase proteins [42], [36]. Therefore, these conditions require protein breakdown in excess of what occurs during fasting, and in some cases, such as extensive burn injury, can require amounts of proteins 4 times in excess of the normal daily intake [40]. This need for excess protein can trigger net breakdown of muscle protein that is difficult to reverse by nutritional support [40]. In fact, patients suffering from trauma or critical illness are less likely

to survive or fully recover if they had lower levels of lean body mass [40]. In the following section I will discuss in more detail the effects and mechanisms of skeletal muscle wasting.

1.2 SKELETAL MUSCLE WASTING

1.2.1 Role of muscle wasting in disease

While muscle protein catabolism can provide tissues with needed amino acids, excessive catabolism of muscle protein can lead to muscle wasting [43], which is characterized by loss of muscle mass and function. Muscle wasting, as seen in patients with catabolic diseases, is caused primarily by increased muscle protein degradation [44], and can lead to death through failure of the diaphragm muscle [45] or the inability to produce the glutamate required to survive a traumatic experience [29]. In contrast to loss of skeletal muscle caused by starvation, the loss of skeletal muscle observed in patients with aging, chronic diseases, or injury cannot be easily reversed [46].

After feeding, protein synthesis in skeletal muscle doubles and accounts for more than half of all the protein synthesis occurring in the body [47]. Protein anabolism by muscle is regulated by the plasma concentrations of amino acids and insulin [48]. Muscle wasting is caused by an imbalance in the amount of muscle protein synthesis and protein degradation. Strategies for treating muscle wasting can then focus either on increasing protein synthesis or decreasing protein degradation. Unfortunately, increased nutrient intake does not increase protein anabolism in many disease states, suggesting that signaling mechanisms of the disease state are not only enhancing degradation, but also inhibiting synthesis. Signaling mechanisms of catabolic diseases include glucocorticoids, cytokines, and oxidative stress, which have all been shown to have negative

impact on the pathways that normally promote anabolism [48]. This effect, as seen in catabolic diseases, has been described as a raise in the "anabolic threshold" [48].

Instead of trying to reset the anabolic threshold, treatments for muscle wasting often focus on increasing amino acid intake to reach the new anabolic threshold. Particularly, supplementing with leucine stimulates protein synthesis, even in the absence of insulin and other amino acids [49]. Still, leucine consumption has been shown to have the most marked effect when taken as part of a whole protein (such as whey protein) and taken all at one meal [48].

An alternative treatment for muscle wasting is to lower the anabolic threshold by modifying the signaling pathways that have led to its rise. A benefit of this strategy is that it would not require complicated feeding schedules and would eliminate the burden placed on nitrogen waste removal mechanisms caused by high protein intake, a matter of important consideration in patients who are frail or have impaired renal function [48]. Despite the fact that many of the signaling pathways causing this rise in the anabolic threshold have been identified, treatments based on this strategy have been largely unexplored [48], mostly due to the complicated nature of trying to re-balance multiple signaling pathways to re-establish a healthy anabolic threshold.

1.2.2 Mechanisms of protein degradation

Degradation can be carried out by lysosomal and non-lysosomal mechanisms. Non-lysosomal mechanisms include the ubiquitin-proteasome system, calpains, and caspases, while lysosomal mechanisms include autophagy [50]. I will briefly discuss the ubiquitin-proteasome system, calpains, and caspases here, although the focus of this work will mostly be on autophagy

and its regulation. This review of non-lysosomal degradative systems will provide a contrast to the mechanisms of autophagy.

The ubiquitin-proteasome system primarily degrades proteins that have been tagged with ubiquitin for degradation. Ubiquitin is a small, 76 amino acid protein. It has a carboxy-terminal glycine residue that is essential for conjugation to other proteins and several lysine residues that are used in making polyubiquitin chains [51].

Tagging of a protein by ubiquitin is a highly regulated process, involving the action of three ubiquitin ligases (E1-E3). The E1 is the ubiquitin-activating enzyme. In mammals, there is only one E1. Once activated, a ubiquitin can be transferred to an E2, a carrier protein. Finally, an E3 transfers the ubiquitin to the target protein. The target can either become mono-, multi-mono-, or polyubiquitylated. Polyubiquitylation occurs when several ubiquitins are attached in a single chain to the substrate. Polyubiquitin chains that are greater than five in length signal for protein degradation [44]. These chains are usually Lys48- and Lys11-linked chains [52]. The type and length of chain is regulated by the E2 [52], of which there are about a dozen in mammals [53], providing a level of specificity and discrimination [51].

The action of the E3 provides even greater specificity to the proteasomal process. Different tissues express different sets of E3s, resulting in tissue-specificity in the proteins degraded by the proteasome. In muscle, the E3 ligases antrogin-1 and MuRF-1 are more highly expressed during atrophy, and mouse models of starvation and denervation show reduced atrophy when these genes are knocked out [51]. These E3s have come to be used as biomarkers for atrophy.

Ubiquitinated proteins are recognized by the proteasome. The proteasome is a large, 60-subunit, protein-degrading machine. The 19S regulatory particles on the ends of the 20S barrel are responsible for recognizing and removing the ubiquitin chains prior to degradation [51]. The

de-ubiquitinated protein is unfolded and translocated into the 20S barrel through an ATP-dependent process. Inside the barrel, the protein is cleaved into peptide fragments. When these fragments exit the proteasome, they are degraded into their constituent amino acids by endo- and aminopeptidases. [51]

Fasting and denervation stimulate ATP-dependent protein degradation 2- to 3-fold in rat leg muscles ([44], [54]) and rat skeletal muscle shows an increase in ubiquitin- conjugated proteins during fasting and denervation. This is accompanied by increases in ubiquitin and proteasome mRNA, despite decreases in total mRNA [55]. These increases suggest that there may be a change in the "transcriptional program" during altered states that lead to atrophy [53].

Two transcription factors implicated in proteasomal protein degradation in muscle are FoxO and NF-kB. FoxO and NF-kB bind the promoters of antrogin-1 and MuRF-1, respectively. In both the case of FoxO and NK-kB, inhibition prevents atrophy and activation causes it [56, 57].

The ubiquitin-proteasome system can only very slowly degrade myofibrils, so they must initially be cleaved by other cytosolic proteases [51]. Evidence suggests that calpains and caspases play this role [51]. The role of calpains and caspases will be discussed in section 1.4.3.

Macroautophagy is responsible for the degradation of long-lived proteins and organelles [3]. It occurs at a basal level in healthy tissue and in muscle is required to maintain mass [50] and prevent myopathy [58]. Up-regulation of autophagy under conditions such as growth factor withdrawal, structural remodeling, protein aggregate accumulation, etc., can be adaptive, but excessive autophagy contributes to muscle loss [59].

Autophagy is negatively regulated by TOR kinase. In response to growth factors and nutrients, TOR turns off autophagy [3] by phosphorylating ATG13 and preventing its interaction with ATG1 [60] (yeast gene names used throughout). Inactivation of TOR leads to

dephosphorylation of ATG13 and its subsequent association with ATG1. This interaction is stabilized by ATG17 [60] and activates the kinase activity of ATG1 [61]. The formation of this complex is required for autophagy, however it is not understood how this complex promotes autophagy [62]. One study [63] suggests that ATG17 is a scaffold required for recruitment of other Atg proteins to the pre-autophagosomal membrane. (Figure 2)

The autophagosomal membrane is a double membrane, whose origin is not entirely known. It begins to form at a punctate structure called the phagophore assembly site (PAS), the structure of which is unknown [63]. ATG proteins are recruited to the PAS, resulting in the nucleation or expansion of the phagophore [64]. The phagophore is a small membrane sac that will elongate and curve to eventually form the closed autophagosome and is also known as the "isolation membrane" [62].

Phosphatidylinositol 3-phosphate (PI3P) is required for formation of the autophagosome, although it is not known why. It may possibly be involved in changing the membrane dynamics of the phagophore origin membrane, or it may simply recruit binding partners required for phagophore formation [65]. PI3P is formed by a type III phosphatidylinositol 3-kinase (PI3K) called Vps34. Vps34 is in a complex with ATG-14, ATG-6 (Beclin-1), and Vps15 [62] (Figure 2). ATG-14 (not shown) localizes the rest of the complex to the PAS though its interaction with ATG-6, which is a binding partner of Vps34 and promotes its association with Vps15 [62]. Vps15 increases the kinase activity of Vps34 and is required for its responsiveness to autophagy induction [62].

The ER is one of the suspected origins of the membrane that makes up the phagophore. ATG14 localizes to the ER during starvation and the ER has increased PI3P content during

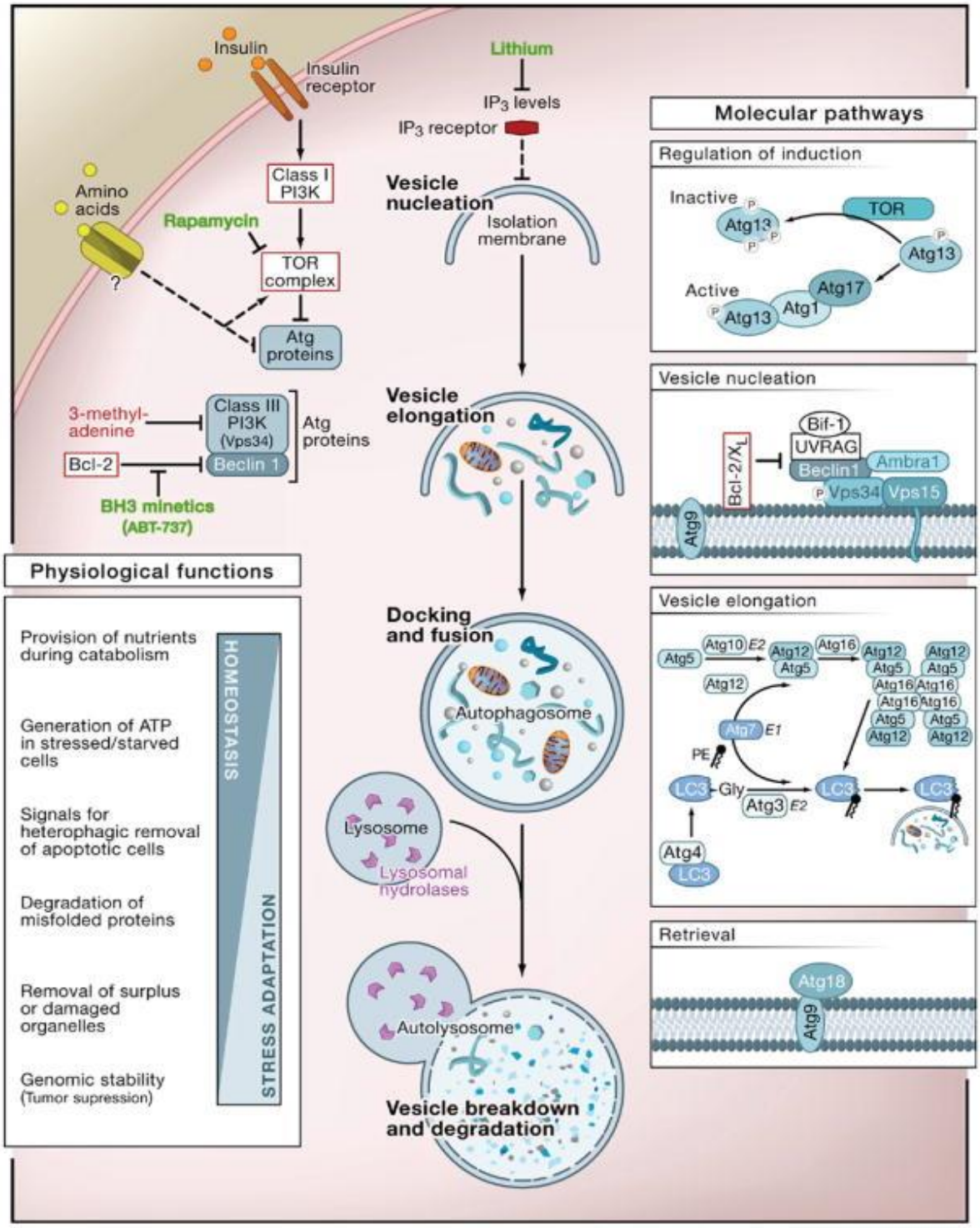

Figure 2

Stages of autophagy. Autophagy is induced upon relief of inhibition by TOR. After induction, an isolation membrane forms and elongates until it forms a complete autophagosome. The autophagosome fuses with the lysosome and its contents are degraded. From Levine, 2008 [3].

starvation [65]. Upon starvation, structures called "omegasomes" are formed on the ER and are proposed as platforms for phagophore formation [65].

Expansion of the phagophore requires two conjugation systems, ATG8 (MAP-LC3) and ATG12 [65] (Figure 2). Both ATG8 and ATG12 are ubiquitin-like proteins, which, although they have no sequence homology to ubiquitin, have similar folds and substrate attachment systems [65]. ATG12 is activated by an E1-like enzyme, transferred to an E2-like enzyme, and finally covalently attached to ATG5. ATG12-ATG5 then associates with ATG16L and oligomerizes to form a large complex [65]. In a similar series of steps, ATG8 becomes covalently attached to phosphatidylethanolamine (PE), with ATG12-ATG5 bound to Atg16L acting as the E3 ligase [65]. ATG12-ATG5 bound to ATG16L seem to have the primary function of conjugating LC3 to PE. Lipidated LC3 is associated with inner and outer autophagosomal membranes. The outer LC3 is not destroyed by maturation of the autophagosome, and is later cleaved off and recycled, so LC3 is a marker of both developing and mature autophagosomes. LC3 is thought to act as a scaffold to support expansion or deformation of the phagophore, as well as an adaptor-coat molecule aiding in cargo selection [65].

Mature autophagosomes can fuse with each other, with endosomes, or with lysosomes [66]. Fusion with the lysosome can either be complete, or can be of the "kiss-and-run" variety, where the autophagosome and the lysosome associate, exchange membrane and content, and disassociate [66]. It is unknown what effect these different types of association have on the degradation of autophagic contents [66].

Degradation of muscle protein involves both the degradation of myofibrillar and non-myofibrillar proteins, which are differentially regulated [67], [68]. Non-lysosomal mechanisms have been implicated in the degradation of myofibrillar proteins, while lysosomal degradation plays a role in the degradation of non-myofibrillar proteins [67], [69]. Although they are

differentially regulated, myofibrillar and non-myofibrillar degradation are often concomitant. For example, *in vitro* studies of denervated rat soleus muscle show that myofibrillar protein is degraded by non-lysosomal mechanisms, but that total protein degradation can be enhanced by combining denervation and conditions that promote lysosomal proteolysis, such as low insulin, low amino acid, or high calcium [69]. In disease states, protein degradation is most likely a combination of myofibrillar and non-myofibrillar degradation, although, historically, myofibrillar degradation has been easier to study *in vivo* through measuring release by the muscle of 3-methyl-histidine (post-translationally modified histidine found in contractile proteins). We have therefore developed *C. elegans* as a model with which to study the degradation of soluble muscle proteins.

1.3 *C. ELEGANS* AS A MODEL TO STUDY MUSCLE PROTEIN DEGRADATION

1.3.1 *C. elegans* muscle structure*

In *C. elegans*, muscle is categorized based on whether it has multiple or single sarcomeres [70]. The muscle with multiple sarcomeres is obliquely striated, with sarcomeres attached to the hypodermis and the cuticle. Body-wall muscle falls into this category. *C. elegans* body-wall muscle is broadly similar in structure and function to human skeletal muscle [71]. There are four

* Information in this section was obtained from the Muscle System chapter of WormAtlas, available at http://www.wormatlas.org/hermaphrodite/muscleintro/MusIntroframeset.html. I have included one citation for each sub-section of the chapter used, although all information in section 1.3.1 was obtained from this source, unless otherwise noted.

quadrants of body-wall muscle, composed of 95, mononucleate cells [72]. Two of the quadrants are dorsal and two are ventral. Each is composed of a double row of muscle cells extending the length of the body and is ensheathed in the basal lamina. Each cell is composed apically of the myofilament lattice and basally of the "muscle belly", which contains the nucleus, cytoplasm, and mitochondria. (Figure 3)

Two myosin proteins are present in *C. elegans* skeletal muscle, MHC A and MHC B. MHC A is encoded by *myo-3* and MHC B is encoded by *unc-54*. Additionally, two other muscle myosins encoded by *myo-2* and *myo-1* are expressed only in the pharyngeal muscle. The myosins in body-wall muscle form homodimers before assembling to form the thick filament. When they assemble, MHC A forms the center of the filament, while MHC B assembles on either end. MHC A is thought to have some role in nucleation of the filament. As in many invertebrates, the thick filament of *C. elegans* also contains paramyosin at its core. Paramyosin has a structure similar to the rod portion of MHC. The actin filament in *C. elegans* is very similar to that of vertebrate skeletal muscle, in that it contains actin, tropomyosin, and troponin. [73]

As in vertebrates, the sarcomeres are composed of interdigitated thick and thin filaments. Thin filaments are anchored to the dense body, the analog of the vertebrate Z-disc, while thick filaments are anchored to an M-line analog. The depth of the myofilament lattice is equal to the length of the dense bodies (approx. 1 μm), which anchor all filaments to the cell membrane, hypodermis, and cuticle. The network of the sarcoplasmic reticulum (SR) surrounds the myofilament lattice, as well as the dense body and the apical plasma membrane. The apical plasma membrane in contact with the SR contains voltage-gated calcium channels, while the SR membrane contains RyRs. (Figure 3)

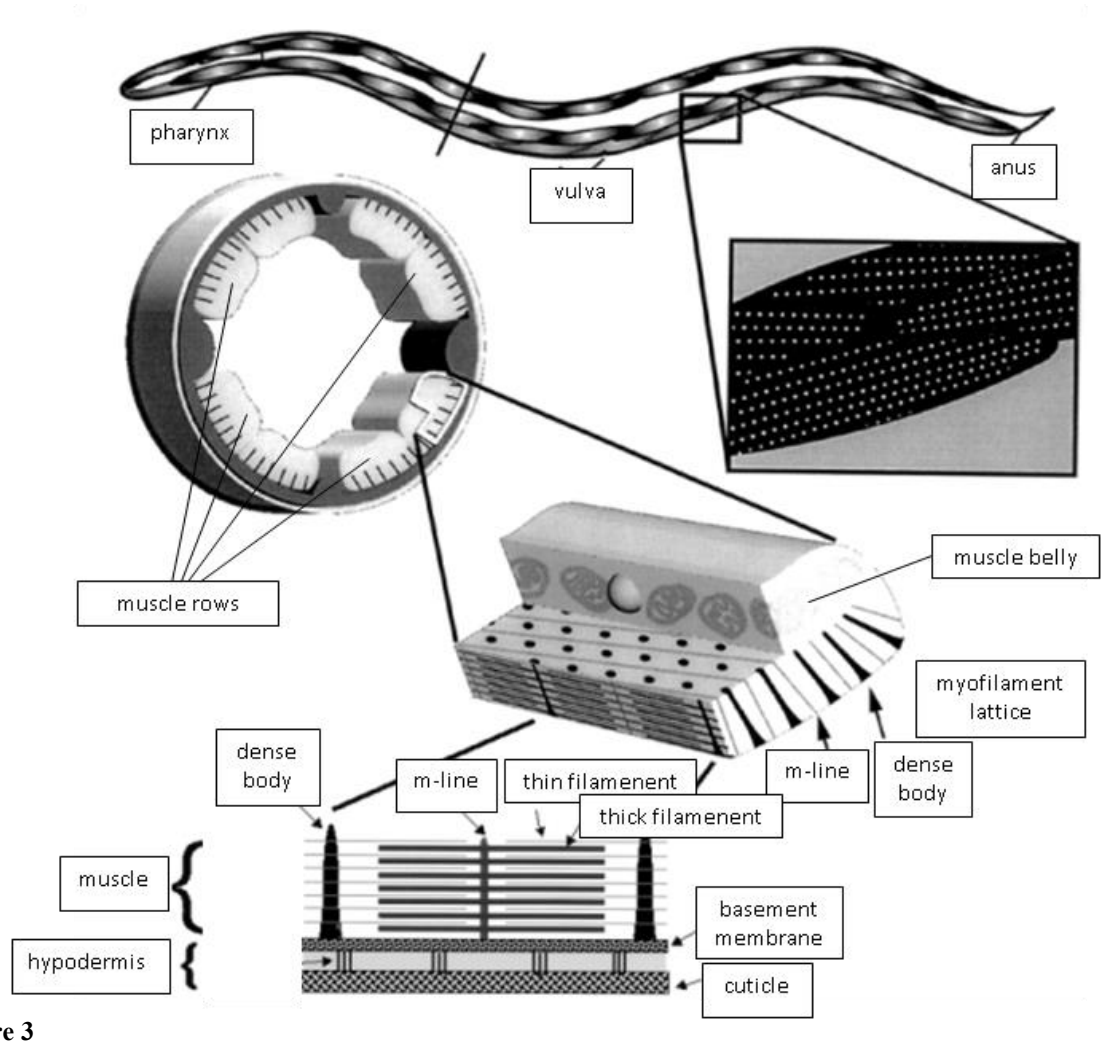

Figure 3

C. elegans muscle structure. The myofilament lattice is composed of sarcomeres and anchored to the cuticle. The myofilament lattice extends into the muscle belly of the muscle cell, which contains the mitochondria and nucleus. Muscle cells are arranged in longitudinal rows to form the four muscle quadrants. Adapted from Hobert, 1999 [1].

Since the SR directly apposes the plasma membrane with only a 12-14 nm gap, no T-tubule system for coupling of excitation and contraction is required, especially since calcium release from the SR through the RyR aids in motility, but is not required. *C. elegans* muscle also does not contain voltage-activated sodium channels. Action potentials are instead generated by influx of calcium through voltage-gated calcium channels (L-type). It is the influx of calcium though these channels that triggers contraction.

The body muscles are innervated by motor neurons arising from the dorsal or ventral nerve cord, which contain cholinergic, stimulatory motor neurons and GABAergic, inhibitory motor neurons. The neck muscles are innervated by the ventral nerve cord and the nerve ring motor neurons. Head muscles are innervated only by the nerve ring motor neurons. Due to this pattern of innervation, the body muscles are only capable of making dorsoventral bends, whereas the head and neck muscles can also make lateral movements.

The neuromuscular junction in *C. elegans* also has its differences from those of vertebrate muscle. In *C. elegans* the muscle sends out arms to meet the motor neuron, housed in the nerve cord. Even at the neuromuscular junction, the muscle cell remains separated from the nerve cord by the basal lamina. Each muscle cell sends out multiple arms to the nerve cord, and each arm varies in size and shape. Gap junctions often occur between the muscle arms of different muscle cells, coupling them electrically.

Because of the many similarities between *C. elegans* body-wall muscle and the skeletal muscle of humans, as well as the numerous advantages of working with *C. elegans*, we have developed *C. elegans* as a model for studying muscle protein degradation. I will discuss the tools we have designed toward this goal in the following section.

1.3.2 Tools for studying muscle in *C. elegans*

By using the expression of muscle-specific reporter proteins in *C. elegans*, we are able to analyze muscle protein degradation in a genetically tractable organism that is amenable to RNAi and drug treatments. In this study I will make use of three different reporter constructs and several different RNAi and drug treatments, as described below.

Reporter Constructs

The first of the three constructs is a chimeric protein consisting of the N-terminal 298 amino acids of MHC (UNC-54) fused to B-galactosidase from *Escherichia coli*. This chimeric protein is encoded by a transgene expressed from the muscle-specific MHC promoter and integrated on chromosome V [74]. Expression of the transgene is confined to the 95 body-wall muscles and eight vulval muscles [74]. Muscle in which the transgene is expressed accumulate the fusion product from embryogenesis through adulthood [74]. This myosin::lacZ fusion is tetrameric, soluble, and stable over at least 2.5 days [74]. When its degradation is induced, its degradation corresponds with its inactivation [74] and occurs at the same rate as native muscle proteins [75]. Therefore, we can use the activity of B-galactosidase in muscle to assay the extent and location of protein degradation in body-wall muscle of individual worms. The second construct is under control of the myo-3 promoter and expresses soluble GFP in body-wall muscle. Both of these reporters are degraded under conditions of starvation [74], denervation [71], excessive FGFR signaling [76], and deficient signaling through the IGFR [77]. Interestingly, the opposed FGFR and IGFR pathways interact directly at the level of the Raf-MEK-MAPK cascade, with FGFR signal promoting activating phosphorylation of Raf and IGFR signal resulting in

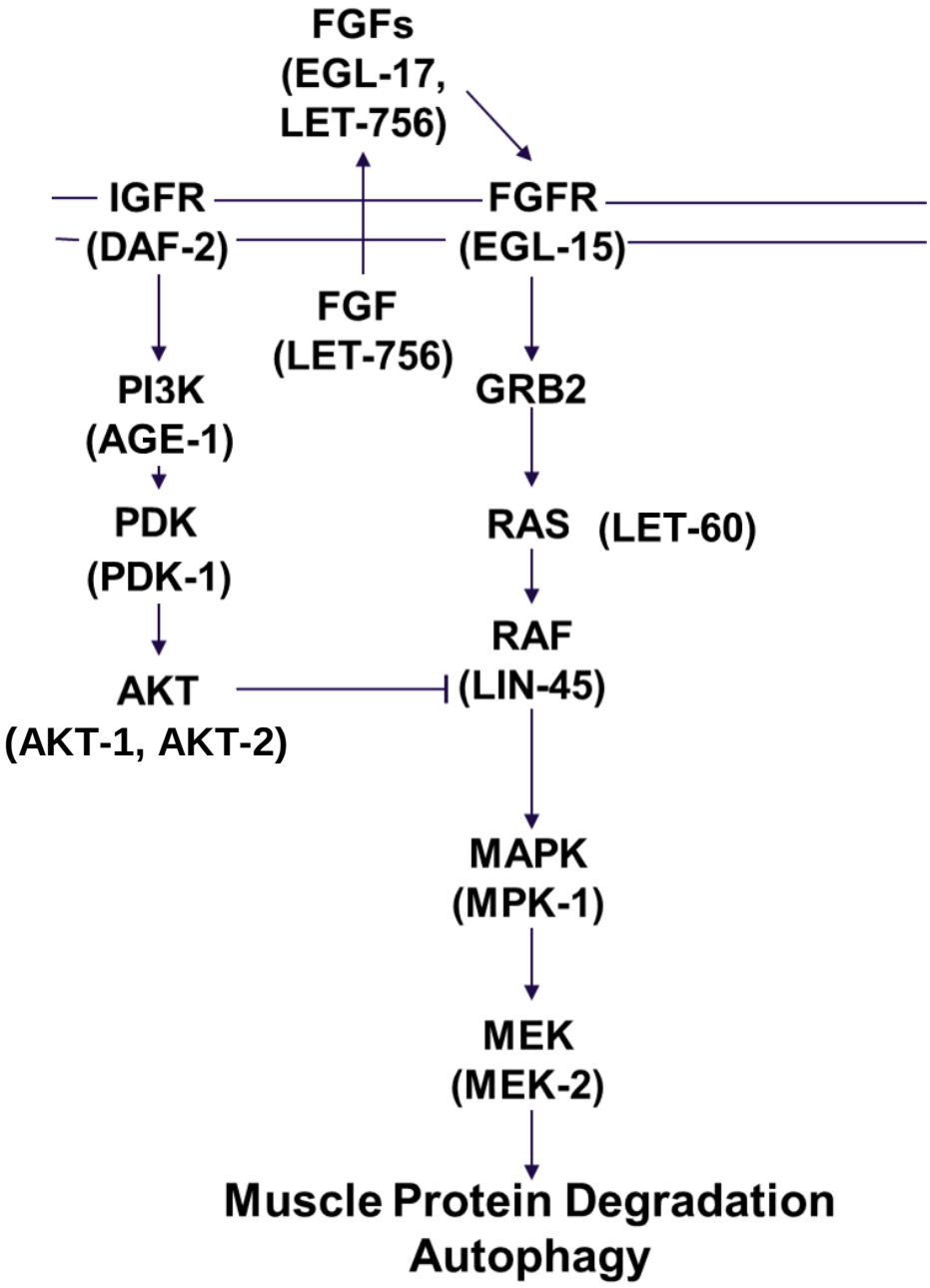

Figure 4

Signaling network regulating muscle protein degradation in *C. elegans*. FGFR signaling promotes muscle protein degradation through activation of the Raf-MEK-MAPK cascade. IGFR signaling inhibits degradation through inhibition of the Raf-MEK-MAPK cascade. In parentheses is the *C. elegans* nomenclature for the mammalian protein names.

inhibitory phosphorylation of Raf via Akt (Figure 4**)** [77]. FGFR and IGFR signaling and their integration at RAF will be reviewed in sections 1.3.3 and 1.3.4.

Here, by applying the third construct, GFP-tagged LGG-1, I demonstrate that this signaling network regulates protein degradation through autophagy. This construct takes advantage of the evolutionary conservation of the autophagic pathway through yeast, worms, and humans [59]. LGG-1 is the worm ortholog of yeast Atg8/Aut7p and mammalian MAP-LC3. LGG-1 localizes to pre-autophagosomal and autophagosomal membranes [78], as discussed in section 1.2.2, as well as the SR and the hypodermis.

RNAi

In *C. elegans*, introduction of dsRNA with the same sequence as a target endogenous gene results in interference with the function of that endogenous gene [79]. When dsRNA enters the cells, it is cleaved by Dicer into fragments of approximately 22 nucleotides in length [80]. These fragments associate with the RISC complex and one of the strands of the dsRNA is degraded [80]. The remaining strand and RISC then bind to the complementary mRNA produced from the target gene, resulting in cleavage of the mRNA and prevention of translation [80]. This process is termed RNA interference (RNAi) and often phenocopies a strong loss-of-function mutation of the target gene [80].

dsRNA can be introduced to *C. elegans* in multiple ways: by injection, soaking, or feeding [81]. RNAi by soaking and injection produce less variable results, but are more labor intensive [81]. For this study, I have used feeding of the worms with bacteria producing the dsRNA as my method. RNAi by feeding is most effective in adults and against non-neuronal targets [82]. After ingestion, the dsRNA is taken up from the environment into the intestinal lumen through SID-1, a

transmembrane protein [83]. The silencing signal is amplified and spreads throughout the organism [83]. Amplification occurs through the action of RNA-dependent RNA polymerases, which generate 5' triphosphate antisense RNAs [83]. Spreading of the signal is thought to occur in a SID-1 independent manner and the silencing signal is thought to be a longer dsRNA [83]. In *C. elegans*, the RNAi signal is also persistent. It persists both in the animal exposed to the dsRNA and through multiple generations, albeit with reduced penetrance [83].

Drug Treatment

Drug treatment of *C. elegans* is used for drug screening and for basic biological research. Methods of applying drugs to *C. elegans* vary. They include adding drugs to live or dead bacterial cultures that will be used for feeding and spotting of drugs directly on plates that are spread with live or dead bacteria [84]. Dead bacteria are sometimes used to eliminate the possibility the bacteria will degrade the drug and effectively reduce the concentration. One study [84] that tested the absorption of a water-soluble and a minimally water-soluble drug found that both drugs reached considerable concentrations in the worms regardless of whether the drugs were added to the bacterial culture or spotted on the plate. Addition of the drug to the bacterial culture was slightly more effective, however, the small increase in effectiveness may not balance the expense of this method requiring the use of more total compound. Both the water-soluble and minimally water-soluble compound reached maximum concentration in the worms between 12 and 24 hours. For my studies, I use the cost-effective strategy of spotting drugs directly on plates spread with live bacteria.

Two drugs used in my work are LY29004 and N6,N6-dimethyladenosine (DMA). LY29004 is a PI3K inhibitor. There are three classes of PI3K, all of which are inhibited by LY29004, a synthetic compound based on the flavonoid quercetin [85]. LY29004 binds the ATP-binding site of PI3K with an IC_{50} of 1.4 μM and a K_d of 0.21 μM [85]. Although this K_d is similar to that of less specific protein kinase inhibitors for PI3K, LY29004 is specific for PI3Ks, and at a concentration of 50uM has no inhibitory effect *in vitro* on other protein kinases that have been tested [85].

DMA is an adenosine analog that has been shown to inhibit autophagic vesicle formation, possibly through the inhibition of a PI3K (see section 1.2.2 for the role of PI3K in autophagic vesicle formation) [86]. Inhibition of autophagy by adenosine analogs is rationalized as a negative feedback mechanism for the degradation of ribosomes and ribosomal RNAs by autophagy [86].

1.3.3 FGFR signaling

Fibroblast growth factor receptors (FGFRs) are members of the receptor tyrosine kinase family [87]. In mammals, there are four FGFRs (1-4), each consisting of an extracellular, ligand-binding domain, a transmembrane helix domain, and a cytoplasmic, tyrosine kinase domain [88]. Combinatorial alternative-splicing yields FGFR that can vary structurally in each of the three domains [89]. The different FGFRs and their splice forms have varying affinities for, and responsiveness to, the more than 20 different FGFs [89]. Upon binding of FGF, activation of the FGFR kinase domain requires dimerization and *trans*-phosphorylation, which is promoted by association with heparan sulfate proteoglycans in a 2:2:2 or 2:2:1 FGF:FGFR:heparin ratio [89, 90] or with the co-receptor Klotho [91]. Different splice forms of the FGFR can heterodimerize,

altering the activity of the complex [89]. This, in combination with the varying tissue-specific expression patterns, ligand affinities, and responsiveness of each receptor, allows one signaling system to control many distinct cellular and developmental processes [89].

The 24 identified FGFs in mammals [92] can have either endocrine or paracrine function [91]. Paracrine FGFs function in patterning during development and in homeostatic processes in adult organisms [91]. Paracrine FGFs are characterized as having a high affinity for cell-surface heparan sulfate proteoglycans and sharing a β-trefoil structure, consisting of 12 anti-parallel β-strands, and variable-length N- and C-terminal tails [92]. Regions of the trefoil bind to heparin [92], while other regions of the trefoil bind the FGFR [87]. Binding of heparan sulfate proteoglycans is required for high-affinity binding FGF to the FGFR [92]. The N- and C-terminal tails provide ligand-receptor specificity [92]. Upon secretion, paracrine FGFs bind cell-surface heparan sulfate proteoglycans, limiting their diffusion, protecting them from proteolysis, and promoting efficient signal transduction [87]. Due to these characteristics, during development paracrine FGFs are often found to pattern the tissue immediately surrounding their source [87].

Endocrine FGFs have a low affinity for heparan and FGFR, and therefore are free to diffuse away from their source, enter the circulation, and induce signaling in other tissues [91]. Endocrine FGFs are often involved in metabolic processes, such as glucose and lipid metabolism, and depend on Klotho co-receptors to activate their FGFRs [91]. Klotho co-receptors are expressed in targets of endocrine FGFs and increase the affinity of the FGFR for endocrine FGFs, while simultaneously decreasing the affinity of FGFR for paracrine FGFs [91]. This safe-guards against off-target signaling and prevents interference by paracrine FGFs [91]

C. elegans has two FGF homologues, EGL-17 and LET-756, and one FGFR, EGL-15 [93]. EGL-15 is structurally similar to vertebrate FGFR [87] and comparative modeling studies suggests

a conserved binding surface for heparin on the *C. elegans* FGF-FGFR complex [93]. Additionally, two redundant homologues of the Klotho co-receptor also are present in *C. elegans* and have been shown to play a role in EGL-17/EGL-15 signaling [94]. However, EGL-17 is not homologous to mammalian endocrine FGFs. In fact, both EGL-17 and LET-756 are homologous to mammalian paracrine FGFs, albeit to FGFs in different subfamilies (FGF8 and FGF9 subfamilies, respectively) [95]. This suggests that the details of paracrine and endocrine FGF signaling as described in mammals cannot be mapped directly onto FGF signaling in *C. elegans*.

The two *C. elegans* FGF ligands signal non-redundantly through distinct splice forms of the FGFR. EGL-17 is secreted by the developing vulva and mutation of EGL-17 leads to abnormal sex myoblast migration and an egg-laying defect [96]. LET-756 is expressed by the body-wall muscle and various neurons [96]. Total loss-of-function mutation in LET-756 is lethal, while reduction-of-function mutation causes a scrawny phenotype [96]. It is thought the LET-756 signal from muscle binds hypodermal EGL-15 and regulates fluid balance [96]. EGL-17 and LET-756 both have roles in axon growth and positioning, but of a non-overlapping subset of neurons [96].

Fibroblast growth factor signaling has been linked to exercise-induced muscle remodeling in rats, with exercise inducing increased FGF expression [97] and degradation of soluble and myofibrillar proteins in skeletal muscle [98]. These non-developmental roles for FGF signaling are interesting, since it was initially thought that FGFRs were not expressed in adult mammalian skeletal muscle. Thinking has since changed [76].

In *C.* elegans, activation of the FGFR by temperature-sensitive (ts) inactivation of its phosphatase, CLR-1, promotes degradation of the *unc-54::lacZ* reporter. This effect does not depend on new protein synthesis, since treatment with cycloheximide six hours prior to temperature shift does not prevent degradation. While reduction-of-function (rf) in the kinase

domain of the FGFR does suppress the protein degradation phenotype of *clr-1* mutants, rf mutation of either of the two FGF ligands present in *C. elegans* is not sufficient to suppress protein degradation, since in this case the two ligands are redundant. As expected then, at least one of the FGF ligands is necessary for the protein degradation caused by rf mutation of *clr-1*. [76]

Ras (LET-60) GTPase is known to have a role in muscle wasting and a ts Ras gain-of-function (gf), mutation promotes reporter degradation at the non-permissive temperature and has a clear (Clr) phenotype [76]. Likewise, rf mutation in the gene for the Ras GTPase-activating protein GAP-1 also promotes degradation of the reporter protein. [99]

In order to determine if activated Ras causes protein degradation through changes in *de novo* gene expression, ts Ras gf mutants were treated with cycloheximide to prevent translation. Treatment with cycloheximide did not block Ras-induced protein degradation, even when the cycloheximide treatment proceeded the temperature shift by six hours. This shows that the degradation induced by Ras does not require the synthesis of new protein and therefore is unlikely to be due to gene expression changes induced by Ras activation. [99]

The effect of Ras on muscle protein degradation was shown to be physiological, rather than developmental. Animals raised for part of their development at the non-permissive temperature and then shifted to the permissive temperature retain LacZ staining in adulthood, while animals raised at the permissive temperature and then shifted to the non-permissive temperature as adults degraded protein. This distinction between development and acute effects of protein activation will become important in the work I will discuss in the Results and Discussion. [99]

These data are consistent with the idea that the FGFR is signaling through Ras to promote muscle protein degradation. Treatment of ts Ras rf mutants with Ras inhibitor suppresses protein

degradation seen in *clr-1* ts mutants. Further experiments show that the FGFR signals to Ras through the *C. elegans* GRB2 and SOS1 homologs.

Since Raf, MEK, and MAPK (*C. elegans* LIN-45, MEK-2, and MPK-1, respectively) had been shown to be downstream of Ras in the development of the hypodermis in *C. elegans* and the Clr phenotype is due to defective FGF signaling in the hypodermis, Szewczyk et al. sought to identify if Raf, MEK, and MAPK are also downstream of Ras in signaling for muscle protein degradation. To do so, ts Ras gf mutation was combined with an additional rf mutation in Raf, MEK, or MAPK. Muscle protein degradation was prevented in each of the double mutants, showing that Raf, MEK, and MAPK act downstream of Ras [99]. Likewise, ts *clr-1* rf mutants with a second rf mutation in the gene coding for any member of the Raf-MEK-MAPK cascade show suppression of protein degradation at the non-permissive temperature, while Raf or MAPK activation is sufficient to induce degradation [77].

It should be noted that the outcome of this pathway is promotion of muscle protein degradation. Since one of the FGF ligands is autocrine, it would seem as if the cell is constantly telling itself to degrade protein. Indeed, this would be the case, if it weren't for an additional, inhibitory input to the pathway, which I will discuss in the next section.

1.3.4 IGFR signaling and Raf as a signaling integrator

In mammalian muscle, insulin signaling has a well-known role in promoting protein accumulation and preventing its degradation. Absence of insulin, as seen in Type I diabetics, causes increased skeletal muscle protein degradation and leads to muscle wasting [36]. Most well-controlled studies show that insulin inhibits protein breakdown, but has little effect on protein

synthesis [36]. Likewise, systemic administration of insulin-like growth factor (IGF) inhibits whole body protein breakdown, but has no effect on whole body protein synthesis [36]. Insulin signaling and IGF signaling have both been shown to target skeletal muscle, although their downstream effects are not identical. IGF signaling is associated with growth, differentiation, and hypertrophy, while insulin signaling is involved with metabolic processes [100]. Insulin is produced by pancreatic beta cells, while IGF-1 is produced by many different cell types [101]. Most of the circulating IGF-1 is produced by hepatocytes [101].

Despite these differences, IGFs are structurally similar to insulin. Human IGF-1 is composed of an alpha and beta chain linked by a disulfide bond, much like insulin [102]. The IGF-1 receptor and the insulin receptor are also structurally similar. Both are disulfide linked homodimers, and IGF-1 receptor/insulin receptor heterodimers can form [103]. Both the IGF-1 receptor and the insulin receptor can bind both IGF-1 and insulin, although with different affinities [103]. Binding of the ligand to the receptor results in formation of the tetrameric receptor, tyrosine phosphorylation, and activation of downstream pathways [100]. Additionally, IGF-1 receptors and insulin receptors require heterotrimerization with G-proteins for some of their biological effects [100]. The partially non-overlapping effects of IGF-1 and insulin signaling are thought to be caused by the different affinities with which they bind each receptor [100].

In *C. elegans*, there is an insulin-like signaling pathway that has been shown to have a role in regulating proteolysis in muscle. *C. elegans* has 38 insulin-like genes expressed throughout the body [101], but only has one receptor homologous to human insulin/insulin-like growth factor receptor (IGFR), *daf-2* [104]. Insulin signaling might be paracrine, autocrine, and/or endocrine in *C. elegans* [101]. Temperature-sensitive, rf mutation in *daf-2* (IGFR) promotes muscle protein degradation at the non-permissive temperature. This effect is seen in adult worms after

temperature shift, is not suppressed by cycloheximide treatment, and can be suppressed by muscle-specific expression of wt *daf-2*. [77]

AGE-1 (PI3K), PDK-1, and AKT-1 or AKT-2 are the proteins canonically found downstream of IGFR. Rf mutation in *age-1* or treatment with a PI3K inhibitor phenocopies the *daf-2* rf mutation. PI3K produces PIP3, stimulating activity of PDK and AKT. Gain-of-function mutation in PDK-1 or AKT-1 suppresses degradation caused by *daf-2* ts mutation. [77]

IGFR signaling negatively regulates activation of the Raf-MEK-MAPK cascade. Reduction-of-function mutation in Raf, MEK, or MAPK are each sufficient to block degradation in *daf-2* ts mutants or LY29004-treated animals. On the other hand, rf mutation in pathway members upstream of Raf does not. This suggests that Raf may be the direct target of Akt. Mutation of a putative Akt phosphorylation site on Raf, S259 (mammalian numbering throughout), to alanine promotes muscle protein degradation [77]. In mammalian systems, phosphorylation of S259 inhibits Raf activity and inhibition of the phosphatases responsible for de-phosphorylation of S259 results in Raf that cannot be activated [105]. Raf activation requires phosphorylation of T491 and S494 [106], which may occur via trans-autophosphorylation after recruitment to the plasma membrane and oligomerization [107]. The propensity of any Raf molecule to become active is modulated by the phosphorylation state of its other regulatory sites, including S259 [105, 108-111]. Therefore, signals from multiple sources result in Raf molecules with different phosphorylation profiles and which have different levels of activity. This allows Raf to integrate signals from multiple inputs and provide the appropriate output.

1.4 CALCIUM SIGNALING IN MUSCLE

In chapter 2.0, I will propose an additional positive input to the FGF/IGFR network I have described—specifically, from calcium signaling, through CaMKII. High intracellular calcium is seen under conditions that cause atrophy, such as sepsis, burn injury, and muscular dystrophy [43, 112]. Treatment with calcium ionophore increases muscle protein degradation, while treatment with calcium antagonists can inhibit it [43]. CaMKII acts as a calcium sensor and decodes calcium frequency-dependent information. CaMKII itself is up-regulated during atrophy [113]. In this section, I will consider the known role of calcium in promoting muscle atrophy, the mechanisms by which calcium enters the cell, and the cellular behaviors stimulated by calcium influx.

1.4.1 Calcium and muscle wasting

The breakdown of muscle protein seen with trauma, burn, and sepsis can be beneficial. Amino acids released from the muscle are used by the liver for gluconeogenesis and the production of acute phase proteins [43]. Acute phase proteins are the liver's response to post-injury inflammatory signals, and include proteins involved in fighting microbes, giving negative feedback to the inflammatory response, and promoting coagulation. Glutamine, specifically, is used by cells in the immune system and can protect the intestinal mucosa in the critically ill [43]. However, extensive muscle wasting is associated with poor clinical outcomes [43].

Levels of calcium in skeletal muscle have been shown to be increased in various conditions that result in muscle wasting [43]. This alteration of calcium homeostasis can lead to, or exacerbate, tissue dysfunction caused by acute injury, such as trauma, burn, and sepsis [114].

Dysfunction can be caused by impairment of functions in resting cells or in cellular behaviors requiring calcium, such as contraction, secretion, signaling, etc. [114]. In the resting state, the concentration of calcium inside the cell is 40-100 nmol/L [114]. This is 10000 times less than the concentration of calcium outside the cell [114]. This gradient is maintained by constant extrusion of calcium from the cell into the extracellular space [114]. When stimulated, the calcium concentration in the cell can rise to 150-1,000 nmol/L [114]. This increase is caused by influx of calcium through voltage-gated or ligand-gated calcium channels and/or release of calcium from ER stores.

Cytosolic calcium levels in septic muscle have been shown to be twice as high as normal [115, 116]. This increase in intracellular calcium promotes loss of muscle mass through activation of calcium sensitive proteases (calpains) and caspases (discussed in section 1.4.3), glucose-uptake insulin resistance [114], increased proteasome activity, apoptosis, and transcriptional changes [43].

It is thought that high intracellular calcium can be caused by glucocorticoid signaling. Inhibitors of glucocorticoid receptors can block muscle wasting with sepsis and treatment with glucocorticoids can increase muscle protein breakdown [43]. Glucocorticoid treatment increases cytoplasmic calcium levels and calcium chelator can block the protein-degradative effects of synthetic glucocorticoid treatment [43]. While it is unknown exactly how glucocorticoid signaling increases cytosolic calcium levels, there is evidence that the calcium is not from extracellular sources, suggesting that increased calcium release from the SR may play a role [43].

1.4.2 Calcium channels in muscle

Most calcium enters the muscle cell from the extracellular space through a voltage-gated calcium channel [117]. Historically, calcium channels have been classified by the voltage at which they open [118, 119]. There is one type of low-voltage calcium channel, T-type, while there are four types of high-voltage calcium channels (L-, N-, P/Q, and R) [119]. *C. elegans* has three multi-subunit, voltage-gated calcium channels. Each channel is defined by the gene coding the alpha subunit. *C. elegans* has the L-type channel, encoded by *egl-19*, the P/Q type channel, encoded by *unc-2*, and the T-type channel, encoded by *cca-1* [117]. Although the P/Q type channel may also be expressed in body-wall muscle [120], the L-type calcium channel is considered the main voltage-gated calcium channel in body-wall muscle. The L-type channel is also the most relevant channel in vertebrate muscle, so I will restrict my discussion to this channel type.

The L-type calcium channel is a heteropentamer of α_1 (EGL-19), α_2, β, γ, and δ subunits [119]. The α_1 subunit is composed of four transmembrane domains, each composed of six alpha helices, similar to the structure of sodium channels [119]. It is believed that the α_1 subunit is responsible for voltage sensing [119]. The α_1 subunit is sufficient for permeation to calcium ions; however, the remaining subunits have important modulatory effects [119].

In fact, behavior of the calcium channel is not only modulated by the additional subunits, but also by diverse signaling events. Calmodulin, a calcium effector discussed in the following section, has been shown to bind and negatively modulate the L-type calcium channel, providing a feedback mechanism. Phosphorylation of the α_1 subunit by various signaling pathways has been shown to affect the calcium current. The β subunit (CCB-1 in worms), which has been implicated in both trafficking and altering the biophysical properties of the alpha subunit, can be modulated

by phosphorylation by PKA, CaMKII, and Akt. Interestingly, it has been shown in zebrafish that a specific β subunit, β1a, is required in muscle for tetrad formation with the RyR and normal movement. [121]

1.4.3 Calcium effectors

Calmodulin

Calmodulin is a relatively small protein of only about 150 amino acids with two N-terminal EF hands and two C-terminal EF hands linked by a flexible alpha helix [122]. Each EF hand is capable of binding one calcium ion [122]. The EF hands at each end have cooperative binding, such that both calcium sites are likely to be occupied [123]. The N- and C-terminal domains are not mirrors of each other; each has its own ion affinities and kinetics [123]. At resting membrane potential, when calcium concentration is low, a large fraction of calmodulin molecules have two calcium ions bound [123]. Since most of calcium-calmodulin's downstream substrates require all of calmodulin's sites to be occupied in order to bind, this form of calmodulin is inactive [123]. When the membrane is depolarized and calcium levels rise, all four sites bind calcium and calmodulin becomes active [122]. Activated calcium-calmodulin can interact with its several hundred target proteins [123]. Modeling of the dynamics of calmodulin activation suggest that these dynamics alone are sufficient for calmodulin to decode calcium spike timing for the activation specific targets [123].

Calpains and Caspases

There are many different calpains, some of which are ubiquitous and others of which have tissue-specific expression [43]. Calpains are often heterodimers, with one subunit containing the catalytic domain and the other having regulatory functions [124]. Calcium-activated calpain is inhibited by two negative feedback mechanisms: 1) binding of an inhibitor, calpastatin, and 2) autolysis [43]. There is also some positive feedback, in that activated calpain is capable of degrading its inhibitor, calpastatin [124]. *C. elegans* has genes encoding multiple calpains, although it lacks the calpain inhibitor, calpastatin [125]

Calpains have been implicated in causing some of the protein degradation seen in sepsis and other muscle-wasting conditions [43]. Expression of calpain genes increases with sepsis; calpastatin expression decreases with sepsis; calcium is required for the release of myofilaments [126]. The last of these is an important point, as it has been shown that the proteasome is incapable of degrading intact myofilaments, suggesting that calpains may have a role in releasing myofilaments so that they may be accessed by the proteasome [126] .

Others have suggested a role for caspase-3 in releasing myofilaments [127]. Caspases are cysteine-dependent aspartic-directed zymogens [128] that are categorized as either initiator or executioner caspases [129]. Upon cleavage, initiator caspases cleave executioner caspases, activating them [129]. *C. elegans* has four caspase genes [130]. Insulin resistance, which occurs during sepsis, has been shown to activate caspase-3 [127]. It is not entirely understood if high calcium can also contribute to glucose-uptake insulin resistance, since calcium signaling can be shown to both promote and inhibit production of the glucose transporter, GLUT4; however, insulin resistance has been shown to accelerate muscle protein degradation [131].

The role of calpains and caspases in myofilament release for protein degradation by the proteasome becomes more complicated when one considers the possibility of cross-talk between the two systems. Caspases have been shown to degrade calpastatin, which would promote activation of calpains, while inhibition of calpains by overexpression of calpastatin has been shown to up-regulate caspase-3 activity [132].

1.4.4 Downstream calcium signaling through CaMKII

CaMKII acts as a calcium sensor and decodes calcium frequency-dependent information. CaMKII itself is up-regulated during atrophy [113]. CaMKII, product of the *C. elegans unc-43* gene, is central in the cell's ability to respond to calcium levels. The CaMKII holoenzyme is a dodecamer composed of two face-to-face rings of six monomers. Each CaMKII monomer consists of a kinase domain, a regulatory domain, and an association domain. The association domain binds to the association domains of other monomers to assemble into the dodecameric holoenzyme. The regulatory domain can act in an autoinhibitory fashion, by binding the kinase domain of CaMKII, or can act as the Ca^{2+}/Calmodulin (CaM) binding domain (Figure 5). [133]

Due to these characteristics of its structure, activation of CaMKII can either be Ca^{2+}/CaM dependent or Ca^{2+}/CaM independent [6]. During Ca^{2+}/CaM dependent activation, Ca^{2+}/CaM binds the regulatory domain, releasing autoinhibition of the kinase domain and exposing Thr 286 (human CaMKIIα numbering throughout) [134]. The exposed Thr 286 is then autophosphorylated by a Ca^{2+}/CaM-activated adjacent subunit. Phosphorylation of Thr 286 prevents rebinding of the regulatory domain to the kinase domain [135] and increases the affinity of Ca^{2+}/CaM for CaMKII by 13,000-fold [136]. When Ca^{2+} concentration is high, phosphorylation of Thr 286 will occur

faster than its dephosphorylation, resulting in a holoenzyme that is phosphorylated on all of its Thr 286 residues. When this occurs, CaMKII activation becomes Ca^{2+}/CaM independent, as even release of Ca^{2+}/CaM will not allow for rebinding of the regulatory domain to the kinase domain. However, when Ca^{2+} levels are low, Thr 286 is dephosphorylated faster than activation can spread through the holoenzyme, maintaining the Ca^{2+}/CaM dependence of activation. I will discuss further details of CaMKII activation as they become relevant in the Results and Discussion.

Figure 5

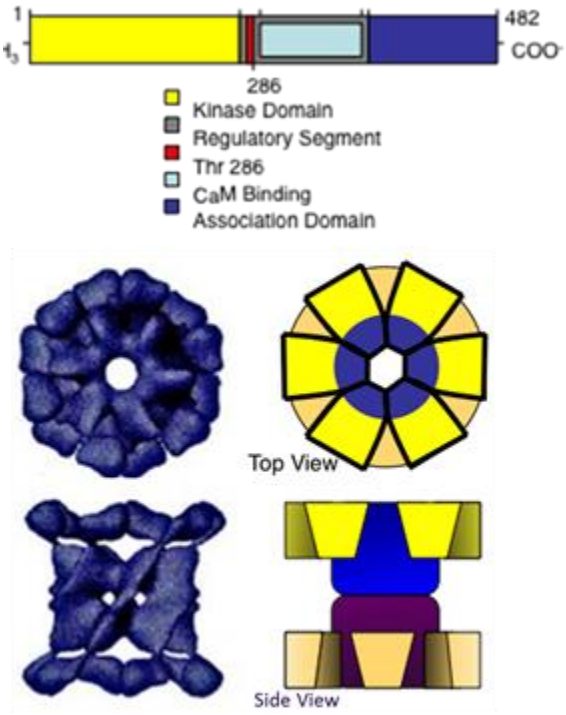

Structure of CaMKII and its activation. CaMKII monomers have a kinase domain (yellow/tan), regulatory segment (grey), and association domain (blue). Monomers assemble into two face-to-face rings of six, resulting in a dodecameric, spindle-like structure. With a short calcium signal, calcium dependent activation of CaMKII is maintained, while with a long calcium signal, calcium-independent activation results. Neighboring subunits phosphorylate each other, preventing re-binding of the autoinhibitory domain, contained in the regulatory segment. Only a phosphatase, FEM-2, can remove the phosphate group and restore calcium dependency. Adapted from Hudmon, 2002 [4] and Lisman, 2002 [6].

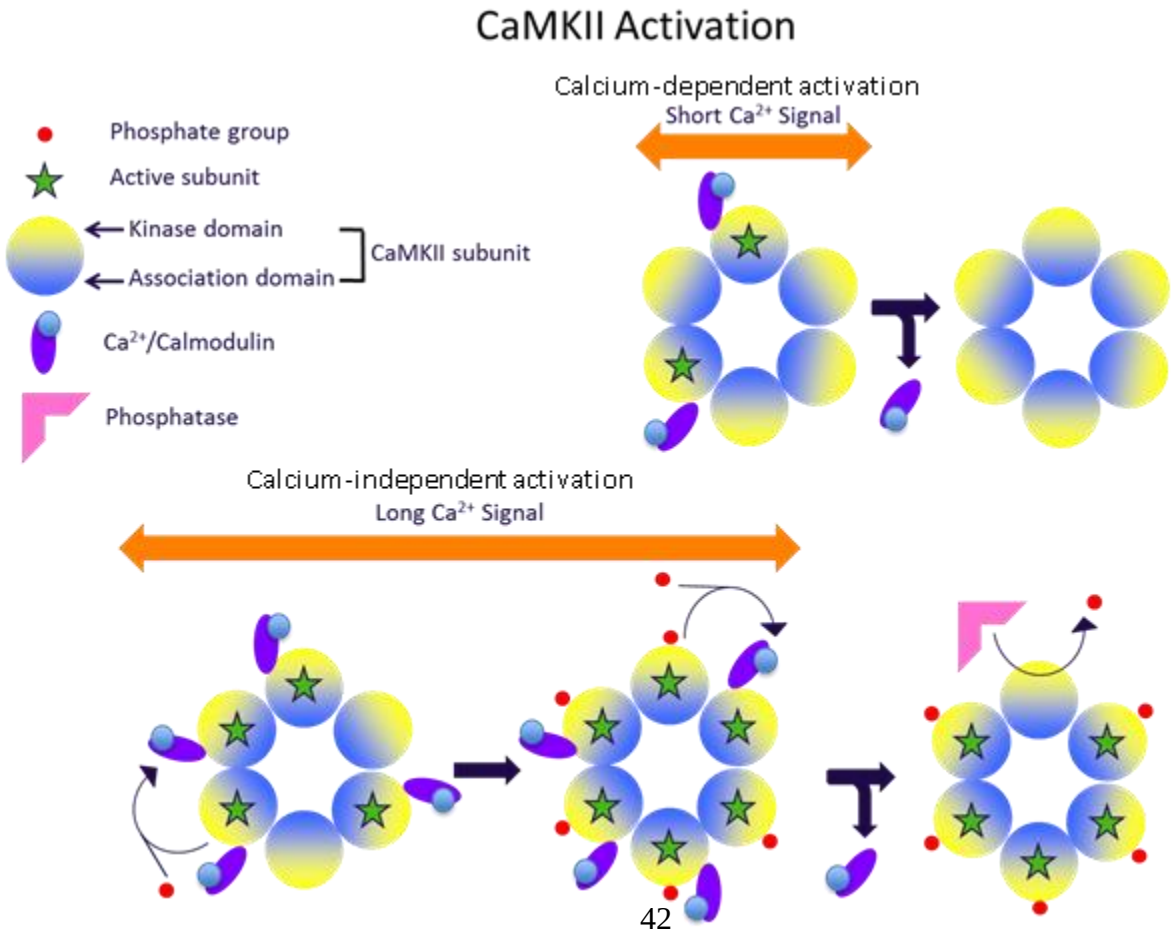

2.0 RESULTS AND DISCUSSION

Here I propose an additional input to the FGF/IGFR network—specifically, calcium signaling through CaMKII (UNC-43). Employing a CaMKII gain-of-function (gf) mutant and a FEM-2 temperature-sensitive (ts), reduction-of-function (rf) mutant, I show that hyperactive CaMKII promotes protein degradation in *C. elegans* body-wall muscle through activation of the Raf-MEK-MAPK cascade. I also propose an *in vivo* role for FEM-2 in *C. elegans* body-wall muscle in de-activating CaMKII. I show that the FGF/IGFR/CaMKII signaling network described herein regulates protein degradation via autophagy. Having detailed the network, questions about the behavior of the network as a whole can be addressed. One such question I address is whether increases or decreases in signaling from one source can be balanced by increases or decreases in signaling from another. This is a particularly interesting question in the network described here, where one protein, Raf, is responsible for integrating signals from multiple sources.

2.1 CAMKII GF MUTATION RESULTS IN PROGRESSIVE MUSCLE PROTEIN DEGRADATION

The CaMKII gf protein (CaMKII*) has an E108K substitution resulting from a missense mutation (allele n498) in the *unc-43* gene [137]. This mutation likely prevents docking of the autoinhibitory domain on the kinase domain [138], causing constitutive activity independent of Ca^{2+}/calmodulin (Figure 5). *unc-43* gf mutants do synthesize LacZ reporter protein in muscle during larval growth (Figure 6a), although delayed relative to wild type (*wt*). However, the LacZ

protein that they do accumulate is lost shortly after entry to adulthood (Figure 6a). This protein degradation is accompanied by the progressive development of uncoordinated movement (Figure 7). As expected for a gf mutation, both the uncoordinated movement and protein degradation phenotypes show partial dominance in *unc*-43gf/+ heterozygotes (data not shown). Additionally, *unc-43* gf worms are egg-retentive and frequently bag (embryos hatch internally). In Figure 8, an internally hatched embryo is visible in the *unc-43* gf worm. Despite these phenotypes, the actin filaments appear intact and appropriately organized, as evidenced by Phalloidin staining (Figure 8).

Fusion of the *unc-43* promoter to *gfp* results in expression of GFP in the neurons, intestines, and body-wall muscle (Figure 9), consistent with the known neuronal [138, 139], intestinal [140], and muscular [138, 141] functions of CaMKII in *C. elegans*. Since knowing the location(s) where CaMKII* activity is required for the phenotypes could provide clues about how CaMKII* is acting to cause the above phenotypes, I wanted to determine this information.

To test if muscular CaMKII* is required for uncoordinated movement and protein degradation, I took advantage of the fact that in *C. elegans* RNAi is ineffective in neurons [82]. Treatment of *unc-43* gf mutants with *unc-43* RNAi suppresses degradation of both LacZ and GFP reporter proteins (Figure 6b), but not the uncoordinated movement phenotype (data not shown) or the egg-laying defect (Figure 6b). This shows that non-neuronal (likely muscular) CaMKII* is required to cause muscle protein degradation in muscle, while neuronal CaMKII* is sufficient to cause uncoordinated movement and the egg-laying defect. From this, I hypothesized that the protein degradation caused by CaMKII* is the result of its signaling intramuscularly, while the uncoordinated movement may originate from problems in neuro-muscular communication.

The *unc-43* gf mutation causes life-long, chronic CaMKII hyper-activation, which is known to cause defects in axonal guidance and morphology [139, 142]. Coordinated movement

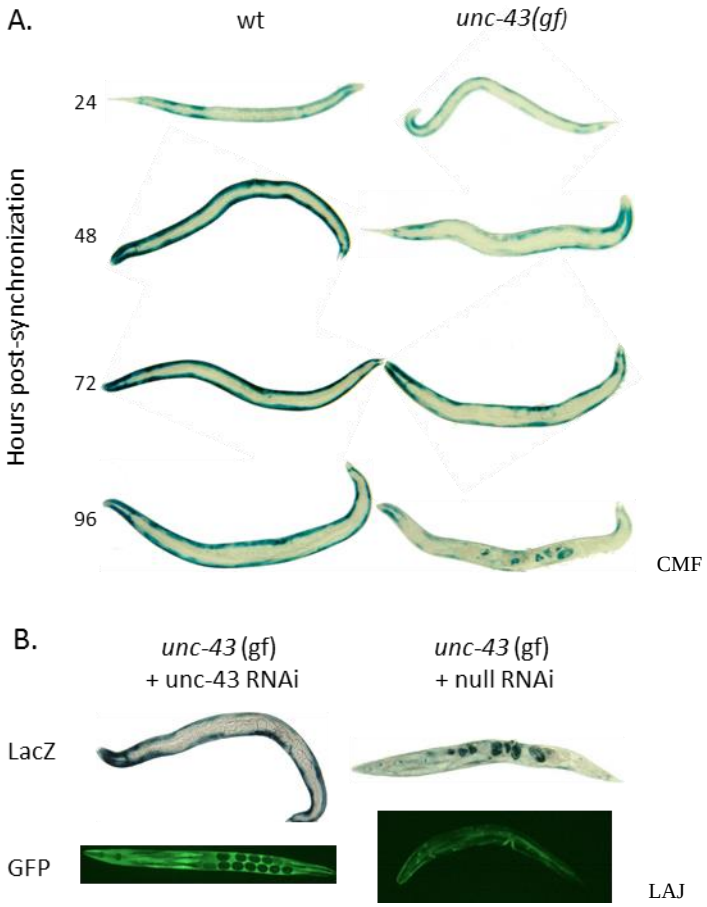

Figure 6
unc-43 gf worms degrade muscle protein, which can be suppressed by treatment with *unc-43* RNAi. a) *unc-43* gf and *wt* worms were synchronized as L1s and raised at 20C. Every 24 hours animals were selected from the population and stained for LacZ. b) L4 *unc-43* gf worms were picked to *unc*-43 or null RNAi plates and raised at 20C. When the F1 reached adulthood, worms were selected for LacZ staining or GFP imaging.

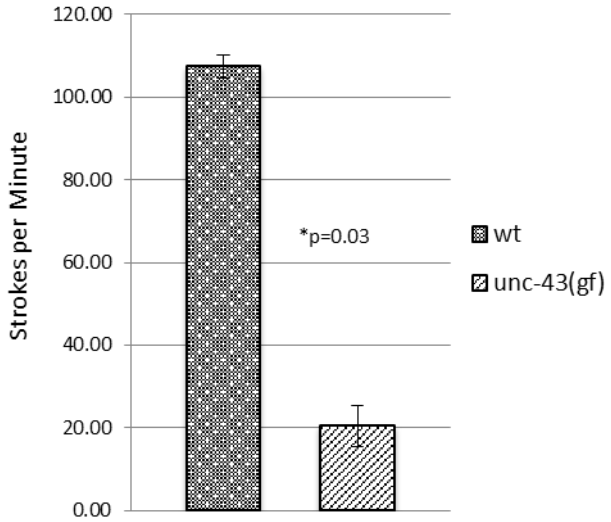

Figure 7

unc-43 gf worms are uncoordinated. Adult *unc-43* gf or *wt* worms were picked into buffer and their swimming rate was measured as strokes per minute. *unc-43* gf worms make fewer strokes per minute then *wt* worms due to their uncoordinated movement. n= 10 replicate measurement on 5 worms of each genotype. The p-value was calculated using the students T-test.

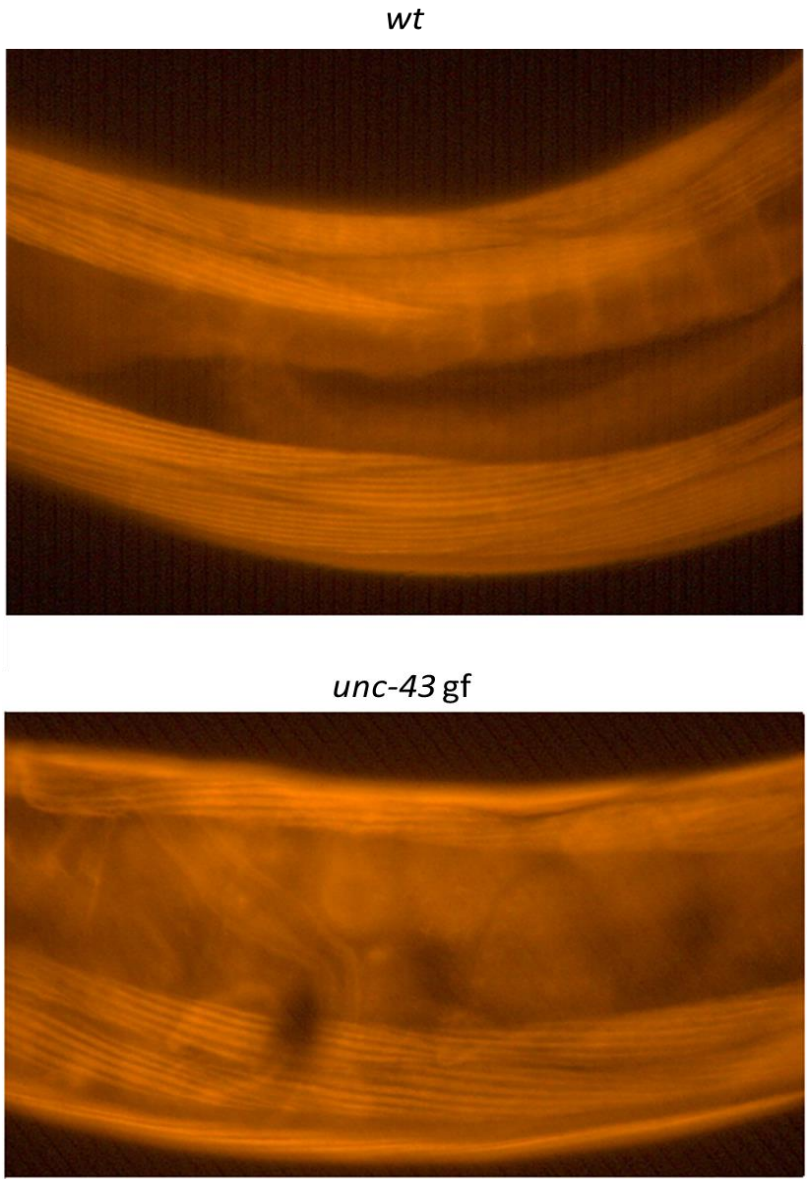

Figure 8
Actin filaments of *unc*-43 gf worms do not appear disorganized. Both *wt* and *unc-43* gf worms were grown at 20C until adulthood, at which point individuals were selected for RITC-labeled Phalloidin staining of actin filaments. After staining overnight, images were collected via fluorescence microscopy. Note the internally hatched embryo in the *unc-43* gf worm.

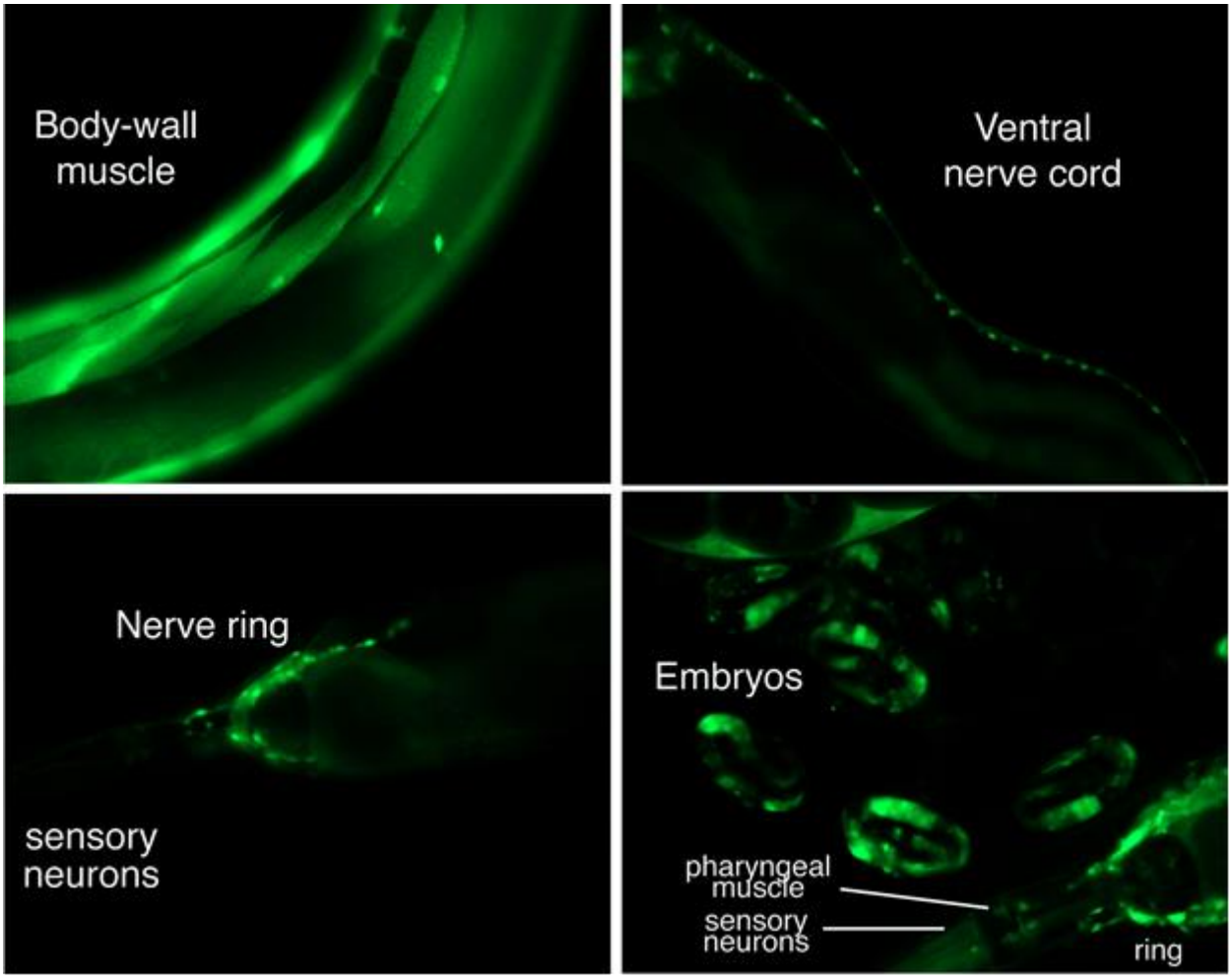

Figure 9
Fusion of the *unc-43* promoter to *gfp* results in GFP expression in muscle, neurons, and the intestine. Worms expressing the *unc-43*::*gfp* fusion were grown at 20C until adulthood, at which point individuals were observed by fluorescence microscopy.

and maintenance of muscle protein levels requires correct formation of the neuromuscular junction (NMJ) during development, maintenance of that junction during larval growth, and proper functioning of neuron and muscle post-development. Defects in any of these can result in uncoordinated movement [143] and muscle protein degradation [71]. Thus, the phenotypes seen in *unc-43* gf worms could be the result of developmental defects or post-developmental defects.

In *unc-43* gf worms, both the cell-specific pattern of LacZ staining and the timing of its loss are distinct from what is observed in genetically denervated animals [71], suggesting that NMJs develop, to some extent, functionally. This is consistent with the observation that *unc-43* gf mutant larvae move quite well. On the other hand, that neuronal CaMKII* is sufficient for progressively uncoordinated movement suggests that neuromuscular communication eventually becomes abnormal. These developmental defects could mask the effect of muscular CaMKII* on movement. Indeed, detailed analysis [138] of the movement defects seen in unc-43 gf and rf mutants show that their movement is characteristic of what would be expected if CaMKII has a role in movement both in neurons and muscles.

I, therefore, sought to distinguish the roles of life-long (chronic) versus post-developmental (acute) hyperactivation of CaMKII in these phenotypes. I hypothesized that post-developmental hyperactivation of CaMKII would cause muscle protein degradation and uncoordinated movement.

For acute activation of CaMKII, no temperature sensitive (ts) *unc-43* gf mutant is available, so we used a *fem-2*^{ts} rf mutant. Research has shown that FEM-2 protein from *C. elegans* dephosphorylates *C. elegans* CaMKII [144] and human CaMKII [145] *in vitro*, causing its inactivation. Therefore, at the non-permissive temperature, reduction of FEM-2 function should

increase CaMKII phosphorylation and activation and lead to phenotypes similar to those seen in *unc-43* gf worms.

At the non-permissive temperature, the *fem-2*^{ts} rf mutation causes an increase in phosphorylated (p) T286-CaMKII (P-CaMKII) (Figure 12). Figure 10a shows that *fem-2*^{ts} rf mutants trigger muscle protein degradation upon shift to the non-permissive temperature (25C). Although both penetrance and expressivity of this phenotype is not 100%, there was a significantly greater frequency of individuals showing muscle protein degradation in the *fem-2*^{ts} rf population compared to *wt*. This degradation required muscular CaMKII, since pre-treatment with *unc-43* RNAi prevented degradation in the *fem-2*^{ts} rf mutants (Figure 10b).

fem-2^{ts} worms also have uncoordinated movement. Again, although there is variable penetrance and expressivity, there is a significantly greater frequency of individuals with uncoordinated movement in the *fem-2*^{ts} population compared to *wt* (Figure 11). Treatment of *fem-2*^{ts} worms with *unc-43* RNAi reduced the frequency of individuals showing uncoordinated movement by swimming assay (Figure 11) and by head-tap response (data not shown)..

These data show that muscular rather than neuronal CaMKII is responsible for the protein degradation seen both with chronic hyper-activation in *unc-43* gf worms and with acute hyper-activation in *fem-2*^{ts} worms. They also show that while chronic, neuronal hyper-activation of CaMKII is sufficient to produce uncoordinated movement, acute hyper-activation of CaMKII causes uncoordinated movement through the action of non-neuronal CaMKII.

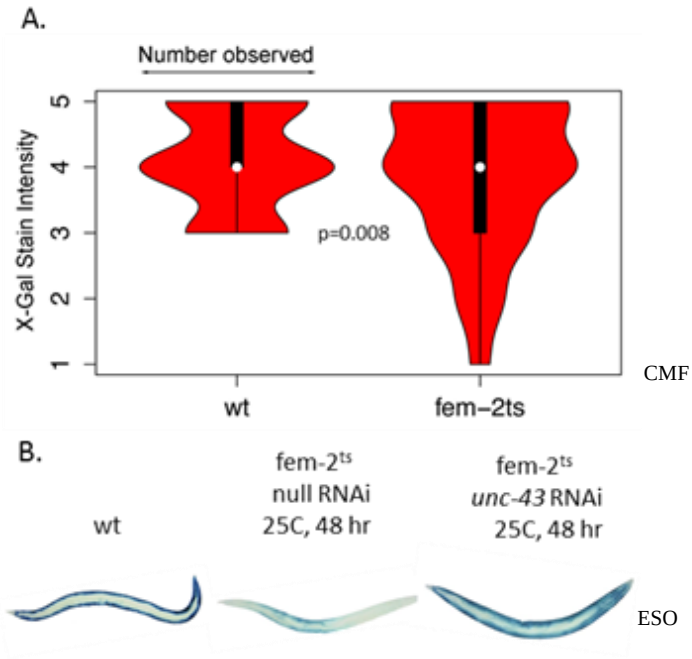

Figure 10

fem-2^{ts} rf causes lacZ degradation, which can be suppressed by *unc-43* RNAi treatment. a) *fem-2*^{ts} rf worms were synchronized as L1s and grown to young-adulthood, at which point they were shifted to 25C for 48 hours. 498 *fem-2*^{ts} rf and *wt* individuals were stained for lacZ and scored for extent of degradation, with 1 being maximal degradation and 5 being no degradation. The distribution of protein degradation in each population was mapped in the above violin plot; the width of the violin represents the number of individuals with a particular protein degradation score, the top and bottom of the thick black line mark quartile 1 and quartile 3, respectively, and the white circle marks the mean. The difference between the populations was calculated using the chi square test for independence. b) L4 *fem-2*^{ts} rf worms were picked to *unc-43* or null RNAi and maintained at 16C. When the F1 reached young-adulthood, the were shifted to 25C. After 48 hr they were stained for LacZ.

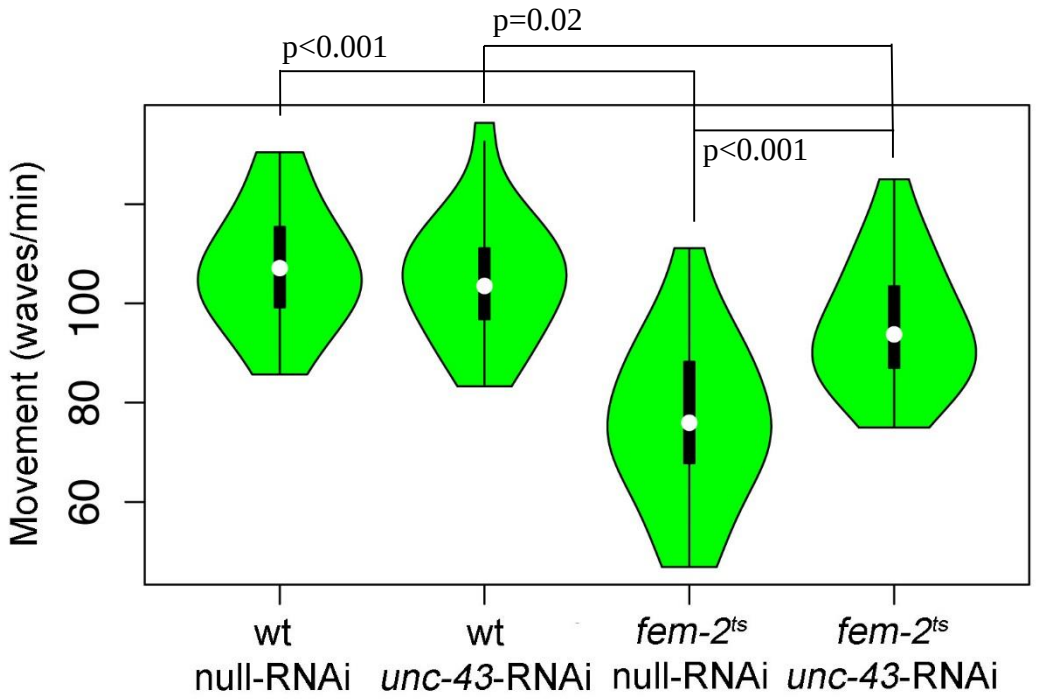

Figure 11

fem-2^{ts} rf causes lacZ uncoordinated movement, which can be suppressed by *unc-43* RNAi treatment. *fem-2*^{ts} rf worms were synchronized as L1s and grown to young-adulthood on *unc-43* or null RNAi, at which point they were shifted to 25C for 48 hours or kept at 20C. *fem-2*^{ts} rf and *wt* individuals were picked into buffer and assayed for swimming rate. In the above violin plot, the width of the violin represents the number of individuals with a particular movement score, the top and bottom of the thick black lines mark quartile 1 and quartile 3, respectively, and the white circle marks the mean. p-values were calculated using the Wilcox Rank Sum Test. n= 5 replicate measurements for 2 worms of each category. Data, ESO. Analysis, CMF.

2.2 CAMKII SIGNALS THROUGH RAF-MEK-MAPK TO PROMOTE MUSCLE PROTEIN DEGRADATION

The protein degradation observed in *unc-43* gf mutants is similar to that found in mutants with hyperactivity in the Raf-MEK-MAPK pathway [76, 77, 99]. This led to the hypothesis that CaMKII signaling might positively regulate the Raf-MEK-MAPK module.

In order to determine if activation of the Raf-MEK-MAPK module is necessary for *unc-43* gf phenotypes, I made an *unc-43*gf; *mpk-1* (MAPK) rf double mutant. The *mpk-1* rf mutation completely suppressed the *unc-43* gf protein degradation phenotype, showing that CaMKII is acting upstream of MAPK (Figure 12a). Thus, although CaMKII may have many cellular targets, its output via MAPK is uniquely required to stimulate protein degradation. However, the movement defect seen in *unc-43* gf animals was not suppressed in the *unc-43* gf; *mpk-1* rf double mutant, suggesting that the effect of chronic CaMKII hyperactivity on movement results from signaling independent of MAPK. This does not eliminate the possibility that the movement defect caused by *acute* hyperactivation of CaMKII requires MAPK, although this is unlikely as activation of any protein in the Raf-MEK-MAPK module does not result in uncoordinated movement phenotypically similar to that observed in CaMKII gf mutants.

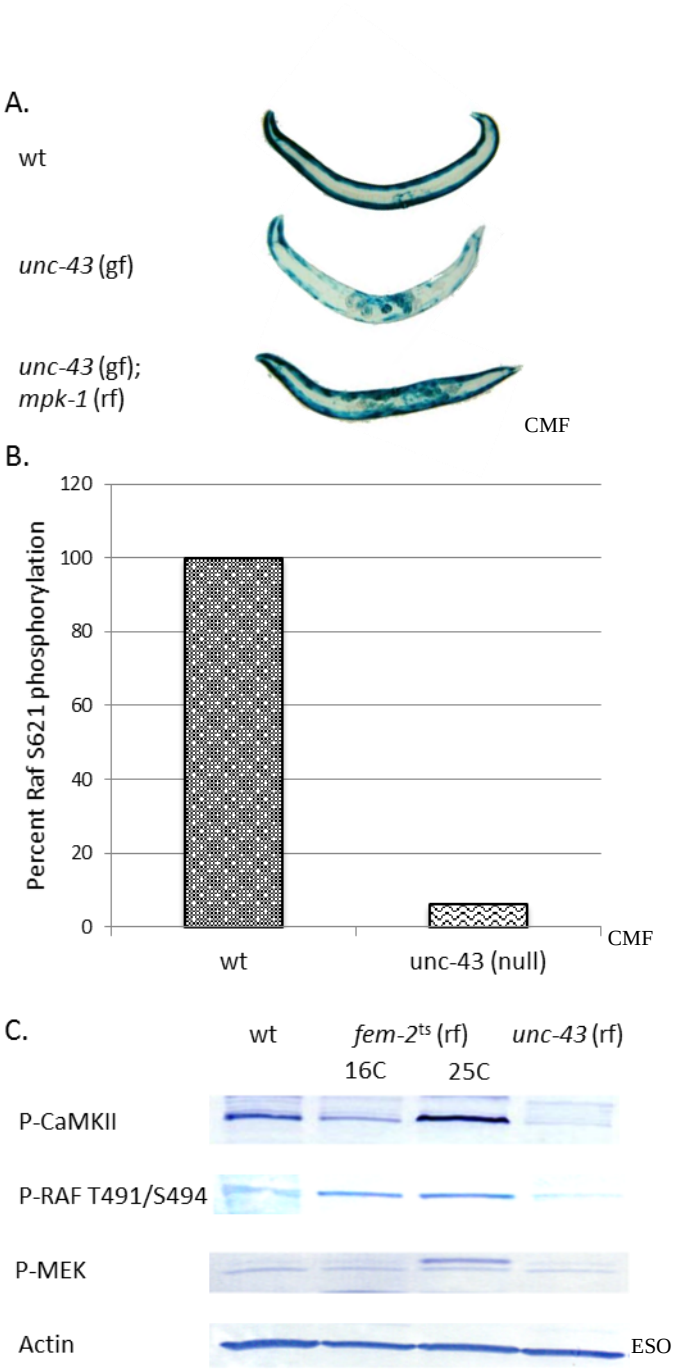

Figure 12

Degradation caused by hyperactive CaMKII requires MAPK and results in activation of Raf and MEK. a) wt, *unc-43* gf, and *unc-43* gf; *mpk-1* rf adults were raised to adulthood at 20C and then stained for LacZ. (**B**) *wt* and *unc-43* null worms were synchronized and grown to adulthood, at which point western blot samples were collected. After blotting, primary antibody for human P-S621 Raf was used. The weak signal was quantified using imageJ software. (**C**) *fem-2*^{ts} rf worms were synchronized, grown to adulthood, and shifted to 25C or held at 15C for 48 hours before collection for western blot samples. All data shown above are from reprobes of the same blot.

We next sought to determine if CaMKII is also upstream of Raf. Raf activation requires phosphorylation of T491 and S494 [106], which may occur via trans-autophosphorylation after recruitment to the plasma membrane and oligomerization [107]. The propensity of any Raf molecule to become active is modulated by the phosphorylation state of its other regulatory sites, specifically S259 and S621 [105, 108-111]. pS621 can be either stimulatory or inhibitory, depending on the context [146]. pS621, in the absence of pS259, stimulates Raf activation.

Mammalian Raf S621 is predicted to be a CaMKII target [147]. The *C. elegans* homologue of Raf-1 is LIN-45. Raf-1 S621 is analogous to LIN-45 S756. Both sites match the CaMKII consensus target sequence rxxS/Txp (Table 1) and the *lin-45* mutant allele ku112 is a weak LIN-45 hypomorph [148]. (I will henceforth denote LIN-45 S756 as "S621" for compatibility with the mammalian Raf literature.)

Table 1 Candidate CaMKII target sites

Raf protein	Sequence (**S** is target)
hRaf-1	RSA**S**EP
hBRaf	RSA**S**EP
LIN-45	RSQ**S**AP
LIN-45 ku1112	RFQ**S**AP

To determine if CaMKII is required for stimulatory phosphorylation of Raf S621, pS621 Raf in *wt* and CaMKII null mutant animals was assayed. CaMKII null mutants were generated and verified as described in the Methods section. Null mutation of CaMKII reduced pS621-Raf

to a nearly undetectable level (Figure 12), showing that CaMKII likely acts directly upstream of Raf to phosphorylate S621.

If CaMKII signals positively through Raf-MEK-MAPK, this implies that acute activation of CaMKII should result in increased activating phosphorylation of Raf, MEK, and MAPK. To acutely activate CaMKII, the *fem*-2^{ts} mutant was used. It was found that increased pT286-CaMKII correlated with increased pT491/pS494 (active) Raf and P-MEK-2 (Figure 12c). These observations confirm the genetic analysis.

2.3 AUTOPHAGY IS REQUIRED FOR PROTEIN DEGRADATION INDUCED BY CAMKII SIGNALING

The muscle protein degradation caused by activation of the Raf-MEK-MAPK cascade does not require the proteasome [99], in contrast to proteasome-dependent protein degradation caused by starvation and denervation [147]. Since the proteasome is not required for degradation induced by the Raf-MEK-MAPK cascade, it was hypothesized [77] that autophagy may be required. To test this, animals expressing a constitutively active *Drosophila* MEK and a heat shock-inducible MAPK (resulting in high levels of active P-MAPK at 25C) were treated with autophagy inhibitors and then assayed for protein degradation by LacZ staining. We inhibited autophagy in two ways: 1) by RNAi knockdown of *bec-1* or *atg-7*, which code for proteins involved in autophagic vesicle nucleation and elongation, respectively (see section 1.2.2), and 2) by rf mutation of the TOR-responsive, *atg-1* homologue, *unc-51*. Both measures suppressed protein degradation (Figure 13), as did treatment with the autophagy inhibitor DMA, showing that autophagy is required for

degradation induced by activation of the Raf-MEK-MAPK cascade (C. Bialas, A. Ayyash, L. Jacobson, unpublished).

Since CaMKII requires MAPK to signal for protein degradation, I tested if *unc-43* gf worms have an increase in autophagy and if autophagy is required for protein degradation. To assay autophagy in *unc-43* gf worms, an *unc-43* gf mutant that expresses a GFP::LGG-1 fusion was constructed. LGG-1 is the *C. elegans* ortholog of yeast Atg8/Aut7p and mammalian MAP-LC3 [59]. Both of these LGG-1 orthologs localize to pre-autophagosomal and autophagosomal membranes, and, notably, the SR [78]. Our construct labels these vesicles in all cells of the *unc-43* gf mutant. The depth of focus of the confocal microscope I used for imaging these worms is approximately equal to the depth of the muscle belly of the body-wall muscle cells. Therefore, I collected one optical slice for each sample and quantified the number of autophagic vesicles in that slice by counting the number of autophagic vesicles per muscle area. Figure 14 shows confocal pictures of *wt* and *unc-43* gf worms. Note the larger number of vesicles in the body-wall muscle of the *unc-43* gf worm.

Wild type worms have a basal number of autophagic vesicles in muscle, which increases between 24 and 48 hours post-L4 (Figure 15a). This level remains constant until 72 hours post-L4. On the other hand, *unc-43* gf mutants initially have a three-fold higher number of autophagic vesicles and these numbers continue to increase through to 72 hours post-L4 (and possibly beyond) (Figure 15a). The increase in the number of autophagic vesicles in *wt* worms between 24 and 48 hours may be a feature of aging. Although the worm lifespan is 12-18 days, worm muscle starts showing aging-related changes as early 7 days after hatching [149]. It is not surprising, then, that autophagy, which has been shown to be required for extended lifespan under multiple conditions and the inactivation of which accelerates aging of tissues in *C. elegans* [150] should be up-

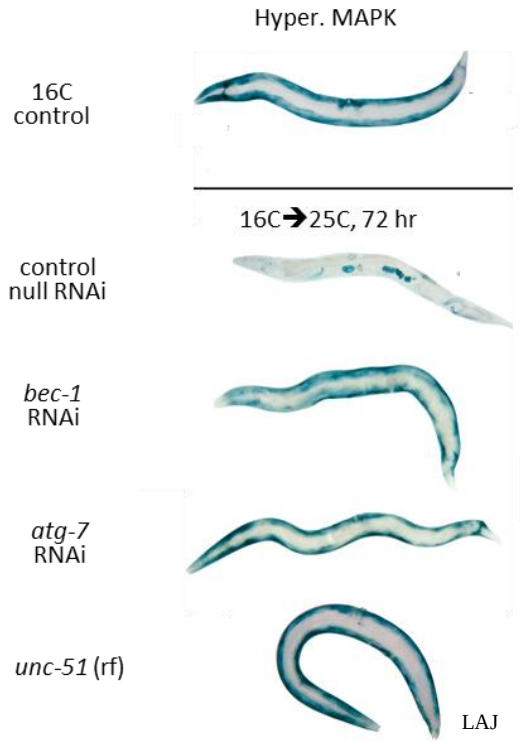

Figure 13

Inhibition of autophagy suppresses muscle protein degradation in hyperactive MAPK worms. Animals were age-synchronized and plated on either *bec-1, atg-7*, or null RNAi plates and grown to mid-adulthood before heat-shock and shift to 25C. Alternatively, *unc-51* rf double mutants were grown to mid-adulthood before heat-shock and shift to 25C. Individuals were then stained for beta-galactosidase activity.

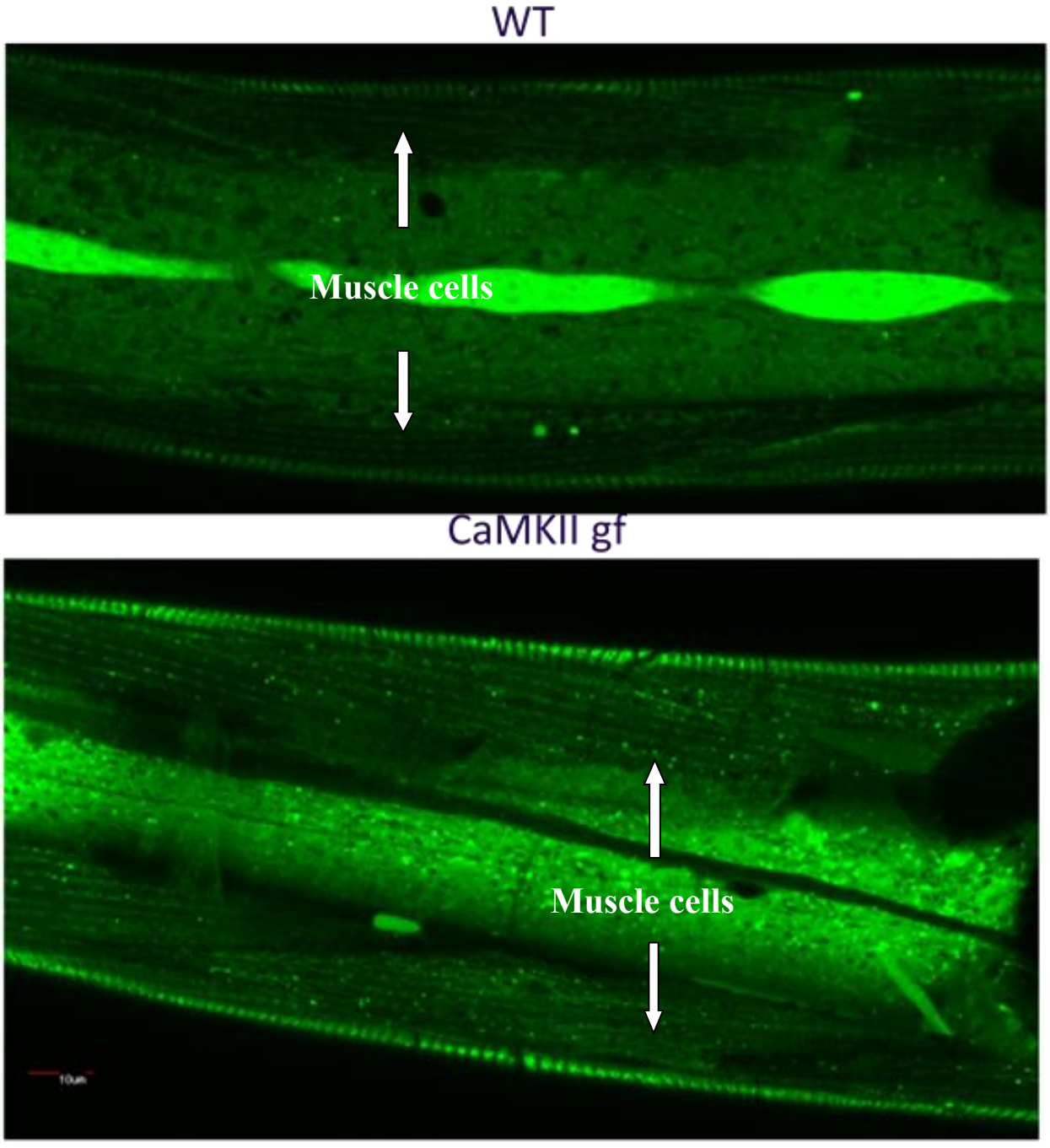

Figure 14
unc-43 gf worms have more LGG-1 positive autophagic vesicles than *wt*. L4 *unc-43* and *wt* worms were picked to fresh plates and grown at 20C for 24 hours before imaging. Confocal microscopy was used to collect images of the muscle belly, as described in Materials and Methods.

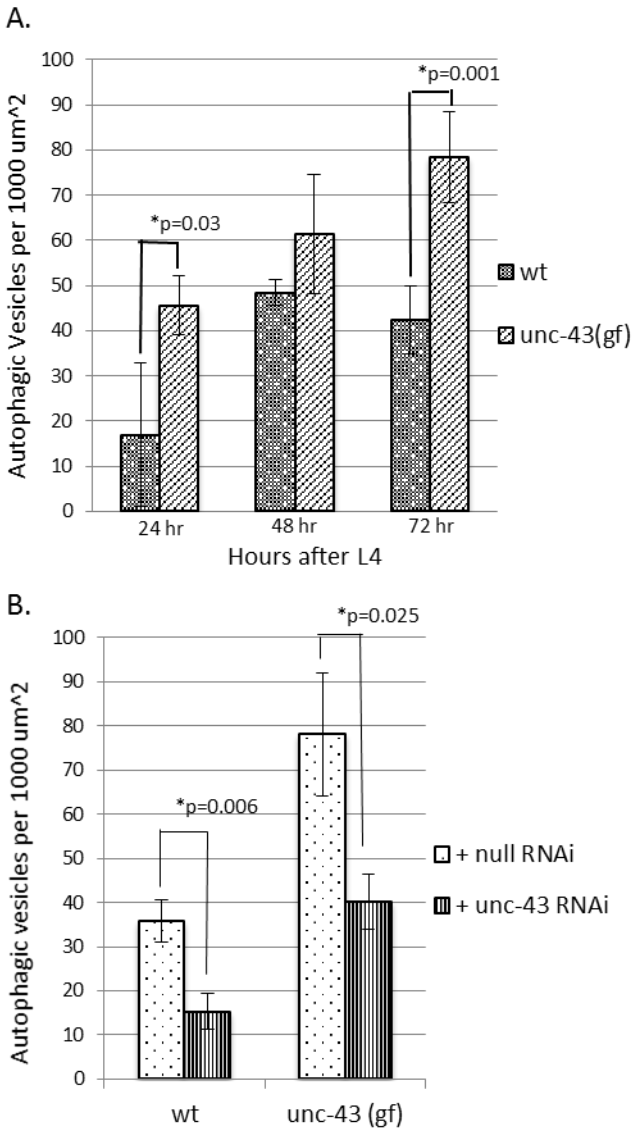

Figure 15
unc-43 gf worms have increased numbers of autophagic vesicles compared to *wt*, which can be suppressed by *unc-43* RNAi treatment. a) L4 *unc-43* gf and *wt* worms were picked to fresh plates and then analyzed every 24 hours for the number of autophagic vesicles present in the muscle cells. At 24 hr, n=14 worms. At 48 hr, n=17. At 72 hr, n=18. b) L4 *unc-43* or *wt* worms were picked to unc-*43* or null RNAi plates. When the F1 reached L4, they were picked to fresh plates and were analyzed for the number of autophagic vesicles 24 hours later. For wt, n=26. For *unc-43* worms, n=21. In all cases, the worms were photographed under the confocal microscope with several muscle cells in the field of view. For each individual worm photographed, the highest quality image was selected for quantification. During quantification, all autophagic vesicles in muscle cells and in the focal plane were counted. p-values were calculated using the Student's T-test.

regulated as early as 5 days after hatching (48 hours post-L4). It could be interesting to follow lifespan and number of autophagic vesicles in the mutants described here.

Subsequent experiments to compare number of autophagic vesicles to *wt* were done at 24 hours post-L4 to reduce aging-related complications.

The high number of autophagic vesicles seen in *unc-43* gf worms can be suppressed by *unc-43* RNAi treatment (Figure 15b). This shows that it is the non-neuronal activity of CaMKII, likely in the muscle, which causes the increase in autophagic vesicles. This is consistent with the data in Figure 6b showing that protein degradation is caused by non-neuronal activity of CaMKII.

Note that even the basal number of autophagic vesicles in *wt* worms is further reduced by treatment with *unc-43* RNAi (Figure 15b). Studies by Shephard et al. have shown that multi-generational *unc-43* RNAi treatment causes defects in myofibril and mitochondrial maintenance [151]. Autophagy is known to be required for maintenance of muscle mass and for prevention of atrophy and myopathy, likely due to the role of autophagy in clearing damaged proteins and organelles [50, 58]. These data suggest that knockdown of CaMKII (*unc-43*) inhibits basal autophagy and thereby might be preventing the normal recycling of used and damaged cellular components leading to myopathy. In light of the autophagy data presented for *wt* animals above, it could likewise be interesting to look at any aging effects of *unc-43* RNAi treatment on aging of the muscle tissue.

To test if autophagy is required for muscle protein degradation induced by CaMKII hyperactivity, I blocked autophagy in *unc-43* gf mutants in two ways. Either I introduced an additional *unc-51* rf mutation into the *unc-43* gf strain or I treated with the autophagy inhibitor DMA. *unc-51* rf mutation prevents protein degradation (Figure 16a) and treatment with DMA

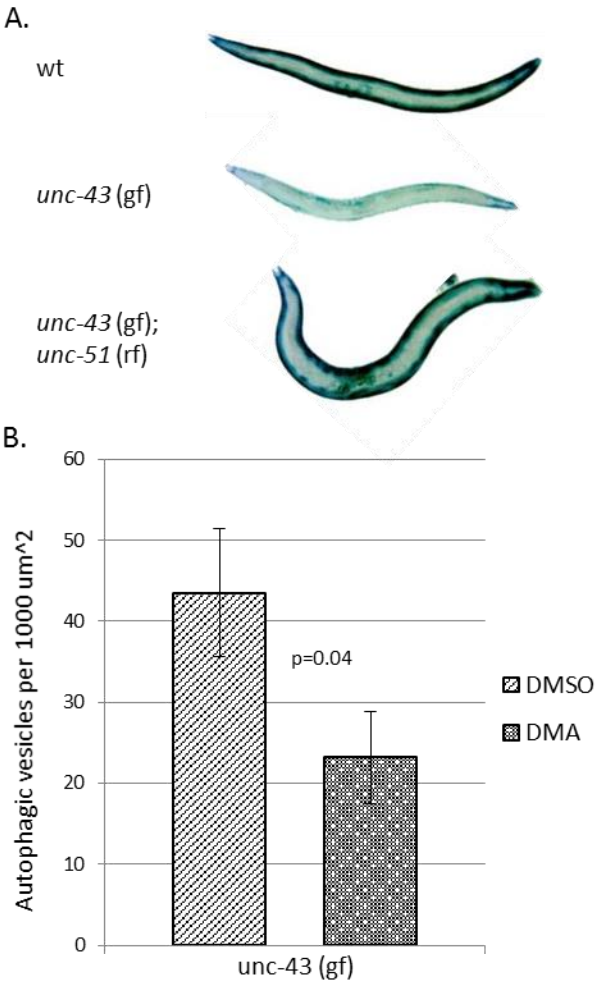

Figure 16

Inhibition of autophagy suppresses autophagic vesicle formation and muscle protein degradation in *unc-43* gf worms. a) Adult *unc-43* gf or *unc-43 gf; unc-51* rf worms were grown to adulthood and stained for LacZ. b) *unc-43* gf worms were treated with DMSO or DMA and then picked to fresh plates as L4s and were analyzed for the number of autophagic vesicles 24 hours later. 19 worms were photographed and, based on quality, one image per worm was selected for quantification.

suppresses the higher level of autophagic vesicles normally seen in *unc-43* gf individuals (Figure 16b), demonstrating that autophagy is required for protein degradation in *unc-43* gf worms.

My observations, taken together with those of Shephard et al. [151], suggest that a basal level of autophagy in muscle is required for "housekeeping" functions, but that excessive autophagy, as seen in *unc-43* gf worms, leads to pathologic levels of protein degradation.

Protein degradation caused by acute increase in Raf-MEK-MAPK signaling or decreased IGFR signaling cannot be blocked by treatment with cycloheximide, a protein synthesis inhibitor [77, 99, 152], showing that degradation is not caused by the downstream effects of transcriptional changes, but by the activation of a pre-existing proteolytic system. To verify that the autophagy caused by hyperactivity of CaMKII acts in a manner consistent with this hypothesis, *fem-2*^{ts} worms were treated with cycloheximide, a protein synthesis inhibitor, and assayed to see if this could prevent any increases in autophagic vesicle formation at the non-permissive temperature.

Interestingly, treatment with cycloheximide increased the number of autophagic vesicles both at the non-permissive and permissive temperature, well beyond anything we have observed with activation of the signaling network described here (Figure 17). Other studies have shown [153] that cycloheximide blocks later stages of autophagy, causing accumulation of autophagic vesicles. We have shown that treatment with cycloheximide does not block inactivation of LacZ when degradation is induced in by activation of Raf by temperature shift after six hours of pre-incubation with cycloheximide [99]. Thus, our results suggests that whatever pre-existing proteins are required for autophagy have a longer life than six hours. Theoretically, if we extended the pre-treatment with cycloheximide, we should eventually prevent autophagy, although obvious complications arise with increased duration of cycloheximide treatment. It should be remembered that degradation, as I have defined it here, is loss of LacZ activity. "Degradation", therefore, does

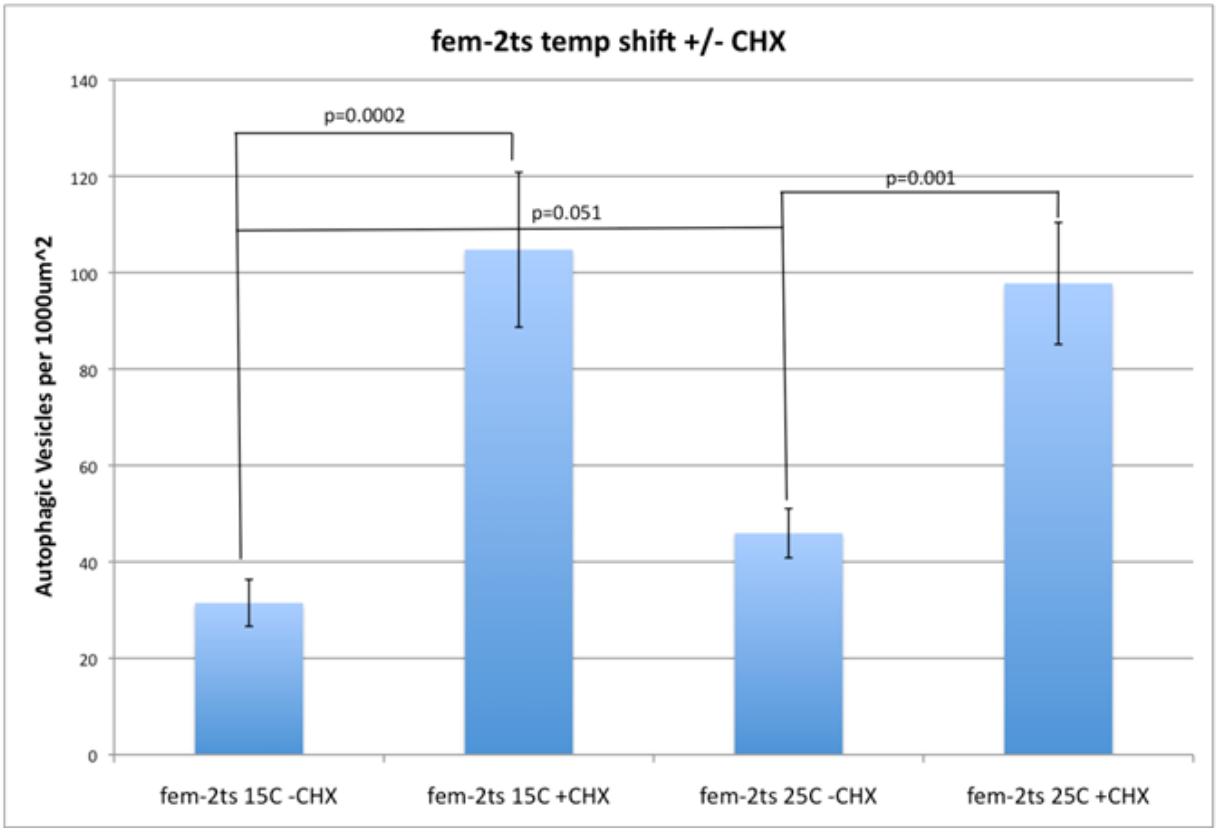

Figure 17

Treatment with cycloheximide causes increased number of autophagic vesicles compared to untreated animals. As L4s, *fem-2* ts worms were picked to plates containing 400 µg/mL cycloheximide and then were either kept at 16C or shifted to 25C. After 48 hours, the number of autophagic vesicles were analyzed. At 15C, n=16 worms. At 25C, n=17 worms. p-values were calculated using the Student's T-test.

not necessarily represent full breakdown of the protein into its constituent amino acids. Early stages of autophagy may be sufficient to cause inactivation of LacZ if vesicles are acidified and LacZ is denatured.

As part of the above experiment I quantified the number of autophagic vesicles caused by acute CaMKII hyperactivation in *fem-2*^{ts} worms. After 48 hours at the non-permissive temperature, *fem-2*^{ts} worms had a significant increase in the number of autophagic vesicles (Figure 17). However, due to the accelerated aging at higher temperature, this increase is likely age-related. Indeed, *wt* controls also show more vesicles after 48 hours at the non-permissive temperature compared to worms at the permissive temperature (data not shown).

2.4 CAMKII SIGNALING COUNTERBALANCES IGFR SIGNALING

Previous work on this signaling network has shown that signaling through the IGFR opposes FGFR signaling through inhibitory phosphorylation of Raf S259. Thus, degradation caused by decreases in inhibitory IGFR signaling can be prevented by simultaneous decreases in stimulatory FGFR signaling [77]. Since signaling is also integrated into the network as a positive input at the level of Raf, I conjectured that increases or decreases in IGFR signaling could be balanced by increases or decreases in CaMKII signaling.

Initially, I tested if protein degradation caused by decreases in IGFR signaling could be suppressed by decreases in CaMKII signaling. I decreased signaling through the IGFR pathway in two ways. First, I treated with the PI3K inhibitor, LY294002. PI3K is downstream of IGFR and its inhibition promotes degradation [77]. Treatment of *wt* worms with LY294002 causes

muscle protein degradation, whereas CaMKII protein null mutants (Q67stop) do not degrade muscle protein when treated with LY294002 (Figure 18). MEK is downstream of both PI3K and CaMKII. Western blots show an increase in P-MEK-2 with LY294002 treatment in *wt* worms, but no such increase in CaMKII protein null worms treated with LY294002 (Figure 18b). MEK-1 is unresponsive. This is consistent with genetic evidence that MEK-2 is necessary for signaling between LIN-45 Raf and MPK-1 MAPK in *C. elegans* muscle [99].

I also made IGFR (*daf-2ts*), CaMKII (*unc-43* rf) double mutants. The *daf-2*^{ts} single mutant degrades protein at the non-permissive temperature, but the double mutant does not (Figure 19a). Likewise, the *daf-2*^{ts} mutant shows an increase in P-MAPK after shift to the non-permissive temperature, while the double mutant does not (Figure 19b).

Lastly I tested the inverse possibility, to see if increases in IGFR signaling could balance the pro-degradative effect of increased CaMKII activity. I increased signaling through the IGFR arm of the pathway by RNAi knockdown of *daf-18*. DAF-18 is a PTEN-class lipid phosphatase that converts the PIP_3 formed by active PI3K back to PIP_2, thereby attenuating the signal. Knockdown of DAF-18 should thus increase the amount of PIP_3 and promote IGFR signaling. As predicted, *unc-43* gf worms treated with *daf-18* RNAi have a reduced number of autophagic vesicles relative to worms treated with null RNAi (Figure 20).

The ability of Raf to integrate signals from the IGFR, FGFR, and CaMKII depends on the multiple phosphorylation sites that regulate its activation [154]. Signaling from the FGFR to Ras promotes localization to the plasma membrane, oligomerization, and activating phosphorylation of Raf [155]. The tendency of Raf to become active is controlled by phosphorylation of the inhibitory S259 site by AKT (downstream of IGFR) and phosphorylation of the stimulatory S621 site by CaMKII (Figure 21).

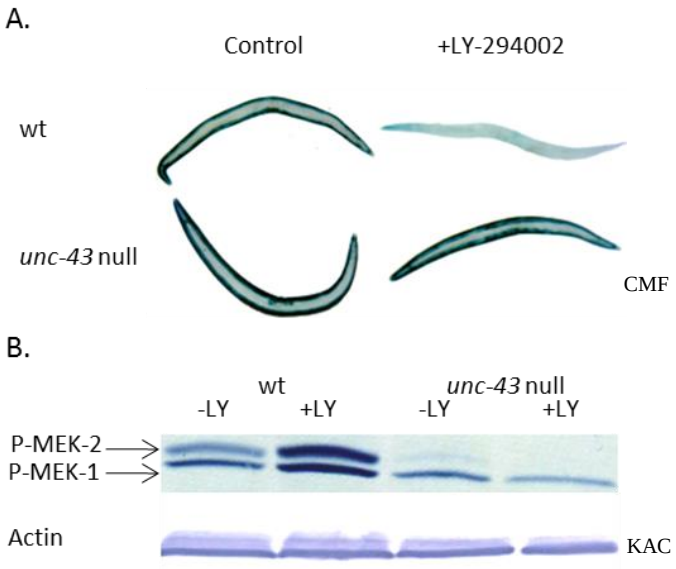

Figure 18

CaMKII null mutation prevents degradation caused by inhibition of IGFR signaling. a) L4 *wt* and *unc-43* null worms were picked as L4s to 160 uM LY-294002 or DMSO plates. 48 hours later they were a) stained for LacZ, or b) were collected for western blot samples with 30 worms/sample. After blotting, the membrane was probed for P-MEK and then re-probed for actin.

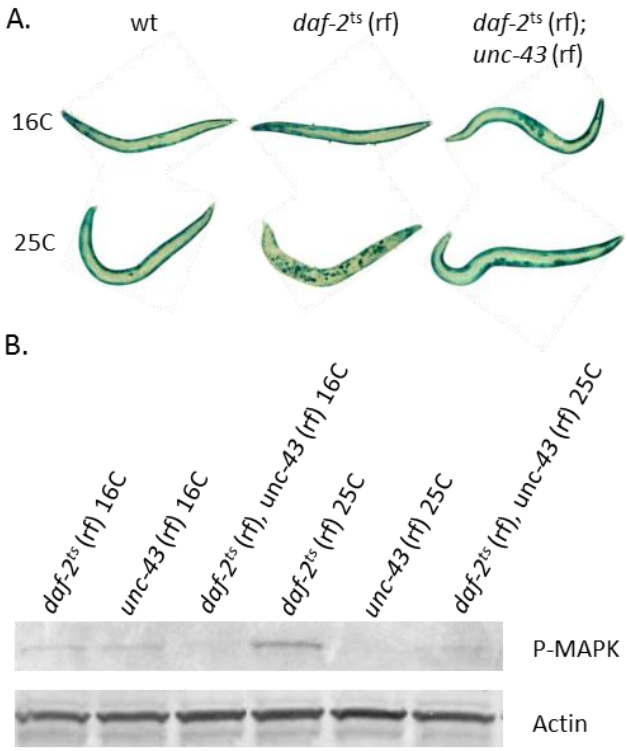

Figure 19
unc-43 rf mutation suppress protein degradation and increased P-MAPK caused by *daf-2*^{ts} rf mutation. Animals were synchronized, grown to young-adulthood and shifted to 25C for 48 hr. They were then stained for LacZ (a) or picked for western blotting, with 30 worms/sample (b). Note that the relevant LacZ stain is in the body-wall muscle, not in embryos seen in egg-retentive individuals (e.g., daf-2 at 25C). The blot was probed for P-MAPK and re-probed for actin.

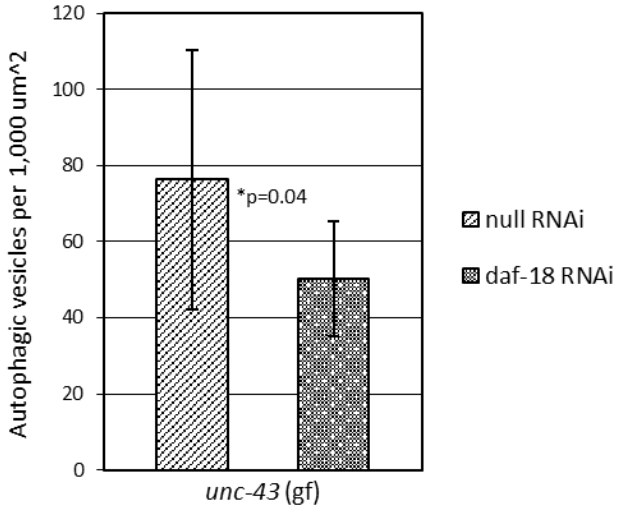

Figure 20
daf-18 RNAi treatment reduces the number of autophagic vesicles in *unc-43* gf worms. L4 *unc-43* gf worms were picked to *daf-18* or null RNAi plates. When the F1 reached the L4 stage, they were picked to fresh plates. 24 hours later they were then analyzed for the number of autophagic vesicles. 20 worms were photographed and the highest quality image for each worm was selected for quantification. The p-value was calculated using the Student's T-test.

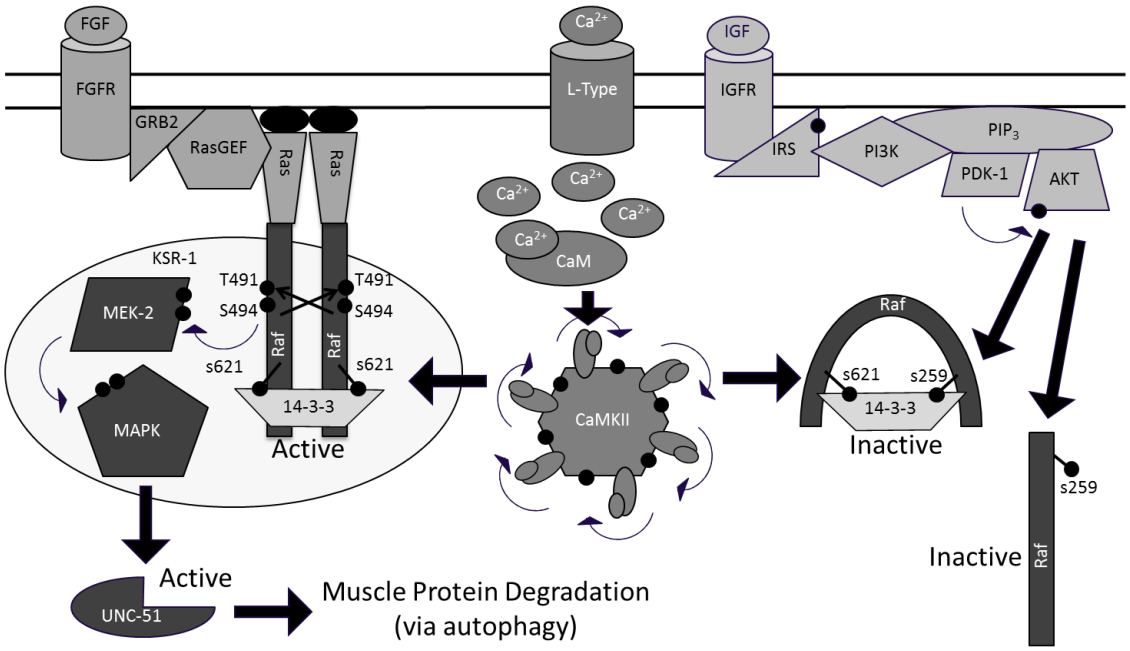

Figure 21
Raf activation. Signaling from CaMKII promotes activation of Raf via phosphorylation of S621. When Ras is active, Raf that is phosphorylated on S621 and dephosphorylated on S259 can localize to the plasma membrane, oligomerize, and become active by phosphorylation of T491/S494. Signaling from the IGFR, via AKT, results in inhibitory phosphorylation of Raf at S259.

Raf pS621 is necessary to promote muscle protein degradation. pS621 in the absence of pS259 (by LY294002 treatment or S259A mutation) causes protein degradation (Figure 18a and Figure 22, respectively). In the absence, or reduction, of CaMKII (and hence pS621), degradation cannot be stimulated by decreased IGFR signaling (Figure 18a) or by S259A mutation of Raf (Figure 22). This is consistent with other studies showing that 14-3-3 binding to pS621 is required for activation of Raf [156].

Raf pS621, however, is not sufficient to promote degradation. In *wt* worms, both S621 and S259 are phosphorylated, leading only to basal levels of Raf activation (Figure 12c) and normal maintenance of muscle protein. In this case, it is thought [157] that 14-3-3 binds to pS259/pS621 Raf and prevents dimerization. Figure 18 and Figure 22 similarly show that, in contrast to pS621, Raf pS259 is sufficient, but not necessary to inhibit muscle protein degradation.

2.5 A ROLE FOR SPLICE FORMS?

While the model of CaMKII activation described in Section 2.5 is useful for a basic understanding of CaMKII activation, the situation *in vivo* is much more complicated. Information encoded by a calcium signal can vary based on its frequency, magnitude, duration, and tempero-spatial localization [158]. CaMKII, as one of the interpreters of these varying signals, must be able to read and respond uniquely to each. In mammals, one way that this is achieved is by the production of a family of CaMK enzymes, four of which are multifunctional (CaMKK, CaMKI, CaMKII, and CaMKIV). CaMKK, CaMKI, and CaMKIV all function as monomers and can diffuse into the nucleus where they affect transcription. CaMKK can be activated either by active

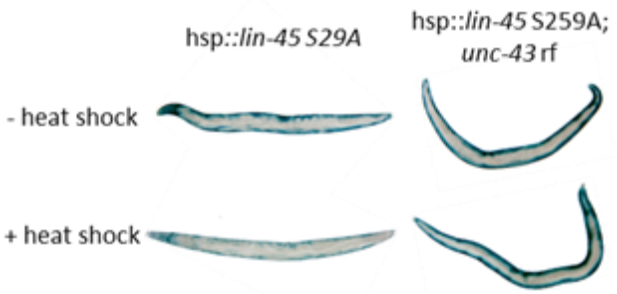

Figure 22

Reduction-of-function mutation in *unc-43* suppresses the protein degradation seen in Raf S259A mutants. Worms were age-synchronized and then heat-shocked for 30 min at 37C. After the heat shock, they were shifted to 25C for 48 hours before LacZ staining.

PKA or Ca^{2+}/CaM, depending on the isoform. Once it is activated, CaMKK goes on to phosphorylate and activate CaMKI and CaMKIV. CaMKI and CaMKIV require both activation by CaMKK and Ca^{2+}/CaM to be active. One of CaMKI and CaMKIV's substrates is the nuclear localization signal (NLS) contained in certain splice variants of CaMKII. Phosphorylation adjacent to the NLS prevents nuclear localization of these CaMKII isoforms [159].

Of the multifunctional CaMKs, only CaMKII oligomerizes to form the dodecameric holoenzyme described above [160]. Human CaMKII includes four isoforms (alpha, gamma, beta, and delta) encoded by separate genes, and more than 20 splice variants of those isoforms [161]. There is also a non-kinase variant, alpha-KAP, whose promoter is intronic to CaMKII and which contains an association domain similar to CaMKII's, but lacks the kinase domain. Different splice variants of alpha-KAP contain a nuclear localization signal and/or an N-terminal hydrophobic domain. These splice variants localize to the nucleus or the SR membrane. [162]

These different forms of CaMK are expressed in an array of combinations in a variety of tissues/cells at appropriate stages of development. At the sub-cellular level, isoforms and splice variants can be differentially localized based on inclusion or exclusion of a localization sequence. During assembly of the holoenzyme, different isoforms can be co-assembled to form a heteromultimer. The number of subunits in the heteromultimer containing a particular localization sequence can alter the localization of the entire holoenzyme [163]. Inclusion of alpha-KAP in the heteromultimer can result in anchoring of the holoenzyme to the sarcoplasmic reticulum in muscle [164]. It has also been shown that CaMKII can decode the frequency, duration, and amplitude of Ca^{2+}spikes into distinct amounts of kinase activity [161]. Isoforms and splice variants of CaMKII are capable of responding with different sensitivities to the frequency of Ca^{2+} oscillations [165].

C. elegans does not have as many multifunctional CaMKs as mammals do. It has genes coding for CaMKK, CaMKI, and CaMKII (*ckk-1*, *cmk-1*, and *unc-43* respectively). However, while there are no isoforms of CaMKII coded by separate genes, there are many different forms produced from the single gene. Wormbase.org lists greater than 15 variants encoded by *unc-43* that have been confirmed by cDNAs (Figure 23). It is possible that some of these variants take on roles usually filled by other proteins in mammals. Most of these are produced by alternative splicing. Notably, several are produced by transcription from internal promoters.

The various forms of CaMKII may be full-length, N-terminal, or C-terminal. Two of the C-terminal forms are produced by transcription from the internal promoter. The C-terminal forms K11E8.1m and K11E8.1o have similarities to a mammalian kinase anchoring protein, αKAP. Like αKAP, they contain a NLS, an association domain, and lack a kinase domain. In mammals, αKAP is capable of assembling in the CaMKII holoenzyme and changing its localization [164]. K11E8.1m and K11E8.1o could serve to localize the holoenzyme to the nucleus or sarcoplasmic reticulum.

N-terminal forms of CaMKII, such as K11E8.1i, have a kinase and CaM binding domain, but lack the association domain. It is not known if the kinase domains of these forms are functional, but if it is, then these forms could act in a manner similar to human monomeric CaMKs. Still other splice variants have unique stretches of amino acids not found in all splice variants or homologous to any portion of a CaMKII in mammals. There is little basis on which to predict the function of these sequences.

We obtained a mutant worm strain that has a deletion of a promoter region internal to full-length CaMKII and required for production of the KAP isoform (allele tm2945). This strain was produced from insertion and imprecise excision of a Mariner transposon, resulting in a

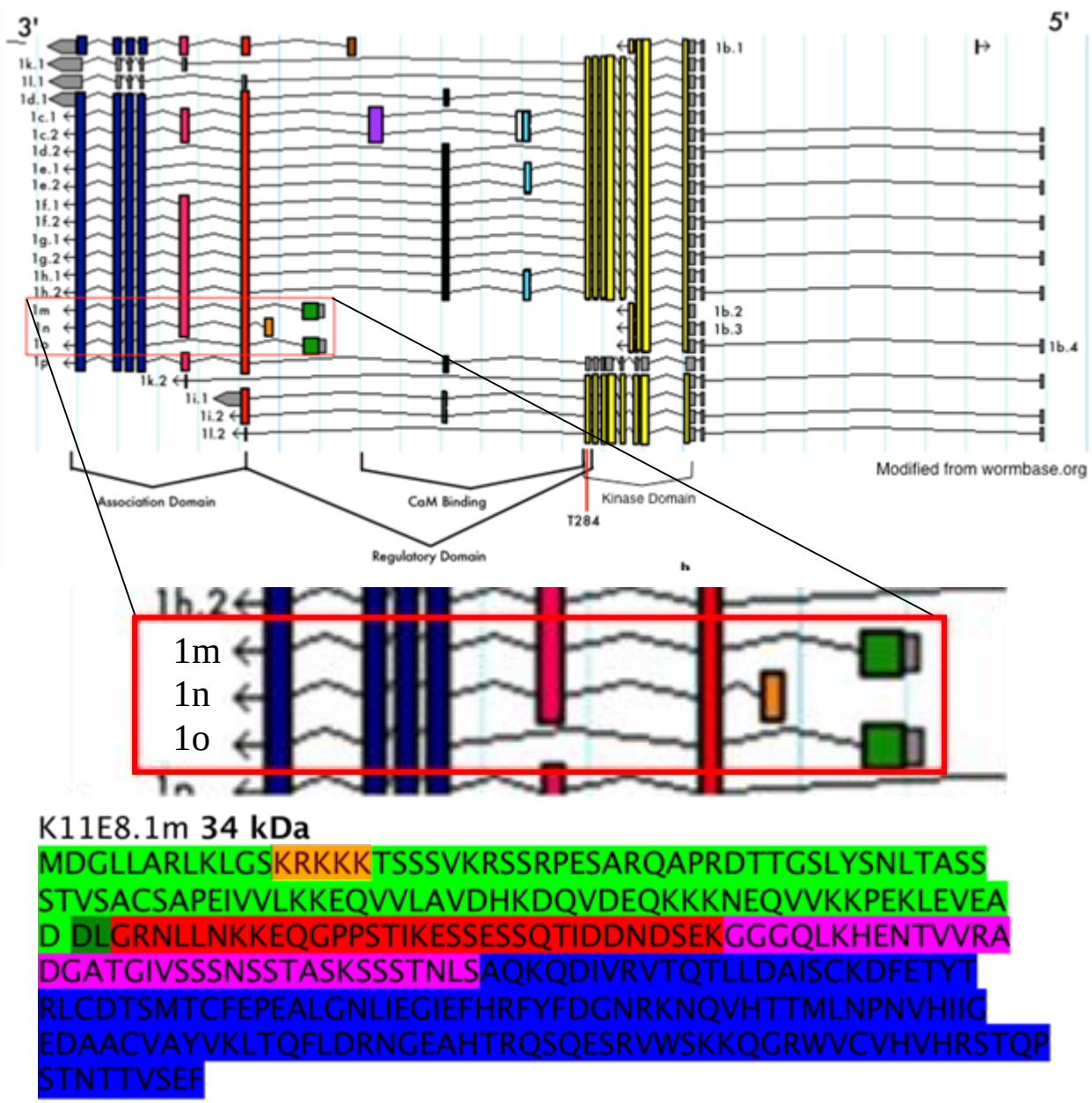

Figure 23
Splice forms of CaMKII. Shown are several of the splice forms of CaMKII found in *C. elegans* and listed on wormbase.org. Bars show exons and thin lines show introns. The kinase domain is shown in yellow and the association domain is shown in blue. Note that several of the splice forms lack one or the other. Splice forms containing a possible localization sequence (1m and 1o) are boxed in red and enlarged. The amino acid sequence for K11E8.1m is shown. Note the putative localization sequence shown in orange.

506bp deletion and a 4 bp insertion. Using the method diagrammed in Figure 24, I constructed a strain that has the KAP promoter deletion and expresses LacZ in the muscle. I verified that the constructed strain has the ~500 bp deletion by PCR of genomic DNA with primers flanking the deletion site (Figure 25). This strain has been named the internal promoter deletion (IPD) strain. The IPD strain does not degrade protein, has a mild movement defect in the swimming and backward crawl assay, and prevents LY-induced degradation (Figure 26). In Western blots, these worms show a reduction in P-CaMKII and P-MEK-2 (Figure 27). In all respects, the IPD strain behaves as a CaMKII rf strain. This is particularly interesting as the KAP form of CaMKII is not catalytically active and contains what may be a localization sequence. The KAP form could assemble into the holoenzyme and then change the localization of the holoenzyme. Although these results are suggestive, it is possible that the internal promoter deletion is altering splicing of full-length CaMKII, resulting in the rf phenotype. To test this possibility, PCR of full-length *unc-43* cDNA could be performed.

RNAi treatment can potentially be used to knock down individual forms of CaMKII. The Jacobson lab previously had unc-43 and unc-43-3' RNAi strains. The unc-43 RNAi is designed to knock down all forms of CaMKII. The unc-43-3' RNAi is designed to knock down full-length, C-terminal, and KAP forms, leaving only N-terminal forms. I constructed unc-43 cDNA, unc-43-5', and KAP RNAi strains (Figure 28), which have been verified by sequencing (Appendix B).

Unlike the unc-43 RNAi strain, the unc-43 cDNA strain does not produce dsRNA that includes introns. The unc-43-5' RNAi is designed to knock down full-length and N-terminal CaMKII, leaving only C-terminal forms. The KAP RNAi is designed to knock down only the KAP form of CaMKII. Exon-specific RNAi sometimes poses a problem in *C. elegans* due to

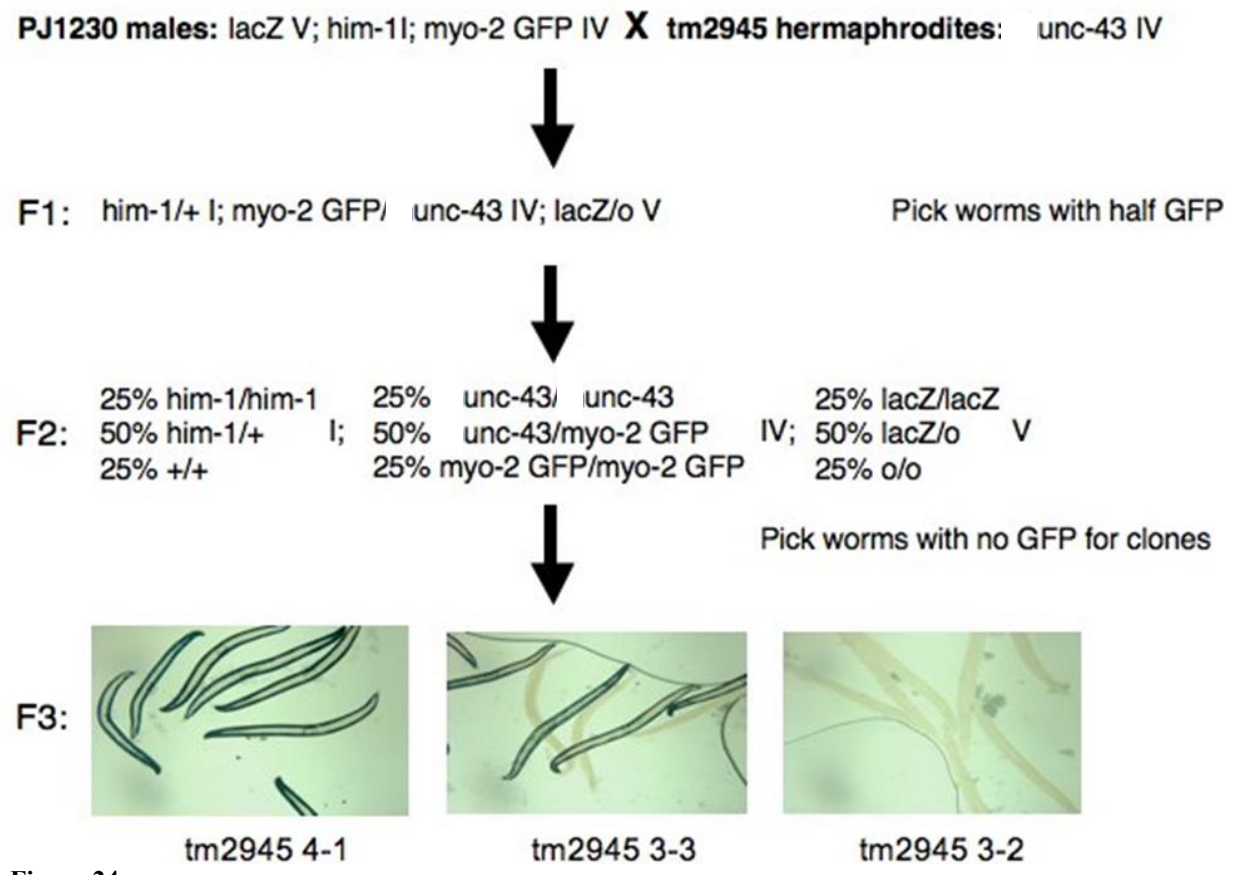

Figure 24

Mating scheme for generation of tm2945 lacZ strain. Males containing LacZ on V and GFP on IV were mated with tm2945 hermaphrodites (the IPD strain with a mutant *unc-43* on IV). Offspring with dim (1/2) GFP were picked to individual plates and allowed to self. From the clones containing GFP, individuals containing no GFP were again picked to individual plates and allowed to self. These individuals should be homozygous for the mutant *unc-43*. Several individuals from each of the clones were stained for LacZ in order to identify which clones are also homozygous for LacZ.

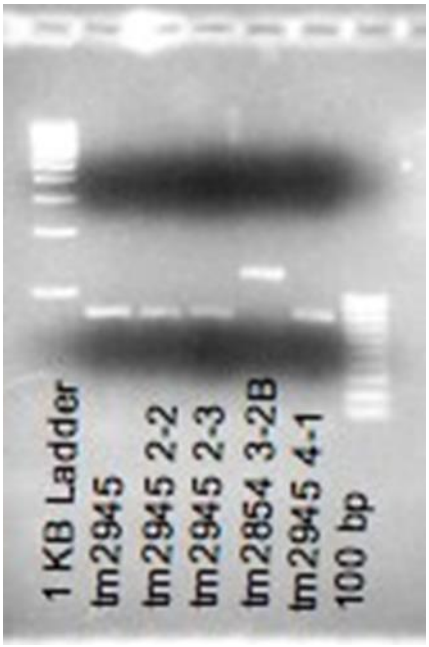

Figure 25
DNA gel of PCR from single-worms showing successful generation of a tm2945 (IPD), LacZ strain. Both the original tm2945 strain and the tm2945 4-1 strain generated by the cross have a PCR product of 790 bp due to the 502 bp deletion, in contrast to tm2854 3-2B, with a 244 bp deletion.

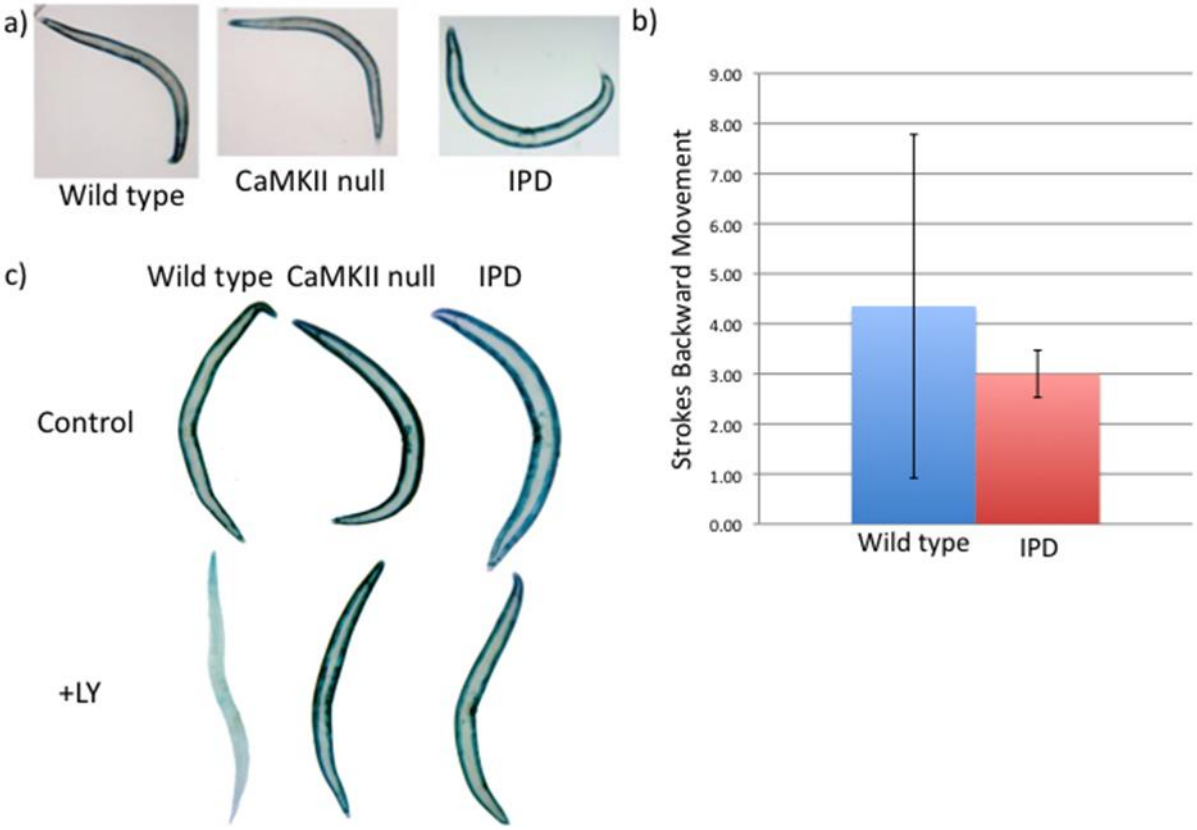

Figure 26

The *unc-43* IPD strain phenocopies the *unc-43* null strain. a) *wt*, CaMKII null, and IPD worms were grown to adulthood at 20C and stained for LacZ. b) Adult *wt* and IPD worms were lightly tapped on the head with a needle and the number of strokes of backwards movement that each worm made was counted (n=20). c) *wt* and *unc-43* null worms were picked as L4s to 160 µM LY294002 or DMSO plates. 48 hours later they were stained for LacZ.

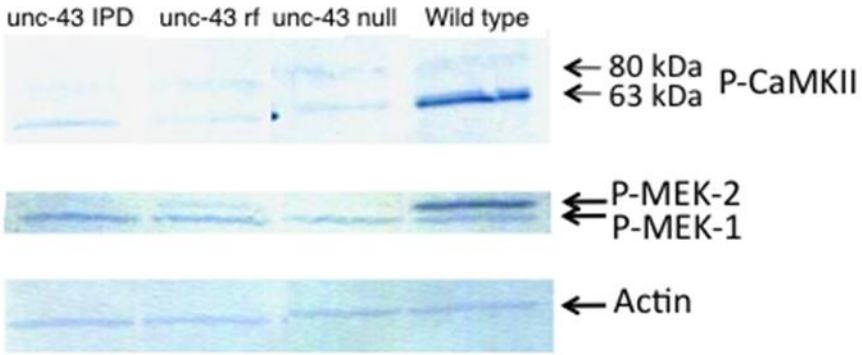

Figure 27

IPD mutation in *unc-43* results in reduced P-CaMKII and P-MEK-2. Adult *wt*, UNC-43 null, *unc-43* rf, and *unc-43* IPD worms raised to adulthood at 20C and collected for western blot samples. After blotting, the membrane was probed for P-CaMKII and then re-probed for P-MEK and actin.

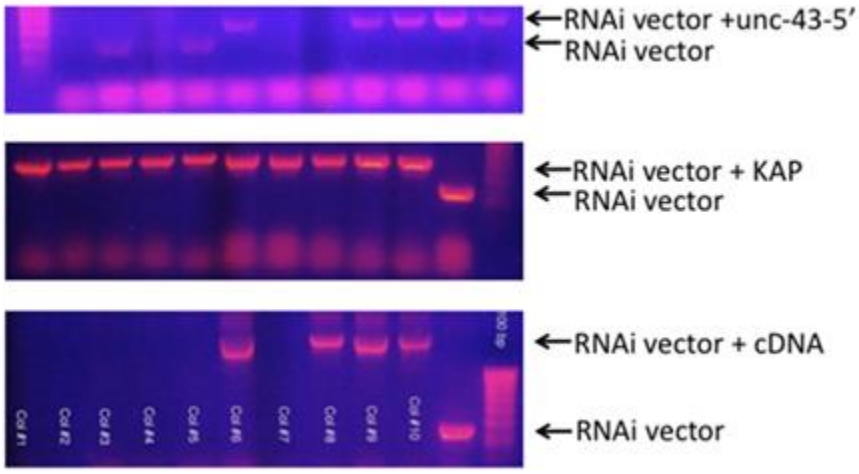

Figure 28

DNA gel showing colony PCR product of each of the successfully generated RNAi strains. In all cases, the RNAi vector with the appropriate insert is larger than the RNAi vector alone. The correct sequence of each strain was further verified by sequencing.

"spreading" in the 5' direction, but we expect that this will not be a problem with the C-terminal and KAP RNAi strains, as there is greater than a 10 kb distance to the catalytic domain. The specificities of these RNAi strains can be tested using RT-PCR. I have done some preliminary work with these RNAi strains, but thus far the results are inconclusive. These strains remain in the lab and can be used by future members to pursue answers to questions revolving around the role of splice forms of CaMKII in signaling for muscle protein degradation.

3.0 SIGNIFICANCE

3.1 CAMKII AND MUSCLE PROTEIN DEGRADATION VIA AUTOPHAGY

3.1.1 CaMKII hyperactivation as a cause of muscle wasting

While increased expression of CaMKII has been observed in denervated and aging rat soleus muscle [166], CaMKII activity has more often been shown to be correlated with muscle hypertrophy [113]. CaMKII calcium-independent activity is induced by both acute exercise and long-term endurance training in animal models and is correlated with increased muscle protein content under these conditions [113] It is, therefore, thought that the increased expression of CaMKII during atrophy in mammalian muscle might actually be a compensatory response, as opposed to part of the signal for degradation [113].

Despite the correlation between increased CaMKII activation and increased muscle protein content with exercise, a causal relationship has not been established. No inferences should be made regarding the role of CaMKII in promoting protein synthesis in animal models of exercise, since it has also been shown that during exercise degradation of non-contractile proteins may increase while degradation of contractile proteins decreases and that in the recovery period after intense exercise degradation of contractile proteins is increased [98]. This is especially true when one considers that in rats the different isoforms of CaMKII have been shown to be differentially activated and expressed under conditions of atrophy and hypertrophy [167]. It is most likely that varying levels of activity of the several isoforms of CaMKII can cause activation of multiple downstream pathways. Some of these pathways may directly or indirectly promote protein

degradation, while others may promote protein synthesis. It will be the combination of signaling through multiple pathways during hypertrophy or atrophy that will determine net gain or loss of protein in a particular state.

What my work has done is to establish a clear link between CaMKII activity and protein degradation via autophagy in muscle, as well as detail the pathway by which they are linked. I have shown that the activation of autophagy by CaMKII is the result of activation of specific, downstream substrates, and not a generalized response to the stress of CaMKII hyperactivation. This is especially evident in the fact that the effects of CaMKII hyperactivation on autophagy can be compensated for by changes in signaling in distant branches of the network.

This link between CaMKII activity and autophagy should be further explored in mammalian models of hypertrophy and atrophy. It is possible that activation of CaMKII and increased autophagy may play a role in the degradation of soluble proteins for energy metabolism during exercise or in exercise-induced muscle remodeling, an adaptive process which includes fiber type transformation, mitochondrial biogenesis, angiogenesis, and improved insulin sensitivity and metabolic flexibility [168]. Likewise, high intracellular calcium levels present in some types of atrophy [43, 114-116] may cause increased CaMKII activity and thereby increased autophagy, which may contribute to net loss of muscle protein. Further studies regarding the role of CaMKII in promoting autophagy in muscle would therefore be of interest both to those looking to build muscle mass and to those looking to prevent its loss.

3.1.2 A novel role for FEM-2

FEM-2 is a serine/threonine phosphatase type-2C (PP2C). Although it has been shown to dephosphorylate human and worm CaMKII *in vitro* [144, 145, 169], it is most well-known for its role in sex-determination in *C. elegans* [144]. Unlike other genes involved in *C. elegans* sex determination, *fem-2* is well conserved in rats and humans and is expressed outside of the worm germ line in both males and females throughout development [145]. This has led to the hypothesis that worm FEM-2 has roles outside of sex determination and that these roles may be conserved for human FEM-2 [144], [145]. One of these roles has been shown to be promotion of apoptosis in mammalian cells, possibly through the inactivation of CaMKII [145].

I have shown that FEM-2 reduction-of-function causes an increase in the amount of active, P-CaMKII *in vivo* in *C. elegans*. Based on the previous *in vitro* studies described above, this is likely due to FEM-2 functioning to directly dephosphorylate CaMKII. Therefore, through dephosphorylation of CaMKII, FEM-2 negatively regulates autophagy in *C. elegans* body-wall muscle. This, then, is another example a function of FEM-2 outside of sex-determination that may be conserved in humans. Historically, protein phosphatases have received less attention in signaling research than kinases; however, phosphatases have been shown to shape the spatiotemporal dynamics of signaling pathways and are now being considered as targets of drug development [170]. Further studies could address whether FEM-2 likewise regulates autophagy in humans, and, if so, in what tissues, under what conditions, and to what effect.

3.1.3 Raf S621 as a CaMKII target

Human C-Raf has been shown to be activated by phosphorylation of S338 by CaMKII [171], providing a possible link between calcium signaling and MAPK signaling. However, S338 is not conserved in *C. elegans* LIN-45 Raf. In *C. elegans,* this residue is a glutamic acid, which may mimic phosphorylation of S338. I have proposed Raf S621 as a site that may be directly phosphorylated by CaMKII, promoting activation of Raf. Further work could be done to show that *C. elegans* Raf and CaMKII physically interact *in vivo* and that CaMKII is capable of phosphorylating Raf S621 *in vitro*. Raf is a proto-oncogene, and the mechanisms of its activation are of interest for cancer biology. If Raf S621 were shown to be a direct target of CaMKII in *C. elegans*, then future work could look to see if CaMKII targets Raf S621 in humans and what effect this has on the activation of Raf, especially since this may mean that CaMKII has multiple Raf target sites. If phosphorylation of this site is necessary for Raf activation (as it appears to be in *C. elegans*) then kinases targeting S621, such as CaMKII, will be required to function at a basal level if Raf activation is to be stimulated by other pathways. If phosphorylation of this site is stimulatory but not necessary, then other pathways will be able to activate Raf without S621 phosphorylation, although S621 phosphorylation will modulate the extent to which activation occurs.

3.1.4 Module assembly and signaling specificity

In this thesis I have described a number of canonical signaling events, such as activation passing from:

A. FGFR→GRB2→RasGEF→Ras

B. IGFR→IRS→PI3K→PDK-1→AKT

C. Raf→MEK→MAPK.

These can be considered signaling modules, and can be assembled en bloc to form a network. Computationally, a signaling module has been defined as "a subset of the original biochemical network, which tends to be self-sufficient and have minimal dependency on the rest of the network" [172]. While the modules themselves may not be unique, the combinations of the modules to form a network in a particular tissue, developmental stage, or organism, may be unique. This allows for a set of inputs to be paired with appropriate, specific outputs, without the need to reinvent the mechanisms of signaling between them [173]. The way the modules interact with each other, for example through feedback, will determine the behavior of the network.

The data presented here describe a signaling network comprised of growth factor signaling and calcium signaling in *C. elegans* muscle, which, combined with our earlier work [71, 74, 76, 77, 99], give a picture of how three signaling modules (FGFR, IGFR, and Ca^{2+}) can interact to regulate a downstream process (autophagy) and muscle proteostasis.

Muscle FGFR is activated by LET-756 FGF, produced constitutively by muscle [174]. This autocrine signal promotes activation of Raf-MEK-MAPK and muscle protein degradation [76]. In worms undergoing oscillatory muscle contraction for sinusoidal movement (i.e. receiving input from motor neurons), calcium signaling fluctuates with a period in the range of 1 second, but is integrated over time by CaMKII [175]. This produces some level of continual kinase activity [165] (note P-CaMKII under basal conditions in *wt* worms, Figure 12), promoting protein degradation. The presence of both FGFR and CaMKII signals means the default state of the network is "on", and the muscle cells are therefore primed to signal for protein degradation. It is only inhibitory IGFR signaling, acting as the brake, which halts this process.

This combination of FGFR, IGFR, and calcium signaling modules to regulate autophagy may be unique to *C. elegans* body-wall muscle, or similar combinations may be found in other tissues/organisms. Regardless, study of this signaling network in *C. elegans* provides an opportunity to dissect how signaling pathways are organized such that the requirements of specificity are met with the relatively small number of gene products [173] controlling cell behavior. An understanding of the organization of signaling pathways can be applied to the engineering of signaling pathways for industrial and pharmacological purposes [176].

3.2 INTEGRATION AND BALANCE

3.2.1 Raf as a signaling hub

Graph theory analysis has shown that signaling networks display a "bow-tie" structure, in that information from multiple extracellular signals is "funneled" to a few intracellular hubs and then dispatched to cause diverse responses [177]. In other words, where multiple modules come together, a hub is required. Signaling hubs, or integrators, are responsible for sensing the various, possibly contradictory inputs, and responding with the appropriate output.

In the network described here, one protein, Raf, is responsible for integrating FGFR, IGFR, and calcium signals. While I have discussed Raf activation in the case of S259A mutation, it must be remembered that when both the S621 and S259 sites are available for phosphorylation, activation of Raf will be a probabilistic process, as both pS259 and pS621 are acted upon by their respective kinases and phosphatases. LIN-45 Raf, then, integrates FGFR, IGFR, and calcium signals through the combinatorial phosphorylation state of its four sites. Although we have a

general idea of the effects of each site, we do not yet know the combinatorial rules that govern Raf activation. Furthermore, neither the phosphorylation rate, nor the dephosphorylation rate at each site is likely to be independent of the state of the other sites.

For illustration, we can consider the hypothesis that pS259 inhibits activation independently of the state of S621. Our data imply that the class of Raf molecules that proceed to activation are probably S259-pS621. In physiological conditions where IGFR signaling and calcium signaling are balanced, net phosphorylation of the two sites happens at approximately the same rate and the majority of Raf molecules are phosphorylated on both S259 and S621 (pS259-pS621), preventing Raf activation. In a high calcium state, such as that modeled with the *unc-43* gf worms, phosphorylation of Raf on S621, in competition with its dephosphorylation, will outpace that of S259 phosphorylation, and a subset of Raf molecules will be in state S259-pS621, promoting Raf relocation, oligomerization, and activation. IGFR signaling, then, exerts its "braking power", by phosphorylation of Raf S259. In a low calcium state, such as that simulated by denervation, S259 phosphorylation will outstrip S621 phosphorylation and Raf will remain inactive. Indeed, although denervation promotes muscle protein degradation, this does not require autophagy, but instead requires the proteasome [71].

Human Raf has four more phosphorylation sites than *C. elegans* Raf [178, 179], expanding the possibilities for regulation. It should be remembered that even the system I have described here for LIN-45 Raf is only a part of the story. Undoubtedly other signals in body-wall muscle additionally converge upon Raf. The mechanisms by which Raf either integrates or isolates incoming signals likely depend on subcellular localization and in the assembly of multi-protein signaling complexes [180]. In the network I have described here, for example, the scaffold protein KSR-1 has been shown to have a role in transduction of the Raf-MEK-MAPK signal. Further

work could be done to understand the mechanism by which Raf integrates the IGFR, FGFR, and CaMKII signals.

The system that I have described here for quantifying the amount of autophagy in a muscle cell can also be further utilized to answer questions about the behavior of the network as a whole. For example, we can ask if the network is functioning as a switch or as a rheostat, or if the system can be turned off once turned on.

3.2.2 A downstream integrator, unc-51?

In this work, I have described signaling from Raf-MEK-MAPK promoting autophagy in an UNC-51-dependent manner. I have not identified what proteins are activated (or inactivated) between MAPK and unc-51 to promote autophagy. Work by other members of the Jacobson Lab has shown that RSK-p90 kinase (encoded by *C. elegans* rskn-1 and/or rskn-2) is likely functioning downstream of MAPK to promote autophagy. Raptor or UNC-51 is possibly downstream of RSK, based on the presence of potential RSK target sites.

Raptor is a scaffold protein that promotes activation of TOR, which inhibits autophagy by preventing the association of Atg1 (UNC-51) with Atg13 [61]. Formation of the Atg1-Atg13-Atg-17 complex is required for autophagy [62]. Raptor scaffolds UNC-51 to TOR and thus regulates the TOR-UNC-51 interaction. For signaling from MAPK to promote autophagy, RSK could either inhibit Raptor upstream of TOR, or RSK could be an independent, activating input downstream of TOR. If RSK is an independent input to UNC-51 downstream of TOR, then simultaneous reduction-of-function in MAPK should prevent protein degradation caused by knockdown of TOR. This has been shown to be the case.

What this then implies is that in order to induce autophagy by inhibition of TOR, wild-type levels of MAPK activity are required. Therefore, UNC-51 may be acting to integrate TOR and MAPK signaling. Further work needs to be done to verify the position of RSK, TOR, and UNC-51 in the network, but what these data suggest is that MAPK can activate autophagy independent of TOR inactivation. Activation of autophagy in starvation by inactivation of TOR has been well-characterized, but not as much is known about activation of autophagy in the fed state, when it is required for the clearing of damaged proteins and organelles and has been shown to be TOR-independent [181].

3.2.3 Maintaining the balance

In higher eukaryotes, autophagy is required for maintenance of tissue and cell homeostasis, as well as for protection from cancer and disease [181]. In muscle, autophagy is required for maintenance of muscle mass and prevention of myopathy [50, 58]. I have shown that knockdown of *unc-43* (CaMKII) by RNAi leads to a decrease in autophagy below that what is seen in null RNAi-treated animals. Shephard et al. [151] have shown that knockdown of *unc-43* leads to defects in myofibril and mitochondrial maintenance.

Due to the role of autophagy in the turnover of damaged organelles and proteins, it is unsurprising that autophagy is important for healthy aging. Lifespan extension is seen in *C. elegans* under conditions which promote autophagy, and it is thought that healthspan may be increased in higher eukaryotes by preventing age-related decreases in autophagy [182].

In *C. elegans*, age-related deterioration of body-wall muscle is correlated with impaired movement and is delayed in PI3K (*age-1*) lifespan-extension mutants [149]. Nuclear localization

of DAF-16, a transcription factor sequestered from the nucleus by Akt, is necessary but not sufficient for life-span extension in *C. elegans* [183]. On the other hand, blockage of Akt activity is both necessary and sufficient for lifespan extension, meaning that Akt likely inhibits other proteins that are involved in processes promoting lifespan extension [183]. Since CaMKII counters Akt activity at Raf, it would be interesting to see if *unc-43* RNAi treatment is sufficient to shorten lifespan and if CaMKII gf mutation is sufficient to extend lifespan. If lifespan is affected by variations in CaMKII activity, then further studies regarding lifespan and healthspan could be done with this system.

3.2.4 Mobilizing a resource

The muscle cell is poised to degrade its contents; in light of its role as a protein reservoir, this may aid in the rapid mobilization of amino acids when they are needed. Unfortunately, excessive protein breakdown can lead to muscle wasting, which is a difficult condition to reverse [48]. It is thought that the signaling mechanisms of disease lead to a change in the set-point of metabolism, such that protein degradation is enhanced and protein synthesis is inhibited [48]. Net protein degradation seen in catabolic conditions might then be treated by increasing protein synthesis and/or decreasing protein breakdown. How this is done will depend on many factors, including the age of the patient, who already may have altered metabolism.

For example, note that the degradation seen in CaMKII gain-of-function animals is progressive—young CaMKII gain-of-function worms do not show net loss of muscle protein, while mature and aging CaMKII gain-of-functions worms do. With the growth that is occurring during development, protein synthesis exceeds protein degradation and there is no net loss of

protein. It is only in the mature and aging animal, that the protein degradation phenotype becomes evident.

In muscle wasting, re-establishment of the balance between protein synthesis and degradation should be the goal, especially since therapies revolving around simply increasing protein intake by the patient have been shown to lack efficacy [48]. Despite this, therapies designed to target the signaling pathways leading to increased protein degradation have yet to be implemented, largely due to an imperfect understanding of the relevant networks. I have shown that co-modulation of seemingly disparate pathways can influence the downstream development of a pathological state. This implies that in diseases such as muscle wasting, where aberrant signaling is leading to disease, therapeutic targets may be found in pathways less obviously associated with the disease. Having targets in alternate pathways can be beneficial for the design of therapeutics if the main pathway is difficult to target. Pathways that may be difficult to target are those through which signaling would need to be increased to produce a desired effect because it is easier to design an inhibitor of a protein than to design a method of stimulating the activity of a protein. Additionally, targeting of pathways with many downstream functions can lead to unintentional effects. Detailed network maps, which can be tedious to generate, provide a resource that can be mined for therapeutic targets as well as reveal possible off-target effects of inhibiting a particular protein or pathway. This means that production of these network maps is potentially useful for the development of therapeutics based on modulation of signaling networks and production of such maps is a valid research goal.

4.0 MATERIALS AND METHODS

4.1 MEDIA AND REAGENTS

TB

10 g Tryptone

5 g NaCl

1.5 mL 1M NaOH

1000 mL ddH_2O

The above were mixed and sterilized by autoclaving.

NGM plates

2.5 g Bacto-peptone

3 g NaCl

17 g Bacto-agar

975 mL ddH_2O

The above was mixed and sterilized by autoclaving. After removal from the autoclave, the following was added: 1 ml 0.5% cholesterol in 95% ethanol

After the mixture had cooled enough that one could hold ones hands to the flask comfortably but before it solidified, the following were added:

2 ml sterile 0.5M $CaCl_2$, 1 ml sterile $MgSO_4$, 25 ml sterile 1M PO_4 buffer, pH 6.

After addition of these final ingredients, the media was poured into Petri dishes of the appropriate size. For general use, about 25 ml of the media was poured into 100 mm X 15 mm

Petri dishes. For mating and clonal selection, about 12.5 ml was added to 60 mm X 15 mm Petri dishes. For drug treatment, exactly 5 ml was added to 60 mm X 15 mm Petri dishes by sterile glass pipette (herein referred to as "drug plates").

BU

7.01 g Na_2HPO_4

4.0 g NaCl

3.0 g KH_2PO_4

1 L ddH_2O

The above were mixed and sterilized by autoclaving.

LacZ Stain

Oxidation Buffer

32 mM NaH_2PO_4

168 mM Na_2HPO_4

1 M $MgCl_2$

5 mM potassium ferrocyanide

5 mM potassium ferriccyanide

5-bromo, 4-chloro-indolyl-β-D-galactosidase (X-gal, 30 mg/mL in N,N-diMe-formamide) and oxidation buffer (in 200 µL aliquots) were stored at -20C. For use, one aliquot of oxidation buffer was thawed and 4 µL of X-gal was added to a final concentration of 0.006 mg/mL. Additionally, the thawed mixture should be warmed in the palm of the hand until no precipitate is visible immediately prior to use.

LB + antibiotic plates

10 g peptone

5 g yeast extract

5 g NaCl

17 g agar

1 L ddH_2O

The above were mixed and sterilized by autoclaving. After the media had cooled sufficiently, 1 µL filter-sterilized, 25 mg/mL Carbenicillin, 10 mg/ml Kanamycin, or 0.1 mg/mL Tetracycline, was added per mL of TB and the plates were poured.

TB + carbenicillin broth

10 g Tryptone

5 g NaCl

1.5 mL 1M NaOH

1 L ddH_2O

The above were mixed and sterilized by autoclaving. Prior to use, 1 µL filter-sterilized, 25 mg/mL Carbenicillin was added per mL of TB.

RNAi lite plates

1.5 g NaCl

4 g tryptone

20 g agar

980 mL ddH_2O

The above were mixed and sterilized by autoclaving. When the media had partially cooled, the following were added and the plates were poured:

25 mL 1M phosphate buffer (108.3 g anhydrous KH_2PO_4 and 35.6 g anhydrous K_2HPO_4 in 1 L ddH_2O and autoclaved.)

2 mL 0.5 M $CaCl_2$

1 mL 5mg/mL cholesterol in ethanol

10 mL lactose (20% solution, autoclaved)

1 mL 0.5M IPTG in ddH_2O

1 mL 25 mg/mL carbenicillin

4X SDS sample buffer

1.6 mL 0.5 M, pH 6.8 Tris (final 0.16M)

1 mL Glycerol (final 20%)

0.4 mL ß-mercaptoethanol (final 0.1%)

2 mL 20% SDS (final 8%)

40 µL 1% bromphenol blue (0.01%)

Running Buffer

12.1 g Tris base (final 25mM)

57.6 g Glycine (final 192mM)

4 g SDS (final 0.1%)

4L ddH_2O

The above were mixed and titrated to a pH of 8.6 with NaOH

Electroblot Buffer

600 mL methanol (final 20%)

9.11 g Tris base (final 25mM)

43.24g Glycine (192mM)

2.4 L ddH_2O

The above were mixed. The pH should be approximately 8.3. This solution should not be titrated.

Tris-buffered saline (TBS)

1.21 g Tris base (final 10 mM)

8.766 g NaCl (final 150mM)

1 L ddH_2O

The above were mixed and titrated to a pH of 8 with HCl. If the protocol called for TBS with Tween, then Tween-20 was added to a final concentration of 0.2%.

4.2 BACTERIAL STRAINS

The *E. coli* strain OP50, a uracil auxotroph, was obtained from the *Caenorhabditis* Genetics center (CGC). For feeding to *C. elegans*, OP50 was grown overnight in approximately 250 ml of TB and then 500 µL was plated per NGM plate. When not used immediately, OP50

culture was stored at 4°C for future use. OP50, a uracil auxotroph, is used due to its limited growth on NGM, preventing the development of an over-thick lawn. Most RNAi bacteria were obtained from the Ahringer Collection (Cambridge GeneService), unless they were constructed in-house as described in section 4.14.

4.3 NEMATODE STRAINS

The nematode strains used in this work are listed in Appendix A. All strains were maintained on NGM plates seeded with OP50 at 20°C, unless the nematode strain is indicated as being temperature sensitive, in which case the strain was maintained at 16°C. For strain maintenance, after the worms had consumed the *E. coli* on their old plate, a chunk of that plate was transferred to a fresh, seeded plate. In some cases, strains were maintained by picking individuals displaying the phenotype of the strain from a spent plate to a fresh plate.

In order to construct strains with more than one unlinked mutation or integrated transgene, standard genetic crosses were done. The scheme shown in Figure 24 is an example of a standard cross. In this case, as in most others, some integrated transgene (e.g., pharyngeal GFP driven by the *myo-2* promoter) or mutation with obvious phenotype (e.g., *daf* mutation) was used as a repulsion marker. In all cases, males for use in crosses were obtained by choosing or creating strains for mating with *him-8* or *him-1* mutation. Worms with *him* mutation have a high incidence of males in the population.

EMS mutagenesis was conducted to obtain suppressors of the *unc-43 n498* gf allele. After mutagenesis, individuals showing increased mobility were selected from the F2. One of these

individuals contained what has become the *n498j037* null allele. Double-stranded sequencing of the *unc-43* gene from these individuals revealed that this allele has the *n498* gf mutation as well as a second mutation resulting in a D236N substitution in the active site of the enzyme (see Appendix C). Western blots have showed that homozygous *n498j037* individuals have no pT286-CaMKII (Figure 29), leading us to conclude that this is likely null for CaMKII protein activity.

4.4 HISTOCHEMICAL STAINING

β-galactosidase activity

10-20 worms were picked into a 20 µL drop of BU placed on a frosted, glass slide. After the worms were picked into the BU, the slides were placed in a vacuum desiccator and allowed to dry at least until no liquid BU was visible and usually for about ninety minutes. Although usually by 45 minutes no liquid BU is visible, longer drying times consistently produce better stains. After drying, the slides were fixed at -20C in acetone in a Coplin jar for 3.5 minutes. Upon removal from the acetone, the slides were placed on aluminum plates at room temperature and allowed to dry for 12 minutes. Shorter drying times do not allow all the acetone to evaporate and result in poorly stained worms. Extended drying times allow the fixed worms to absorb moisture from the air and also results in poor staining. Drying times post-fixation in acetone may need to be adjusted based on room humidity. After drying, 20 µL of X-gal stain was added to each sample, as described [74] for 1.5-3h at room temperature. Every experiment included control animals, such that the length of staining was appropriate and did not result in over- or under-stained animals. During staining, slides are kept in a humidor composed of a large petri

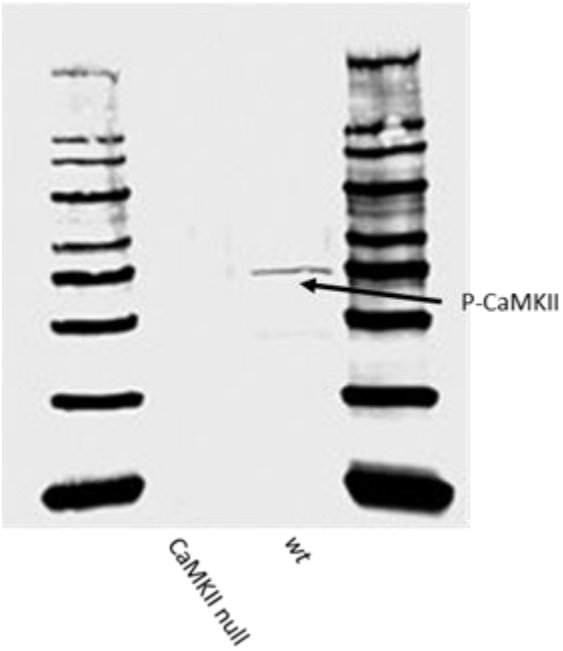

Figure 29

CaMKII null mutants lack P-CaMKII. a) *wt* and *unc-43* null worms were grown to adulthood at 20C and harvested for western blotting for pT286 CaMKII. 30 worms/lane.

dish containing a wet paper towel and sealed with parafilm to prevent drying of the slides. The worms stain blue where β-galactosidase is present (Figure 30). A benefit of this method, as opposed to a fluorometric assay of β-galactosidase activity, is that it is possible to see in which muscles and in what individuals β-galactosidase activity is present, instead of it being averaged.

Phalloidin Staining

Slides were prepared as for β-galactosidase staining, except they were fixed in acetone at -20C for 5 minutes. After fixation, slides were allowed to dry as above and then 20 µL of Phalloidin stain (2 units RITC-labeled Phalloidin from Molecular Probes, Inc. in 5% methanol) was added to each sample. After addition of stain, slides were sealed in a humidor and incubated overnight in the dark at room temperature before imaging.

4.5 BRIGHT-FIELD AND FLUORESCENCE MICROSCOPY AND IMAGING

For LacZ stains, after staining was completed, each slide was covered with a cover slip and observed with bright-field microscopy. Digital images were taken at approximately the same exposure for all images. Later, images were processed with Adobe Photoshop or Corel PHOTO-PAINT X6. Processing of the images involved equalization of color and illumination quality, as well as construction of composite images. When color corrections were made, they were applied equally to all areas of a composite.

GFP-expressing or phalloidin-stained worms were illuminated with UV light and observed with the appropriate filter. For GFP images, live worms were picked into 20 µL of BU

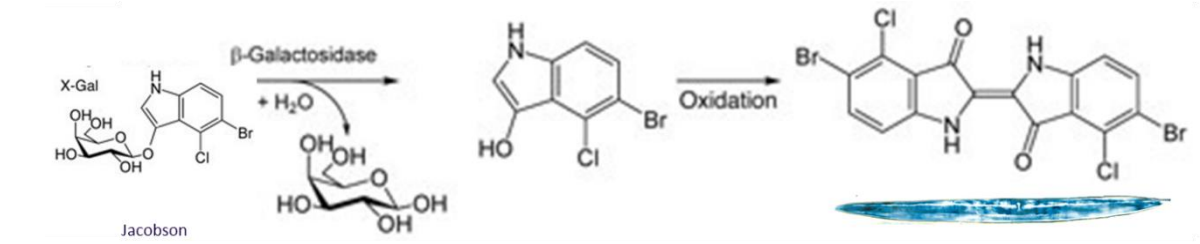

Figure 30

Diagram of the mechanism by which LacZ staining produces blue color.

and covered with a cover slip. When the worms' movement slowed enough for photography, images were collected at the same exposure.

4.6 RNAI TREATMENT

E. coli bacteria expressing gene-specific dsRNA were maintained on LB + carb plates. For use, one colony from the stock plate was picked into 5 mL of TB + carb broth and grown overnight by shaking in a 37C water bath. In all cases, null RNAi, consisting of the RNAi plasmid with no gene insert, was prepared and used concurrently with treatment RNAis as a negative control. After overnight growth, 250 µL of each culture was added to 750 µL of fresh LB + carb broth. To this, 10 µL of 0.5M IPTG was added and the tube was shaken in the 37C water bath for 4-5 hours. While the cultures grew, RNAi lite plates were placed on the bench to warm to room temperature. After the 4-5 hour incubation, 250 µL of RNAi culture was spread on the RNAi lite plate. Seeded plates were then incubated at 37C overnight. The next day, 5-10 L4 worms of the nematode strain of interest as well as the control strain were picked to the treatment and control RNAi plates. The plates were then stored at the temperature appropriate for the strain of interest. The L4s initially plated were allowed to grow to adulthood and lay the F1 on the RNAi plates. When the F1 reached L4 or adulthood (as appropriate for the experiment), they were harvested for further use. If the worms were being used for LacZ stains, they were picked to OP50 and allowed to crawl around for 2-24 hours to excrete the RNAi bacteria, which also contain ß-galactosidase.

4.7 SYNCHRONIZING WORM GROWTH

Plates of worms were grown until there was a large population of L1s and the *E. coli* food source had decreased. 3 mL of BU was then added to the surface of the plate, was swirled around, and then pipetted back up from the surface of the plate. The BU containing the worms was then added to a 15 mL centrifuge tube and allowed to sit for 2 minutes. Larger worms sink faster, and after 2 minutes the top 0.5 mL of BU, containing all L1s, was pipetted off and plated.

4.8 MOVEMENT ASSAYS

Well-fed, young-adult worms were picked into 20 µL of BU on a frosted, glass slide and observed under the dissecting scope. With a stop watch, the number of seconds it took for each worm to wag its head back and forth ten times was counted. This was converted into strokes/minute. For each worm observed, ten measurements were collected.

4.9 TEMPERATURE SHIFT

Prior to a temperature shift experiment, all worm strains, including controls, were kept at 16C. When the plates contained worms of the appropriate age, the worms were either settle synchronized, as described above, and allowed to grow to L4/young adult before use, or were hand-picked as L4s by inspection. For experiments requiring larger numbers of animals, the first method was used, while for experiments requiring less than about one hundred animals the second

method was used, since it allows for tighter control of age. Control animals were kept at 16C, while the experimental group was shifted to 25C. The experimental group remained at 25C for 24, 48, or 72 hours, as indicated, at which point they were stained for LacZ, used for movement assays, or collected for Western blot samples.

For heat shock experiments, worms were placed at 37C for 30 minutes before being transferred to 25C for 48 hours. Afterwards, samples were treated as described above.

4.10 IMMUNOBLOTTING

For Western blot samples, thirty worms were picked into 20 µL sterile ddH_2O. Immediately following picking, samples were frozen in liquid nitrogen and stored at -20C until use. 4X SDS buffer was warmed in the palm of the hand until fully liquid, then 8 µL was added to the frozen samples. A hot water bath was prepared by bringing a tray of water to boiling and then allowing to cool for two minutes. After cooling, the samples were placed in the hot water bath for two minutes. After the bath, the samples were agitated on a vortex mixer for five minutes and then centrifuged for 1 minute. Samples were then loaded into 12% or 4-20% gel cassettes from Lonza and run at approximately 120 volts for 1.5 hours.

To prep the Immobilon-P PVDF membrane (Millipore) for blotting, it was soaked for 3 minutes in methanol, 2 minutes in ddH_2O, and then left sit in electroblot buffer. The gels were loaded with the membrane into the electroblotter and allowed to sit for 15 minutes before blotting. They were electroblotted for 45 minutes at 12V, at which point the membrane was removed and blocked for 1 hour in a concentration of bovine serum albumin (BSA) or non-fat dry milk (NFDM)

in TBS + tween at a concentration optimized for the particular antibody. After blocking, the membrane was washed four times for five minutes each in TBS. The membrane was then incubated with the primary antibody in an optimized percentage of BSA or NFDM in TBS + tween overnight at 4°C with shaking. Primary antibodies used are listed below. In the morning, the membrane was washed with TBS four times for five minutes each and then incubated with the secondary antibody in the appropriate concentration of BSA or NFDM in TBST. The secondary antibodies were obtained from Jackson Immunoresearch and were peroxidase-conjugated, affinity-purified, donkey anti-mouse or anti-rabbit. After the blots were again rinsed in TBS four times for five minutes each, they were incubated with TMB peroxidase substrate (KPL) for detection. After detection they were rinsed in ddH_2O and allowed to dry. After drying, they were scanned and, where indicated, were analyzed with ImageJ software.

In all cases, blots were stripped by incubation in Restore PLUS stripping buffer (Thermo Scientific) for 7 minutes and then re-blocked and re-probed for actin as a loading control. Where blots were quantified, the amount of signal for each sample was calculated by dividing the amount of signal for the first primary antibody by the amount of actin signal. In some cases, blots were stripped and re-probed multiple times to detect various proteins of interest.

Primary antibodies

anti-pT286-CaMKII (Cell Signaling Technologies, no. 3361)

anti-QETVD CaMKII (Signosis, Ab-286)

anti-pS621 Raf (Abcam ab58542)

anti-P-MEK (Cell Signaling Technologies, no. 9121)

anti-P-MAPK (Cell Signaling, #9101)

anti-actin (Developmental Studies Hybridoma Bank, JLA-20)

The following primary antibodies were purchased from Cell Signaling Technologies: anti-pTpY-ERK (no. 9101), anti-ERK (no. 9102), anti-MEK (no. 9122). Anti -pT598pS601-BRaf (no. sc-28006) was from Santa Cruz Biotechnologies.

4.11 STATISTICAL ANALYSIS

Unless otherwise noted, all error bars represent standard errors of the mean. Statistical significances in differences between treatments were calculated using the Student's T-test, unless otherwise noted. Other methods of determining statistical significance used in this work are the chi-square test for independence and the Wilcox Rank Sum Test. In the case of the Chi square test, data were binned for each population prior to application of the test. p values less than 0.05 were considered significant.

4.12 CONFOCAL MICROSCOPY

For confocal microscopy, live animals were picked into 20 µL of BU on a frosted, glass slide and covered with a cover slip suspended by two dots of ink from a hydrophobic pen at opposite corners. After movement of live worms had slowed enough for photography, an Olympus FV1000 confocal microscope was used to observe autophagic vesicles in the muscle "belly". The depth of focus of the microscope exceeds the thickness of the muscle belly, so images at multiple focal planes were not taken. The focal plane containing the belly region of the muscle cells was

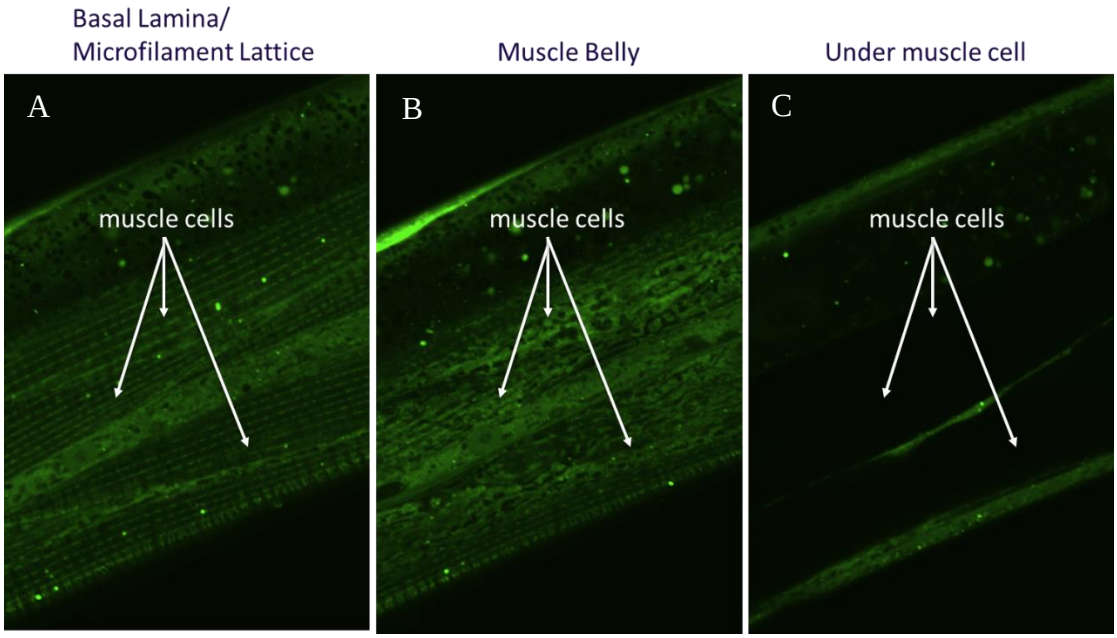

Figure 31

Characteristic LGG-1::GFP fluorescence in three different planes of *C. elegans* muscle cells as viewed by confocal microscopy: a) myofilament lattice, b) muscle belly, c) under the muscle cells. When collecting images for quantification of autophagic vesicles, the muscle belly plane was located relative to the myofilament lattice. It was additionally verified that other fluorescent structures did not underlie the muscle belly, to avoid complicating the analysis.

located relative to the rows of GFP::LGG-1 fluorescence associated with the sarcoplasmic reticulum, which is associated with the microfilament lattice (Figure 31). Autophagic vesicles were counted manually from the confocal images, and normalized to the area examined using ImageJ software.

4.13 DRUG TREATMENT

N^6,N^6-dimethyladenosine (DMA)

To prepare DMA plates, 50 µL of 50mM DMA in DMSO (Toronto Research Chemicals) was added to 5 mL NGM drug plates (prepared as described in section 4.1) to a final concentration of 0.5mM. The drug was sprinkled over the surface of the plate, and then the plate was rocked at room temperature for 24 hours. Approximately thirty L4 worms (experimental or control) were added to each plate. Worms were also added to control plates, which contained 1% v/v DMSO and were prepared in the same manner as the DMA plates. Plates were then maintained at 20C. After 48 hours, an additional dose of 50 µL of 50mM DMA was added to each plate. 72 hours later pictures of autophagic vesicles were obtained by the method described in section 4.12 of young-adult F1 worms (24 hours post-L4).

Cycloheximide

To prepare cycloheximide plates, 100 µL of 20 mg/mL cycloheximide (in H_2O) was added to 5 mL NGM drug plates, prepared as described in section 4.1. The final concentration of cycloheximide was 400 µg/mL. Plates were incubated on a rocker overnight at room temperature

and then were sealed and refrigerated for no more than one week before use. L4 worms were picked to cycloheximide plates and were incubated for 48 hours at the temperatures needed for the experiment. DMSO plates at 1% v/v were prepared and maintained in the same fashion. The survival rate of worms on cycloheximide at the non-permissive temperature was approximately 10% after 48 hours.

LY294002

To prepare LY294002 (BioMol, Enzo Life Sciences) plates, 50 µL of 16mM LY294002 in DMSO was plated onto 5 mL drug plates to a final concentration of 160uM. Plates were incubated at room temperature for 24 hours. Young adult or L4 worms were added to the plates and collected 48 hours later for Western blotting and LacZ staining. Control plates contained DMSO alone at 1% v/v.

4.14 RNAI STRAIN CONSTRUCTION

RNAi strains are constructed by transforming *E. coli* containing T7 polymerase under control of the lac operon with a plasmid (L44440, Fire collection) containing the gene of interest flanked 5' and 3' by the T7 promoter. Upon induction with IPTG, T7 polymerase is produced and transcribes the gene of interest, resulting in dsRNA.

To construct the plasmid containing the gene of interest, the gene of interest was amplified by PCR from the source and using the primers listed below (Go Taq polymerase, Promega). The L4440 plasmid, which we use for null RNAi treatments and which contains a multiple cloning

region and an ampicillin resistance gene, was isolated from *E. coli* maintained in the lab (QIAprep Spin Miniprep Kit, Qiagen). Both the PCR product and the L4440 plasmid were digested with the appropriate restriction enzymes, as listed below (NEB). If the plasmid was treated with Calf Intestinal Alkaline Phosphatase (CIP, NEB), it was subsequently gel-purified (Wizard SV gel and PCR clean-up system). The digested PCR product was also gel-purified. After purification, the PCR product and digested plasmid were ligated (T4 ligase, NEB). After ligation, the resultant plasmids were digested with a restriction enzyme (NEB) whose site in the multiple cloning region of L4440 was no longer present in the recombinant plasmid. This served to counter-select against plasmids that did not contain the gene of interest. Competent cells (OneShot Omnimax 2-T1^{R}, Invitrogen) were transformed with the recombinant plasmid. Colony PCR (Go Taq Polymerase, Promega), using the following primers external to the insert, was performed to identify colonies containing the recombinant plasmid.

Primers: R 5'GGC CTC TTC GCT ATT ACG C

L 5'GGA GAC CGG CAG ATC TGA TA

After colonies containing the recombinant plasmid were identified, plasmid DNA was isolated and sent for sequencing (Genewiz). Plasmids containing the gene of interest with no sequencing variations were selected for further use and were transformed into the bacterial strain used for RNAi, HT115 (DE3), which contains the gene for T7 polymerase under control of the lac operon, and lacks double-stranded RNAse III. RNAi plasmids in HT115 are maintained on LB + carb plates to select for the RNAi plasmid, but resultant strains were also streaked on Tet to verify the Tet-resistance of the HT115 strain. Colonies able to grow on both Carb and Tet were further verified to contain the RNAi plasmid by colony PCR.

unc-43-5'

PCR template: pKU24, plasmid containing *unc-43* cDNA

Primers: R 5'CGC GCG TCG ACT CAA AA CCA GAT AA

L 5'TAT ATA CTG CAG GGT GCC TTC TCA

Restriction enzymes: SalI, Pst1, counter-selection - HindIII

NLS RNAi

PCR template: *C. elegans* genomic DNA

Primers: R 5'TAT ATA GCG GCC GCA CAT CAT CGT CAG TAA TA

L 5'CGC GCG CTG CAG ACT TCT AAC TTC TCA GGT T

Restriction Enzymes: NotI, PstI, counter-selection – NheI

***unc-43* cDNA RNAi**

No PCR was needed in the construction of this strain, as a plasmid, pKU24, already containing the *unc-43* cDNA, was present in the lab. The portion of pKU24 to be inserted into the RNAi plasmid was removed by digestion of pKU24 with KpnI and NheI. After ligation of the fragment with L4440, plasmids were counter-selected with PstI.

APPENDIX A

STRAINS OF *C. ELEGANS* USED

Description	Strain code	Genotype
wt	PD55	tra-3(e1107) IV; sup-7; unc-54::lacZ (ccIs55) V
unc-43 (CaMKII) gf	PJ1182	unc-43(n498) IV; ccIs55 unc-54::lacZ V; Punc-54::daf-2+, Pgoa-1::GFP, rol-6 extrachromosomal (njex38)
unc-43 promoter::*gfp*	BC11417	dpy-5(e907); sEx 11417 [rCes K11E8.1d::GFP + pCeh361) unc-43::GFP
fem-2^{ts} rf	PJ1703	fem-2(b245ts) III; ccIs55 (unc-54::lacZ) V
unc-43 gf*; mpk-1* rf	PJ1720	mpk-1(n2521) III; him-8 (e1489), unc-43(n498) IV; unc-54::lacZ (ccIs55) V; Punc-54::daf-2+, Pgoa-1::GFP, rol-6 extrachromosomal (njex38)
CaMKII activity null	PJ1304	unc-43(n498) IV; ccIs55 unc-54::lacZ V; ??? (j037); Punc-54::daf-2+, Pgoa-1:GFP, rol-6 extrachromosomal (njex38)
unc-43 rf	PJ1088	unc-43(e408) IV; ccIs55a(unc-54::lacZ) V
CaMKII IPD	PJ1295	unc-43(tm2945) IV; unc-54::lacZ (ccIs55) V
CaMKII protein null	PJ1251	unc-43(n1186 n498) IV; unc-54::lacZ(ccIs55) V
Constitutively active *Dros.* MEK with heat shock-inducible MAPK	PJ1115	gaIs37 (pEF1α::Dmek hs::mpk-1) IV; ccIs55 (unc-54::lacZ) V
Hyper MAPK; *unc-51* rf	PJ1236	gaIs37(EF1a::Dmek hs::mpk-1) IV; unc-51(e369) unc-54::lacZ(ccIs55) V

unc-43 gf; *unc-51* rf	PJ1726	unc-43(n498) IV; unc-51(e369) unc-54::lacZ(ccIs55) V
unc-43 gf; *lgg-1::gfp*	PJ749	unc-43(n498gf) IV; adIs2122 [lgg-1::GFP + pRF4(rol-6(su1006)] ?
lgg-1::gfp	DA2123	adIs2122 [gfp::lgg-1 + pRF4(rol-6(su1006)] ?
unc-43 rf; *daf-2*^{ts} rf	PJ1729	daf-2(m41ts) III; unc-43 (e408) IV; unc-54::lacZ (ccIs55) V
daf-2^{ts} rf	PJ1123	daf-2(m41ts) III; ccIs55(unc-54::lacZ) V

APPENDIX B

RNAi SEQUENCE DATA

unc-43 cDNA RNAi vs. *unc-43* spliced

```
Comparison of: (A) ./wwwtmp/.30097.1.seq cDNA unc-43-L 1190 bp
- 1190 nt (B) ./wwwtmp/.30097.2.seq unc-43e spliced 2505 bp
- 2505 nt  using matrix file: DNA (5/-4), gap-open/ext: -14/-4 E(limit)   0.05
94.1% identity in 1140 nt overlap (66-1189:225-1361); score: 5080 E(10000):

          70        80        90       100       110       120
cDNA   ATGATGAACGCAAGCACCAAGTTTAGTGACAATTACGATGTGAAGGAGGAACTTGGAAAA
       ::::::::::::::::::::::::::::::::::::::::::::::::::::::::::::
unc-43 ATGATGAACGCAAGCACCAAGTTTAGTGACAATTACGATGTGAAGGAGGAACTTGGAAAA
          230       240       250       260       270       280

         130       140       150       160       170       180
cDNA   GGTGCCTTCTCAGTTGTTCGTCGTTGTGTTCATAAAACCACGGGCCTCGAGTTTGCTGCC
       ::::::::::::::::::::::::::::::::::::::::::::::::::::::::::::
unc-43 GGTGCCTTCTCAGTTGTTCGTCGTTGTGTTCATAAAACCACGGGCCTCGAGTTTGCTGCC
          290       300       310       320       330       340

         190       200       210       220       230       240
cDNA   AAAATCATCAACACAAAGAAGCTATCCGCTCGTGACTTTCAGAAACTTGAGAGGGAAGCC
       ::::::::::::::::::::::::::::::::::::::::::::::::::::::::::::
unc-43 AAAATCATCAACACAAAGAAGCTATCCGCTCGTGACTTTCAGAAACTTGAGAGGGAAGCC
          350       360       370       380       390       400

         250       260       270       280       290       300
cDNA   AGAATTTGCAGAAAACTCCAGCATCCAAATATTGTTAGACTACACGACAGTATTCAAGAG
       ::::::::::::::::::::::::::::::::::::::::::::::::::::::::::::
unc-43 AGAATTTGCAGAAAACTCCAGCATCCAAATATTGTTAGACTACACGACAGTATTCAAGAG
          410       420       430       440       450       460

         310       320       330       340       350       360
cDNA   GAATCATTCCATTATCTGGTTTTTGATCTCGTTACCGGAGGAGAACTGTTTGAGGACATT
       ::::::::::::::::::::::::::::::::::::::::::::::::::::::::::::
unc-43 GAATCATTCCATTATCTGGTTTTTGATCTCGTTACCGGAGGAGAACTGTTTGAGGACATT
          470       480       490       500       510       520

         370       380       390       400       410       420
cDNA   GTTGCTCGCGAGTTTTATTCAGAAGCGGATGCAAGTCATTGCATTCAACAAATTCTCGAA
       ::::::::::::::::::::::::::::::::::::::::::::::::::::::::::::
unc-43 GTTGCTCGCGAGTTTTATTCAGAAGCGGATGCAAGTCATTGCATTCAACAAATTCTCGAA
          530       540       550       560       570       580

         430       440       450       460       470       480
cDNA   TCGATTGCTTATTGCCACTCTAACGGTATTGTTCACAGAGACTTGAAGCCAGAAAACTTG
       ::::::::::::::::::::::::::::::::::::::::::::::::::::::::::::
unc-43 TCGATTGCTTATTGCCACTCTAACGGTATTGTTCACAGAGACTTGAAGCCAGAAAACTTG
          590       600       610       620       630       640
```

```
         490       500       510       520       530       540
cDNA   CTTCTCGCATCTAAAGCGAAGGGAGCTGCTGTAAAGCTTGCCGATTTTGGTCTTGCAATC
       ::::::::::::::::::::::::::::::::::::::::::::::::::::::::::::
unc-43 CTTCTCGCATCTAAAGCGAAGGGAGCTGCTGTAAAGCTTGCCGATTTTGGTCTTGCAATC
          650       660       670       680       690       700

         550       560       570       580       590       600
cDNA   GAAGTGAACGATAGTGAAGCATGGCACGGATTTGCTGGAACTCCAGGATACTTGTCGCCA
       ::::::::::::::::::::::::::::::::::::::::::::::::::::::::::::
unc-43 GAAGTGAACGATAGTGAAGCATGGCACGGATTTGCTGGAACTCCAGGATACTTGTCGCCA
          710       720       730       740       750       760

         610       620       630       640       650       660
cDNA   GAAGTTCTCAAGAAGGATCCATACTCAAAGCCAGTTGATATCTGGGCTTGTGGTGTCATT
       ::::::::::::::::::::::::::::::::::::::::::::::::::::::::::::
unc-43 GAAGTTCTCAAGAAGGATCCATACTCAAAGCCAGTTGATATCTGGGCTTGTGGTGTCATT
          770       780       790       800       810       820

         670       680       690       700       710       720
cDNA   CTGTACATCCTTCTTGTTGGATACCCACCATTCTGGGATGAGGACCAACACCGTTTATAC
       ::::::::::::::::::::::::::::::::::::::::::::::::::::::::::::
unc-43 CTGTACATCCTTCTTGTTGGATACCCACCATTCTGGGATGAGGACCAACACCGTTTATAC
          830       840       850       860       870       880

         730       740       750       760       770       780
cDNA   GCACAAATCAAGGCTGGAGCCTATGATTACCCGAGCCCCGAATGGGATACGGTGACCCCG
       ::::::::::::::::::::::::::::::::::::::::::::::::::::::::::::
unc-43 GCACAAATCAAGGCTGGAGCCTATGATTACCCGAGCCCCGAATGGGATACGGTGACCCCG
          890       900       910       920       930       940

         790       800       810       820       830       840
cDNA   GAGGCAAAAAGCCTCATCGACAGCATGCTGACGGTGAACCCAAAGAAGCGTATCACCGCT
       ::::::::::::::::::::::::::::::::::::::::::::::::::::::::::::
unc-43 GAGGCAAAAAGCCTCATCGACAGCATGCTGACGGTGAACCCAAAGAAGCGTATCACCGCT
          950       960       970       980       990      1000

         850       860       870       880       890       900
cDNA   GATCAGGCCTTGAAAGTCCCATGGATTTGCAATCGCGAACGCGTTGCATCAGCTATCCAC
       ::::::::::::::::::::::::::::::::::::::::::::::::::::::::::::
unc-43 GATCAGGCCTTGAAAGTCCCATGGATTTGCAATCGCGAACGCGTTGCATCAGCTATCCAC
         1010      1020      1030      1040      1050      1060

         910       920       930       940       950       960
cDNA   AGACAGGATACTGTTGACTGCTTGAAGAAATTCAATGCNANGGCGGAAGTTGAAGGNGGC
       :::::::::::::::::::::::::::::::::::: : ::::::::::::::: :::
unc-43 AGACAGGATACTGTTGACTGCTTGAAGAAATTCAATGCAA-GGCGGAAGTTGAAGGCGGC
        1070      1080      1090      1100       1110      1120

         970       980       990      1000      1010      1020
cDNA   AATATCGACTGTCAAAATGGTGACACGAATGTCGGNAGTTCTTCNAACTTCCGACTCCCA
       ::::::: :::::::::::::::::::::::::: :::::::: :::::::::::: :
unc-43 AATATCGGCTGTCAAAATGGTGACACGAATGTCGGGAGTTCTTCGAACTTCCGACTCC-A
         1130      1140      1150      1160      1170      1180



       1030      1040      1050      1060      1070       1080
cDNA   CTGGNTCAGNTCGCATCGAATGGATCAACGACGCACGATGCGTCNNNGGNNN-AGGAN-A
       :::: :::: :::::::::::::::::::::::::::::::   ::    ::::  :
unc-43 CTGGATCAG-TCGCATCGAATGGATCAACGACGCACGATGCGTCACAGGTGGCAGGAACA
        1190       1200      1210      1220      1230      1240
```

NLS RNAi vs. *unc-43*

```
Comparison of: (A) ./wwwtmp/.12748.1.seq RNAi NLS-L 792 bp
- 792 nt (B) ./wwwtmp/.12748.2.seq unc-43m genomic 6826 bp
- 6826 nt  using matrix file: DNA (5/-4), gap-open/ext: -14/-4 E(limit)   0.05
99.6% identity in 242 nt overlap (23-264:220-461); score: 1201 E(10000): 6.3e-91

             30        40        50        60        70        80
RNAi   ACATCATCGTCAGTAAAACGAAGTAGTCGACCGGAAAGTGCACGACAGGCACCAAGAGAT
       ::::::::::::::::::::::::::::::::::::::::::::::::::::::::::::
unc-43 ACATCATCGTCAGTAAAACGAAGTAGTCGACCGGAAAGTGCACGACAGGCACCAAGAGAT
     220       230       240       250       260       270

             90       100       110       120       130       140
RNAi   ACCACAGGATCCCTTTACTCAAATTTAACAGCTTCCTCATCAACAGTATCTGCGTGTTCG
       ::::::::::::::::::::::::::::::::::::::::::::::::::::::::::::
unc-43 ACCACAGGATCCCTTTACTCAAATTTAACAGCTTCCTCATCAACAGTATCTGCGTGTTCG
     280       290       300       310       320       330

            150       160       170       180       190       200
RNAi   GCGCCAGAAATTGTTGTGCTCAAAAAAGAGCAGGTGGTTTTGGCAGTAGATCATAAAGAT
       ::::::::::::::::::::::::::::::::::::::::::::::::::::::::::::
unc-43 GCGCCAGAAATTGTTGTGCTCAAAAAAGAGCAGGTGGTTTTGGCAGTAGATCATAAAGAT
     340       350       360       370       380       390

            210       220       230       240       250       260
RNAi   CAAGTGGACGAACAGAAAAAGAGGAATGAACAAGTGGTTAAGAAACCTGAGAAGTTAGAA
       :::::::::::::::::::: ::::::::::::::::::::::::::::::::::::::
unc-43 CAAGTGGACGAACAGAAAAAGAAGAATGAACAAGTGGTTAAGAAACCTGAGAAGTTAGAA
     400       410       420       430       440       450

RNAi   GT
       ::
unc-43 GT
     460
```

unc-43-5' RNAi vs. *unc-43* spliced

```
Comparison of: (A) ./wwwtmp/.30099.1.seq 5'RNAi unc-43-L 1094 bp
- 1094 nt (B) ./wwwtmp/.30099.2.seq unc-43e spliced 2505 bp
- 2505 nt  using matrix file: DNA (5/-4), gap-open/ext: -14/-4 E(limit)   0.05
99.5% identity in 208 nt overlap (87-294:283-490); score: 1031 E(10000): 4.8e-77

          90       100       110       120       130       140
5'RNAi AGGGTGCCTTCTCAGTTGTTCGTCGTTGTGTTCATAAAACCACGGGCCTCGAGTTTGCTG
       : ::::::::::::::::::::::::::::::::::::::::::::::::::::::::::::
unc-43 AAGGTGCCTTCTCAGTTGTTCGTCGTTGTGTTCATAAAACCACGGGCCTCGAGTTTGCTG
            290       300       310       320       330       340



         150       160       170       180       190       200
5'RNAi CCAAAATCATCAACACAAAGAAGCTATCCGCTCGTGACTTTCAGAAACTTGAGAGGGAAG
       ::::::::::::::::::::::::::::::::::::::::::::::::::::::::::::
unc-43 CCAAAATCATCAACACAAAGAAGCTATCCGCTCGTGACTTTCAGAAACTTGAGAGGGAAG
```

```
            350       360       370       380       390       400


        210       220       230       240       250       260
5'RNAi CCAGAATTTGCAGAAAACTCCAGCATCCAAATATTGTTAGACTACACGACAGTATTCAAG
       ::::::::::::::::::::::::::::::::::::::::::::::::::::::::::::
unc-43 CCAGAATTTGCAGAAAACTCCAGCATCCAAATATTGTTAGACTACACGACAGTATTCAAG
            410       420       430       440       450       460

        270       280       290
5'RNAi AGGAATCATTCCATTATCTGGTTTTTGA
       ::::::::::::::::::::::::::::
unc-43 AGGAATCATTCCATTATCTGGTTTTTGA
            470       480       490
```

APPENDIX C

SEQUENCE DATA FOR THE *UNC-43 n498j037* ALLELE

wt and UNC-43 *n498j037* protein sequences

unc-43 *wt*
MMNASTKFSDNYDVKEELGKGAFSVVRRCVHKTTGLEFAAKIINTKKLSARDFQKLER
EARICRKLQHPNIVRLHDSIQEESFHYLVFDLVTGGELFEDIVAREFYSEADASHCIQQILE
SIAYCHSNGIVHRDLKPENLLLASKAKGAAVKLADFGLAIEVNDSEAWHGFAGTPGYLS
PEVLKKDPYSKPVDIWACGVILYILLVGYPPFWDEDQHRLYAQIKAGAYDYPSPEWDTV
TPEAKSLIDSMLTVNPKKRITADQALKVPWICNRERVASAIHRQDTVDCLKKFNARRKL
KVAICZ
E108K = gf, D236 = catalytic domain residue conserved in 70% of all CaMKII orthologues/paralogues, T286 = autophosphorylation site, R283 = autoinhibitory domain residue that purportedly interacts with D236

PJ1304 (D236N)
MMNASTKFSDNYDVKEELGKGAFSVVRRCVHKTTGLEFAAKIINTKKLSARDFQKLER
EARICRKLQHPNIVRLHDSIQEESFHYLVFDLVTGGELFEDIVAREFYSEADASHCIQQILE
SIAYCHSNGIVHRDLKPENLLLASKAKGAAVKLADFGLAIEVNDSEAWHGFAGTPGYLS
PEVLKKDPYSKPVDIWACGVILYILLVGYPPFWDEDQHRLYAQIKAGAYDYPSPEWNTV
TPEAKSLIDSMLTVNPKKRITADQALKVPWICNRERVASAIHRQDTVDCLKKFNARRKL
KVAICZ
D236N = CaMKII activity null substitution

unc-43 n498j037 (PJ1304) vs. *wt unc-43*

```
Comparison of:(A) ./wwwtmp/lalign/.12323.1.seq 1304mid
- 771 nt(B) ./wwwtmp/lalign/.12323.2.seq wt
- 2062 nt using matrix file: DNA, gap penalties: -14/-4

  98.7% identity in 773 nt overlap; score: 3786 E(10,000): 5.3e-307



               10          20        30        40        50
1304mi TATTCTTTTNNNNNN--CTTTCNTAATTTTTTTTCGGTTTCAAAAGTTGTGATATATCTG
       :::::::::        ::::: ::::::::::::::::::::::::::::::::::::
wt     TATTCTTTTGAAAACAACTTTCATAATTTTTTTTCGGTTTCAAAAGTTGTGATATATCTG
      1270      1280      1290      1300      1310      1320
```

```
        60         70         80         90        100        110
1304mi TGATTAATATCAGAAGAGATTTCTTTAAAAAAAATTACATTTTCAGCCAGAAAACTTGCT
       ::::::::::::::::::::::::::::::::::::::::::::::::::::::::::::
wt      TGATTAATATCAGAAGAGATTTCTTTAAAAAAAATTACATTTTCAGCCAGAAAACTTGCT
       1330       1340       1350       1360       1370       1380

       120        130        140        150        160        170
1304mi TCTCGCATCTAAAGCGAAGGGAGCTGCTGTAAAGCTTGCCGATTTTGGTCTTGCAATCGA
       ::::::::::::::::::::::::::::::::::::::::::::::::::::::::::::
wt      TCTCGCATCTAAAGCGAAGGGAGCTGCTGTAAAGCTTGCCGATTTTGGTCTTGCAATCGA
       1390       1400       1410       1420       1430       1440

       180        190        200        210        220        230
1304mi AGTGAACGATAGTGAAGCATGGCACGGATTTGCTGGAACTCCAGGATACTTGTCGCCAGA
       ::::::::::::::::::::::::::::::::::::::::::::::::::::::::::::
wt      AGTGAACGATAGTGAAGCATGGCACGGATTTGCTGGAACTCCAGGATACTTGTCGCCAGA
       1450       1460       1470       1480       1490       1500

       240        250        260        270        280        290
1304mi AGTTCTCAAGAAGGATCCATACTCAAAGCCAGTTGATATCTGGGCTTGTGGTATGTATTT
       ::::::::::::::::::::::::::::::::::::::::::::::::::::::::::::
wt      AGTTCTCAAGAAGGATCCATACTCAAAGCCAGTTGATATCTGGGCTTGTGGTATGTATTT
       1510       1520       1530       1540       1550       1560

       300        310        320        330        340        350
1304mi TAAAGTTTAATATTTCGAGTTAAGAATCTAATTTATAGGTGTCATTCTGTACATCCTTCT
       ::::::::::::::::::::::::::::::::::::::::::::::::::::::::::::
wt      TAAAGTTTAATATTTCGAGTTAAGAATCTAATTTATAGGTGTCATTCTGTACATCCTTCT
       1570       1580       1590       1600       1610       1620

       360        370        380        390        400        410
1304mi TGTTGGATACCCACCATTCTGGGATGAGGACCAACACCGTTTATACGCACAAATCAAGGC
       ::::::::::::::::::::::::::::::::::::::::::::::::::::::::::::
wt      TGTTGGATACCCACCATTCTGGGATGAGGACCAACACCGTTTATACGCACAAATCAAGGC
       1630       1640       1650       1660       1670       1680

       420        430        440        450        460        470
1304mi TGGAGCCTATGATGTATGTTGAGCTTAAACTAGTTGAAACTATTTTAAAAATTCAAAATT
       ::::::::::::::::::::::::::::::::::::::::::::::::::::::::::::
wt      TGGAGCCTATGATGTATGTTGAGCTTAAACTAGTTGAAACTATTTTAAAAATTCAAAATT
       1690       1700       1710       1720       1730       1740

       480        490        500        510        520        530
1304mi TCAGTACCCGAGCCCCGAATGGAATACGGTGACCCCGGAGGCAAAAAGCCTCATCGACAG
       :::::::::::::::::::::: ::::::::::::::::::::::::::::::::::::
wt      TCAGTACCCGAGCCCCGAATGGGATACGGTGACCCCGGAGGCAAAAAGCCTCATCGACAG
       1750       1760       1770       1780       1790       1800



       540        550        560        570        580        590
1304mi CATGCTGACGGTGAACCCAAAGAAGCGTATCACCGCTGATCAGGCCTTGAAAGTCCCATG
       ::::::::::::::::::::::::::::::::::::::::::::::::::::::::::::
wt      CATGCTGACGGTGAACCCAAAGAAGCGTATCACCGCTGATCAGGCCTTGAAAGTCCCATG
       1810       1820       1830       1840       1850       1860
```

```
      600       610       620       630       640       650
1304mi GATTTGCGTATGTTTTTTTTTGAATTATTTTTTGAATTCGAGAATTTATGATTTTCAAAT
       ::::::::::::::::::::::::::::::::::::::::::::::::::::::::::::
wt     GATTTGCGTATGTTTTTTTTTGAATTATTTTTTGAATTCGAGAATTTATGATTTTCAAAT
      1870      1880      1890      1900      1910      1920

      660       670       680       690       700       710
1304mi TTTTCTATAAACATTTAAAGAATTTCAGAATCGCGAACGCGTTGCATCAGCTATCCACAG
       ::::::::::::::::::::::::::::::::::::::::::::::::::::::::::::
wt     TTTTCTATAAACATTTAAAGAATTTCAGAATCGCGAACGCGTTGCATCAGCTATCCACAG
      1930      1940      1950      1960      1970      1980

      720       730       740       750       760       770
1304mi ACAGGATACTGTTGACTGCTTGAAGAAATTCAATGCAAGGCGGAAGTTGAAGG
       :::::::::::::::::::::::::::::::::::::::::::::::::::::
wt     ACAGGATACTGTTGACTGCTTGAAGAAATTCAATGCAAGGCGGAAGTTGAAGG
      1990      2000      2010      2020      2030      2040
```

BIBLIOGRAPHY

1. Hobert, O., et al., *A conserved LIM protein that affects muscular adherens junction integrity and mechanosensory function in Caenorhabditis elegans.* J Cell Biol, 1999. **144**(1): p. 45-57.
2. Exeter, D. and D.A. Connell, *Skeletal muscle: functional anatomy and pathophysiology.* Semin Musculoskelet Radiol, 2010. **14**(2): p. 97-105.
3. Levine, B. and G. Kroemer, *Autophagy in the pathogenesis of disease.* Cell, 2008. **132**(1): p. 27-42.
4. Hudmon, A. and H. Schulman, *Structure-function of the multifunctional Ca2+/calmodulin-dependent protein kinase II.* Biochem J, 2002. **364**(Pt 3): p. 593-611.
5. Brooks, S.V., *Current topics for teaching skeletal muscle physiology.* Adv Physiol Educ, 2003. **27**(1-4): p. 171-82.
6. Lisman, J., H. Schulman, and H. Cline, *The molecular basis of CaMKII function in synaptic and behavioural memory.* Nat Rev Neurosci, 2002. **3**(3): p. 175-90.
7. Lynch, G.S., *Tackling Australia's future health problems: developing strategies to combat sarcopenia--age-related muscle wasting and weakness.* Intern Med J, 2004. **34**(5): p. 294-6.
8. Evans, W.J. and W.W. Campbell, *Sarcopenia and age-related changes in body composition and functional capacity.* J Nutr, 1993. **123**(2 Suppl): p. 465-8.
9. Welle, S., *Cellular and molecular basis of age-related sarcopenia.* Can J Appl Physiol, 2002. **27**(1): p. 19-41.
10. Di Iorio, A., et al., *Sarcopenia: age-related skeletal muscle changes from determinants to physical disability.* Int J Immunopathol Pharmacol, 2006. **19**(4): p. 703-19.
11. Lin, J., et al., *Age-related cardiac muscle sarcopenia: Combining experimental and mathematical modeling to identify mechanisms.* Exp Gerontol, 2008. **43**(4): p. 296-306.
12. Parise, G. and M. De Lisio, *Mitochondrial theory of aging in human age-related sarcopenia.* Interdiscip Top Gerontol, 2010. **37**: p. 142-56.
13. Liu, L.K., et al., *Age-related skeletal muscle mass loss and physical performance in Taiwan: Implications to diagnostic strategy of sarcopenia in Asia.* Geriatr Gerontol Int, 2013.
14. Paniagua, R., et al., *Ultrastructure of invertebrate muscle cell types.* Histol Histopathol, 1996. **11**(1): p. 181-201.
15. Firulli, A.B. and E.N. Olson, *Modular regulation of muscle gene transcription: a mechanism for muscle cell diversity.* Trends Genet, 1997. **13**(9): p. 364-9.
16. Brand, T., *Heart development: molecular insights into cardiac specification and early morphogenesis.* Dev Biol, 2003. **258**(1): p. 1-19.
17. Topouzis, S. and M.W. Majesky, *Smooth Muscle Lineage Diversity in the Chick Embryo.* Dev Biol, 1996. **178**(2): p. 430-45.
18. Kelvin, D.J., et al., *A model for the modulation of muscle cell determination and differentiation by growth factors.* Biochem Cell Biol, 1989. **67**(9): p. 575-80.

19. Webb, R.C., *Smooth muscle contraction and relaxation.* Adv Physiol Educ, 2003. **27**(1-4): p. 201-6.
20. Van Lierop, J.E., et al., *Activation of smooth muscle myosin light chain kinase by calmodulin. Role of LYS(30) and GLY(40).* J Biol Chem, 2002. **277**(8): p. 6550-8.
21. Hashimoto, Y. and T.R. Soderling, *Phosphorylation of smooth muscle myosin light chain kinase by Ca2+/calmodulin-dependent protein kinase II: comparative study of the phosphorylation sites.* Arch Biochem Biophys, 1990. **278**(1): p. 41-5.
22. Bijnens, B., et al., *Myocardial motion and deformation: What does it tell us and how does it relate to function?* Fetal Diagn Ther, 2012. **32**(1-2): p. 5-16.
23. Pinnell, J.T., SImon; and Simon Howell, *Cardiac Muscle Physiology.* Continuing Education in Anaesthesia, Critical Care and Pain, 2007. **7**(3): p. 85-88.
24. Ishikawa, Y. and R. Kurotani, *Cardiac myosin light chain kinase: a new player in the regulation of myosin light chain in the heart.* Circ Res, 2008. **102**(5): p. 516-8.
25. Swaminathan, P.D., et al., *Calmodulin-dependent protein kinase II: linking heart failure and arrhythmias.* Circ Res, 2012. **110**(12): p. 1661-77.
26. Mok, G.F. and D. Sweetman, *Many routes to the same destination: lessons from skeletal muscle development.* Reproduction, 2011. **141**(3): p. 301-12.
27. Bismuth, K. and F. Relaix, *Genetic regulation of skeletal muscle development.* Exp Cell Res, 2010. **316**(18): p. 3081-6.
28. Takagaki, Y., H. Yamagishi, and R. Matsuoka, *Factors involved in signal transduction during vertebrate myogenesis.* Int Rev Cell Mol Biol, 2012. **296**: p. 187-272.
29. Goldspink, G., *Gene expression in muscle in response to exercise.* J Muscle Res Cell Motil, 2003. **24**(2-3): p. 121-6.
30. Ito, K., et al., *Deficiency of triad junction and contraction in mutant skeletal muscle lacking junctophilin type 1.* J Cell Biol, 2001. **154**(5): p. 1059-67.
31. Hoh, J.F., *Muscle fiber types and function.* Curr Opin Rheumatol, 1992. **4**(6): p. 801-8.
32. Nelson, T.E., *Heat production during anesthetic-induced malignant hyperthermia.* Biosci Rep, 2001. **21**(2): p. 169-79.
33. Faulkner, J.A., *Terminology for contractions of muscles during shortening, while isometric, and during lengthening.* J Appl Physiol, 2003. **95**(2): p. 455-9.
34. Brooks, S.V. and J.A. Faulkner, *Skeletal muscle weakness in old age: underlying mechanisms.* Med Sci Sports Exerc, 1994. **26**(4): p. 432-9.
35. Block, B.A., *Thermogenesis in muscle.* Annu Rev Physiol, 1994. **56**: p. 535-77.
36. Rooyackers, O.E. and K.S. Nair, *Hormonal regulation of human muscle protein metabolism.* Annu Rev Nutr, 1997. **17**: p. 457-85.
37. Yamaoka, I., *Modification of core body temperature by amino acid administration.* Asia Pac J Clin Nutr, 2008. **17 Suppl 1**: p. 309-11.
38. Eyer, F. and T. Zilker, *Bench-to-bedside review: mechanisms and management of hyperthermia due to toxicity.* Crit Care, 2007. **11**(6): p. 236.
39. Lecker, S.H. and A.L. Goldberg, *Slowing muscle atrophy: putting the brakes on protein breakdown.* J Physiol, 2002. **545**(Pt 3): p. 729.
40. Wolfe, R.R., *The underappreciated role of muscle in health and disease.* Am J Clin Nutr, 2006. **84**(3): p. 475-82.
41. Cahill, G., Jr., et al., *Metabolic adaptation to prolonged starvation in man.* Nord Med, 1970. **83**(3): p. 89.

42. Reeds, P.J., C.R. Fjeld, and F. Jahoor, *Do the differences between the amino acid compositions of acute-phase and muscle proteins have a bearing on nitrogen loss in traumatic states?* J Nutr, 1994. **124**(6): p. 906-10.
43. Hasselgren, P.O., et al., *Novel aspects on the regulation of muscle wasting in sepsis.* Int J Biochem Cell Biol, 2005. **37**(10): p. 2156-68.
44. Lecker, S.H., et al., *Muscle protein breakdown and the critical role of the ubiquitin-proteasome pathway in normal and disease states.* J Nutr, 1999. **129**(1S Suppl): p. 227S-237S.
45. Reid, W.D. and N.A. MacGowan, *Respiratory muscle injury in animal models and humans.* Mol Cell Biochem, 1998. **179**(1-2): p. 63-80.
46. Holecek, M., *Muscle wasting in animal models of severe illness.* Int J Exp Pathol, 2012. **93**(3): p. 157-71.
47. Rennie, M.J., et al., *Muscle protein synthesis measured by stable isotope techniques in man: the effects of feeding and fasting.* Clin Sci (Lond), 1982. **63**(6): p. 519-23.
48. Dardevet, D., et al., *Muscle wasting and resistance of muscle anabolism: the "anabolic threshold concept" for adapted nutritional strategies during sarcopenia.* ScientificWorldJournal, 2012. **2012**: p. 269531.
49. Dardevet, D., et al., *Stimulation of in vitro rat muscle protein synthesis by leucine decreases with age.* J Nutr, 2000. **130**(11): p. 2630-5.
50. Masiero, E., et al., *Autophagy is required to maintain muscle mass.* Cell Metab, 2009. **10**(6): p. 507-15.
51. Lecker, S.H., A.L. Goldberg, and W.E. Mitch, *Protein degradation by the ubiquitin-proteasome pathway in normal and disease states.* J Am Soc Nephrol, 2006. **17**(7): p. 1807-19.
52. Ye, Y. and M. Rape, *Building ubiquitin chains: E2 enzymes at work.* Nat Rev Mol Cell Biol, 2009. **10**(11): p. 755-64.
53. Jagoe, R.T. and A.L. Goldberg, *What do we really know about the ubiquitin-proteasome pathway in muscle atrophy?* Curr Opin Clin Nutr Metab Care, 2001. **4**(3): p. 183-90.
54. Wing, S.S. and A.L. Goldberg, *Glucocorticoids activate the ATP-ubiquitin-dependent proteolytic system in skeletal muscle during fasting.* Am J Physiol, 1993. **264**(4 Pt 1): p. E668-76.
55. Medina, R., S.S. Wing, and A.L. Goldberg, *Increase in levels of polyubiquitin and proteasome mRNA in skeletal muscle during starvation and denervation atrophy.* Biochem J, 1995. **307 (Pt 3)**: p. 631-7.
56. Sandri, M., et al., *Foxo transcription factors induce the atrophy-related ubiquitin ligase atrogin-1 and cause skeletal muscle atrophy.* Cell, 2004. **117**(3): p. 399-412.
57. Cai, D., et al., *IKKbeta/NF-kappaB activation causes severe muscle wasting in mice.* Cell, 2004. **119**(2): p. 285-98.
58. Masiero, E. and M. Sandri, *Autophagy inhibition induces atrophy and myopathy in adult skeletal muscles.* Autophagy, 2010. **6**(2): p. 307-9.
59. Sandri, M., *Autophagy in health and disease. 3. Involvement of autophagy in muscle atrophy.* Am J Physiol Cell Physiol, 2010. **298**(6): p. C1291-7.
60. Diaz-Troya, S., et al., *The role of TOR in autophagy regulation from yeast to plants and mammals.* Autophagy, 2008. **4**(7): p. 851-65.
61. Kamada, Y., et al., *Tor directly controls the Atg1 kinase complex to regulate autophagy.* Mol Cell Biol, 2010. **30**(4): p. 1049-58.

62. Stipanuk, M.H., *Macroautophagy and its role in nutrient homeostasis.* Nutr Rev, 2009. **67**(12): p. 677-89.
63. Suzuki, K., et al., *Hierarchy of Atg proteins in pre-autophagosomal structure organization.* Genes Cells, 2007. **12**(2): p. 209-18.
64. Kawamata, T., et al., *Organization of the pre-autophagosomal structure responsible for autophagosome formation.* Mol Biol Cell, 2008. **19**(5): p. 2039-50.
65. Tooze, S.A. and T. Yoshimori, *The origin of the autophagosomal membrane.* Nat Cell Biol, 2010. **12**(9): p. 831-5.
66. Jahreiss, L., F.M. Menzies, and D.C. Rubinsztein, *The itinerary of autophagosomes: from peripheral formation to kiss-and-run fusion with lysosomes.* Traffic, 2008. **9**(4): p. 574-87.
67. Hasegawa, M., et al., *Differential regulation of gene expression and insulin-induced activation of phosphodiesterase 3B in adipocytes of lean insulin-resistant IRS-1 (-/-) mice.* Diabetes Res Clin Pract, 2002. **58**(2): p. 79-85.
68. Meyer, T., et al., *Progressive muscle atrophy with hypokalemic periodic paralysis and calcium channel mutation.* Muscle Nerve, 2008. **37**(1): p. 120-4.
69. Furuno, K., M.N. Goodman, and A.L. Goldberg, *Role of different proteolytic systems in the degradation of muscle proteins during denervation atrophy.* J Biol Chem, 1990. **265**(15): p. 8550-7.
70. Altun, Z.F.a.H., D.H, *Muscle System, Introduction.* In WormAtlas, 2009.
71. Szewczyk, N.J., et al., *Genetic defects in acetylcholine signalling promote protein degradation in muscle cells of Caenorhabditis elegans.* J Cell Sci, 2000. **113 (Pt 11)**: p. 2003-10.
72. Altun, Z.F.a.H., D.H., *Muscle System, Somatic muscle.* In WormAtlas, 2009.
73. Riddle, D.L., *C. elegans II*. Cold Spring Harbor monograph series,. 1997, Plainview, N.Y.: Cold Spring Harbor Laboratory Press. xvii, 1222 p.
74. Zdinak, L.A., et al., *Transgene-coded chimeric proteins as reporters of intracellular proteolysis: starvation-induced catabolism of a lacZ fusion protein in muscle cells of Caenorhabditis elegans.* J Cell Biochem, 1997. **67**(1): p. 143-53.
75. Fostel, J.L., L. Benner Coste, and L.A. Jacobson, *Degradation of transgene-coded and endogenous proteins in the muscles of Caenorhabditis elegans.* Biochem Biophys Res Commun, 2003. **312**(1): p. 173-7.
76. Szewczyk, N.J. and L.A. Jacobson, *Activated EGL-15 FGF receptor promotes protein degradation in muscles of Caenorhabditis elegans.* EMBO J, 2003. **22**(19): p. 5058-67.
77. Szewczyk, N.J., et al., *Opposed growth factor signals control protein degradation in muscles of Caenorhabditis elegans.* EMBO J, 2007. **26**(4): p. 935-43.
78. Melendez, A., et al., *Autophagy genes are essential for dauer development and life-span extension in C. elegans.* Science, 2003. **301**(5638): p. 1387-91.
79. Fire, A., et al., *Potent and specific genetic interference by double-stranded RNA in Caenorhabditis elegans.* Nature, 1998. **391**(6669): p. 806-11.
80. Maine, E.M., *RNAi As a tool for understanding germline development in Caenorhabditis elegans: uses and cautions.* Dev Biol, 2001. **239**(2): p. 177-89.
81. Ahringer, J., ed., *Reverse Genetics.* WormBook, ed., 2006.
82. Timmons, L., D.L. Court, and A. Fire, *Ingestion of bacterially expressed dsRNAs can produce specific and potent genetic interference in Caenorhabditis elegans.* Gene, 2001. **263**(1-2): p. 103-12.

83. Fischer, S.E., *Small RNA-mediated gene silencing pathways in C. elegans.* Int J Biochem Cell Biol, 2010. **42**(8): p. 1306-15.
84. Zheng, S.Q., et al., *Drug absorption efficiency in Caenorhbditis elegans delivered by different methods.* PLoS One, 2013. **8**(2): p. e56877.
85. Walker, E.H., et al., *Structural determinants of phosphoinositide 3-kinase inhibition by wortmannin, LY294002, quercetin, myricetin, and staurosporine.* Mol Cell, 2000. **6**(4): p. 909-19.
86. Kovacs, A.L., et al., *Inhibition of hepatocytic autophagy by adenosine, adenosine analogs and AMP.* Biol Chem, 1998. **379**(11): p. 1341-7.
87. Ornitz, D.M., *FGFs, heparan sulfate and FGFRs: complex interactions essential for development.* Bioessays, 2000. **22**(2): p. 108-12.
88. Plotnikov, A.N., et al., *Crystal structures of two FGF-FGFR complexes reveal the determinants of ligand-receptor specificity.* Cell, 2000. **101**(4): p. 413-24.
89. Shi, E., et al., *Control of fibroblast growth factor receptor kinase signal transduction by heterodimerization of combinatorial splice variants.* Mol Cell Biol, 1993. **13**(7): p. 3907-18.
90. Schlessinger, J., et al., *Crystal structure of a ternary FGF-FGFR-heparin complex reveals a dual role for heparin in FGFR binding and dimerization.* Mol Cell, 2000. **6**(3): p. 743-50.
91. Goetz, R. and M. Mohammadi, *Exploring mechanisms of FGF signalling through the lens of structural biology.* Nat Rev Mol Cell Biol, 2013. **14**(3): p. 166-80.
92. Tulin, S. and A. Stathopoulos, *Extending the family table: Insights from beyond vertebrates into the regulation of embryonic development by FGFs.* Birth Defects Res C Embryo Today, 2010. **90**(3): p. 214-27.
93. Nagendra, H.G., et al., *Sequence analyses and comparative modeling of fly and worm fibroblast growth factor receptors indicate that the determinants for FGF and heparin binding are retained in evolution.* FEBS Lett, 2001. **501**(1): p. 51-8.
94. Chateau, M.T., et al., *Klotho interferes with a novel FGF-signalling pathway and insulin/Igf-like signalling to improve longevity and stress resistance in Caenorhabditis elegans.* Aging (Albany NY), 2010. **2**(9): p. 567-81.
95. Goetz, R., et al., *Molecular insights into the klotho-dependent, endocrine mode of action of fibroblast growth factor 19 subfamily members.* Mol Cell Biol, 2007. **27**(9): p. 3417-28.
96. Birnbaum, D., C. Popovici, and R. Roubin, *A pair as a minimum: the two fibroblast growth factors of the nematode Caenorhabditis elegans.* Dev Dyn, 2005. **232**(2): p. 247-55.
97. Olfert, I.M., et al., *Skeletal muscle capillarity and angiogenic mRNA levels after exercise training in normoxia and chronic hypoxia.* J Appl Physiol, 2001. **91**(3): p. 1176-84.
98. Dohm, G.L., E.B. Tapscott, and G.J. Kasperek, *Protein degradation during endurance exercise and recovery.* Med Sci Sports Exerc, 1987. **19**(5 Suppl): p. S166-71.
99. Szewczyk, N.J., B.K. Peterson, and L.A. Jacobson, *Activation of Ras and the mitogen-activated protein kinase pathway promotes protein degradation in muscle cells of Caenorhabditis elegans.* Mol Cell Biol, 2002. **22**(12): p. 4181-8.
100. Espinosa, A., M. Estrada, and E. Jaimovich, *IGF-I and insulin induce different intracellular calcium signals in skeletal muscle cells.* J Endocrinol, 2004. **182**(2): p. 339-52.

101. Gami, M.S. and C.A. Wolkow, *Studies of Caenorhabditis elegans DAF-2/insulin signaling reveal targets for pharmacological manipulation of lifespan.* Aging Cell, 2006. **5**(1): p. 31-7.
102. Laron, Z., *Insulin-like growth factor 1 (IGF-1): a growth hormone.* Mol Pathol, 2001. **54**(5): p. 311-6.
103. Lawrence, M.C., N.M. McKern, and C.W. Ward, *Insulin receptor structure and its implications for the IGF-1 receptor.* Curr Opin Struct Biol, 2007. **17**(6): p. 699-705.
104. Kaletsky, R. and C.T. Murphy, *The role of insulin/IGF-like signaling in C. elegans longevity and aging.* Dis Model Mech, 2010. **3**(7-8): p. 415-9.
105. Jaumot, M. and J.F. Hancock, *Protein phosphatases 1 and 2A promote Raf-1 activation by regulating 14-3-3 interactions.* Oncogene, 2001. **20**(30): p. 3949-58.
106. Chong, H., J. Lee, and K.L. Guan, *Positive and negative regulation of Raf kinase activity and function by phosphorylation.* EMBO J, 2001. **20**(14): p. 3716-27.
107. Goetz, C.A., J.J. O'Neil, and M.A. Farrar, *Membrane localization, oligomerization, and phosphorylation are required for optimal raf activation.* J Biol Chem, 2003. **278**(51): p. 51184-9.
108. Hekman, M., et al., *Dynamic changes in C-Raf phosphorylation and 14-3-3 protein binding in response to growth factor stimulation: differential roles of 14-3-3 protein binding sites.* J Biol Chem, 2004. **279**(14): p. 14074-86.
109. Light, Y., H. Paterson, and R. Marais, *14-3-3 antagonizes Ras-mediated Raf-1 recruitment to the plasma membrane to maintain signaling fidelity.* Mol Cell Biol, 2002. **22**(14): p. 4984-96.
110. Rommel, C., et al., *Activated Ras displaces 14-3-3 protein from the amino terminus of c-Raf-1.* Oncogene, 1996. **12**(3): p. 609-19.
111. Rommel, C., et al., *Negative regulation of Raf activity by binding of 14-3-3 to the amino terminus of Raf in vivo.* Mech Dev, 1997. **64**(1-2): p. 95-104.
112. Sayeed, M.M., *Alterations in calcium signaling and cellular responses in septic injury.* New Horiz, 1996. **4**(1): p. 72-86.
113. Chin, E.R., *Role of Ca2+/calmodulin-dependent kinases in skeletal muscle plasticity.* J Appl Physiol, 2005. **99**(2): p. 414-23.
114. Sayeed, M.M., *Signaling mechanisms of altered cellular responses in trauma, burn, and sepsis: role of Ca2+.* Arch Surg, 2000. **135**(12): p. 1432-42.
115. Benson, D.W., et al., *Effect of sepsis on calcium uptake and content in skeletal muscle and regulation in vitro by calcium of total and myofibrillar protein breakdown in control and septic muscle: results from a preliminary study.* Surgery, 1989. **106**(1): p. 87-93.
116. Song, S.K., et al., *Increased intracellular Ca2+: a critical link in the pathophysiology of sepsis?* Proc Natl Acad Sci U S A, 1993. **90**(9): p. 3933-7.
117. Kwok, T.C., et al., *A small-molecule screen in C. elegans yields a new calcium channel antagonist.* Nature, 2006. **441**(7089): p. 91-5.
118. McDonald, T.F., et al., *Regulation and modulation of calcium channels in cardiac, skeletal, and smooth muscle cells.* Physiol Rev, 1994. **74**(2): p. 365-507.
119. Varadi, G., et al., *Molecular elements of ion permeation and selectivity within calcium channels.* Crit Rev Biochem Mol Biol, 1999. **34**(3): p. 181-214.
120. Schafer, W.R. and C.J. Kenyon, *A calcium-channel homologue required for adaptation to dopamine and serotonin in Caenorhabditis elegans.* Nature, 1995. **375**(6526): p. 73-8.

121. Dolphin, A.C., *Calcium channel diversity: multiple roles of calcium channel subunits.* Curr Opin Neurobiol, 2009. **19**(3): p. 237-44.
122. Finn, B.E. and S. Forsen, *The evolving model of calmodulin structure, function and activation.* Structure, 1995. **3**(1): p. 7-11.
123. Slavov, N., J. Carey, and S. Linse, *Calmodulin transduces Ca(2+) oscillations into differential regulation of its target proteins.* ACS Chem Neurosci, 2013. **4**(4): p. 601-12.
124. Smith, I.J., S.H. Lecker, and P.O. Hasselgren, *Calpain activity and muscle wasting in sepsis.* Am J Physiol Endocrinol Metab, 2008. **295**(4): p. E762-71.
125. Joyce, P.I., et al., *The atypical calpains: evolutionary analyses and roles in Caenorhabditis elegans cellular degeneration.* PLoS Genet, 2012. **8**(3): p. e1002602.
126. Williams, A.B., et al., *Sepsis stimulates release of myofilaments in skeletal muscle by a calcium-dependent mechanism.* FASEB J, 1999. **13**(11): p. 1435-43.
127. Du, J., et al., *Activation of caspase-3 is an initial step triggering accelerated muscle proteolysis in catabolic conditions.* J Clin Invest, 2004. **113**(1): p. 115-23.
128. MacKenzie, S.H. and A.C. Clark, *Death by caspase dimerization.* Adv Exp Med Biol, 2012. **747**: p. 55-73.
129. Snigdha, S., et al., *Caspase-3 activation as a bifurcation point between plasticity and cell death.* Neurosci Bull, 2012. **28**(1): p. 14-24.
130. Shaham, S., *Identification of multiple Caenorhabditis elegans caspases and their potential roles in proteolytic cascades.* J Biol Chem, 1998. **273**(52): p. 35109-17.
131. Wang, X., et al., *Insulin resistance accelerates muscle protein degradation: Activation of the ubiquitin-proteasome pathway by defects in muscle cell signaling.* Endocrinology, 2006. **147**(9): p. 4160-8.
132. Neumar, R.W., et al., *Cross-talk between calpain and caspase proteolytic systems during neuronal apoptosis.* J Biol Chem, 2003. **278**(16): p. 14162-7.
133. Rosenberg, O.S., et al., *Structure of the autoinhibited kinase domain of CaMKII and SAXS analysis of the holoenzyme.* Cell, 2005. **123**(5): p. 849-60.
134. Goldberg, J., A.C. Nairn, and J. Kuriyan, *Structural basis for the autoinhibition of calcium/calmodulin-dependent protein kinase I.* Cell, 1996. **84**(6): p. 875-87.
135. Pelloux, S., et al., *Identification of a cryptic protein kinase CK2 phosphorylation site in human complement protease Clr, and its use to probe intramolecular interaction.* FEBS Lett, 1996. **386**(1): p. 15-20.
136. Meyer, T., et al., *Calmodulin trapping by calcium-calmodulin-dependent protein kinase.* Science, 1992. **256**(5060): p. 1199-202.
137. Park, E.C. and H.R. Horvitz, *Mutations with dominant effects on the behavior and morphology of the nematode Caenorhabditis elegans.* Genetics, 1986. **113**(4): p. 821-52.
138. Reiner, D.J., et al., *Diverse behavioural defects caused by mutations in Caenorhabditis elegans unc-43 CaM kinase II.* Nature, 1999. **402**(6758): p. 199-203.
139. Wang, Q. and W.G. Wadsworth, *The C domain of netrin UNC-6 silences calcium/calmodulin-dependent protein kinase- and diacylglycerol-dependent axon branching in Caenorhabditis elegans.* J Neurosci, 2002. **22**(6): p. 2274-82.
140. Nehrke, K., J. Denton, and W. Mowrey, *Intestinal Ca2+ wave dynamics in freely moving C. elegans coordinate execution of a rhythmic motor program.* Am J Physiol Cell Physiol, 2008. **294**(1): p. C333-44.
141. LeBoeuf, B., T.R. Gruninger, and L.R. Garcia, *Food deprivation attenuates seizures through CaMKII and EAG K+ channels.* PLoS Genet, 2007. **3**(9): p. 1622-32.

142. Tam, T., et al., *Voltage-gated calcium channels direct neuronal migration in Caenorhabditis elegans.* Dev Biol, 2000. **226**(1): p. 104-17.
143. Richmond, J., *Dissecting and recording from the C. Elegans neuromuscular junction.* J Vis Exp, 2009(24).
144. Zhang, Y., et al., *Structural insight into Caenorhabditis elegans sex-determining protein FEM-2.* J Biol Chem, 2013. **288**(30): p. 22058-66.
145. Tan, K.M., et al., *The Caenorhabditis elegans sex-determining protein FEM-2 and its human homologue, hFEM-2, are Ca2+/calmodulin-dependent protein kinase phosphatases that promote apoptosis.* J Biol Chem, 2001. **276**(47): p. 44193-202.
146. Mischak, H., et al., *Negative regulation of Raf-1 by phosphorylation of serine 621.* Mol Cell Biol, 1996. **16**(10): p. 5409-18.
147. Illario, M., et al., *Calcium/calmodulin-dependent protein kinase II binds to Raf-1 and modulates integrin-stimulated ERK activation.* J Biol Chem, 2003. **278**(46): p. 45101-8.
148. Sundaram, M. and M. Han, *The C. elegans ksr-1 gene encodes a novel Raf-related kinase involved in Ras-mediated signal transduction.* Cell, 1995. **83**(6): p. 889-901.
149. Herndon, L.A., et al., *Stochastic and genetic factors influence tissue-specific decline in ageing C. elegans.* Nature, 2002. **419**(6909): p. 808-14.
150. Toth, M.L., et al., *Longevity pathways converge on autophagy genes to regulate life span in Caenorhabditis elegans.* Autophagy, 2008. **4**(3): p. 330-8.
151. Shephard, F., et al., *Identification and functional clustering of genes regulating muscle protein degradation from amongst the known C. elegans muscle mutants.* PLoS ONE, 2011. **6**(9): p. e24686.
152. Szewczyk, N.J. and L.A. Jacobson, *Signal-transduction networks and the regulation of muscle protein degradation.* Int J Biochem Cell Biol, 2005. **37**(10): p. 1997-2011.
153. Lawrence, B.P. and W.J. Brown, *Inhibition of protein synthesis separates autophagic sequestration from the delivery of lysosomal enzymes.* J Cell Sci, 1993. **105 (Pt 2)**: p. 473-80.
154. Morrison, D.K., *Mechanisms regulating Raf-1 activity in signal transduction pathways.* Mol Reprod Dev, 1995. **42**(4): p. 507-14.
155. Rajakulendran, T., et al., *A dimerization-dependent mechanism drives RAF catalytic activation.* Nature, 2009. **461**(7263): p. 542-5.
156. Dhillon, A.S., et al., *The C-terminus of Raf-1 acts as a 14-3-3-dependent activation switch.* Cell Signal, 2009. **21**(11): p. 1645-51.
157. Yip-Schneider, M.T., et al., *Regulation of the Raf-1 kinase domain by phosphorylation and 14-3-3 association.* Biochem J, 2000. **351**(Pt 1): p. 151-9.
158. Bootman, M.D., P. Lipp, and M.J. Berridge, *The organisation and functions of local Ca(2+) signals.* J Cell Sci, 2001. **114**(Pt 12): p. 2213-22.
159. Heist, E.K., M. Srinivasan, and H. Schulman, *Phosphorylation at the nuclear localization signal of Ca2+/calmodulin-dependent protein kinase II blocks its nuclear targeting.* J Biol Chem, 1998. **273**(31): p. 19763-71.
160. Swulius, M.T. and M.N. Waxham, *Ca(2+)/calmodulin-dependent protein kinases.* Cell Mol Life Sci, 2008. **65**(17): p. 2637-57.
161. Bayer, K.U., P. De Koninck, and H. Schulman, *Alternative splicing modulates the frequency-dependent response of CaMKII to Ca(2+) oscillations.* EMBO J, 2002. **21**(14): p. 3590-7.

162. Bayer, K.U., J. Lohler, and K. Harbers, *An alternative, nonkinase product of the brain-specifically expressed Ca2+/calmodulin-dependent kinase II alpha isoform gene in skeletal muscle.* Mol Cell Biol, 1996. **16**(1): p. 29-36.
163. Srinivasan, M., C.F. Edman, and H. Schulman, *Alternative splicing introduces a nuclear localization signal that targets multifunctional CaM kinase to the nucleus.* J Cell Biol, 1994. **126**(4): p. 839-52.
164. Bayer, K.U., K. Harbers, and H. Schulman, *alphaKAP is an anchoring protein for a novel CaM kinase II isoform in skeletal muscle.* EMBO J, 1998. **17**(19): p. 5598-605.
165. De Koninck, P. and H. Schulman, *Sensitivity of CaM kinase II to the frequency of Ca2+ oscillations.* Science, 1998. **279**(5348): p. 227-30.
166. Chin, E.R., *The role of calcium and calcium/calmodulin-dependent kinases in skeletal muscle plasticity and mitochondrial biogenesis.* Proc Nutr Soc, 2004. **63**(2): p. 279-86.
167. Brett, W., *CaMKII Protein Expression and Phosphorylation in Mouse Skeletal Muscle Following Atrophy and Hypertrophy.* 2012.
168. Yan, Z., et al., *Regulation of exercise-induced fiber type transformation, mitochondrial biogenesis, and angiogenesis in skeletal muscle.* J Appl Physiol (1985), 2011. **110**(1): p. 264-74.
169. Harvey, B.P., S.S. Banga, and H.L. Ozer, *Regulation of the multifunctional Ca2+/calmodulin-dependent protein kinase II by the PP2C phosphatase PPM1F in fibroblasts.* J Biol Chem, 2004. **279**(23): p. 24889-98.
170. Nguyen, L.K., et al., *Signalling by protein phosphatases and drug development: a systems-centred view.* FEBS J, 2013. **280**(2): p. 751-65.
171. Salzano, M., et al., *Calcium/calmodulin-dependent protein kinase II (CaMKII) phosphorylates Raf-1 at serine 338 and mediates Ras-stimulated Raf-1 activation.* Cell Cycle, 2012. **11**(11): p. 2100-6.
172. Nayak, L. and R.K. De, *An algorithm for modularization of MAPK and calcium signaling pathways: comparative analysis among different species.* J Biomed Inform, 2007. **40**(6): p. 726-49.
173. Pawson, T. and P. Nash, *Protein-protein interactions define specificity in signal transduction.* Genes Dev, 2000. **14**(9): p. 1027-47.
174. Bulow, H.E., T. Boulin, and O. Hobert, *Differential functions of the C. elegans FGF receptor in axon outgrowth and maintenance of axon position.* Neuron, 2004. **42**(3): p. 367-74.
175. Robatzek, M. and J.H. Thomas, *Calcium/calmodulin-dependent protein kinase II regulates Caenorhabditis elegans locomotion in concert with a G(o)/G(q) signaling network.* Genetics, 2000. **156**(3): p. 1069-82.
176. Rohlin, L., M.K. Oh, and J.C. Liao, *Microbial pathway engineering for industrial processes: evolution, combinatorial biosynthesis and rational design.* Curr Opin Microbiol, 2001. **4**(3): p. 330-5.
177. Ma'ayan, A., *Insights into the organization of biochemical regulatory networks using graph theory analyses.* J Biol Chem, 2009. **284**(9): p. 5451-5.
178. Morrison, D.K., et al., *Identification of the major phosphorylation sites of the Raf-1 kinase.* J Biol Chem, 1993. **268**(23): p. 17309-16.
179. Schramm, K., et al., *Phosphorylation of c-Raf-1 by protein kinase A interferes with activation.* Biochem Biophys Res Commun, 1994. **201**(2): p. 740-7.

180. Kyriakis, J.M., *The integration of signaling by multiprotein complexes containing Raf kinases.* Biochim Biophys Acta, 2007. **1773**(8): p. 1238-47.
181. Lipinski, M.M., et al., *A genome-wide siRNA screen reveals multiple mTORC1 independent signaling pathways regulating autophagy under normal nutritional conditions.* Dev Cell, 2010. **18**(6): p. 1041-52.
182. Salminen, A. and K. Kaarniranta, *AMP-activated protein kinase (AMPK) controls the aging process via an integrated signaling network.* Ageing Res Rev, 2012. **11**(2): p. 230-41.
183. Lin, K., et al., *Regulation of the Caenorhabditis elegans longevity protein DAF-16 by insulin/IGF-1 and germline signaling.* Nat Genet, 2001. **28**(2): p. 139-45.